Université de Sherbrooke

Nuclear import mechanism of Php4 under iron deprivation in fission yeast *Schizosaccharomyces pombe.*

By

Md Gulam Musawwir Khan

Département de Biochimie

Faculté de Médecine et des Sciences de la Santé,

Université de Sherbrooke, Sherbrooke, QC, Canada

Memory submitted at

La Faculté de Médecine et des Sciences de la Santé

To fulfill the requirement for the degree of

Master of Science (M.Sc.) in Biochemistry

TABLE OF CONTENT

TABLE OF CONTENT……..II
LIST OF FIGURES……IV
LIST OF TABLES……VI
LIST OF ABBREVIATIONS……VII
ABSTRACT……VIII
INTRODUCTION……1
1. Iron: An essential element for living organisms……1
2. Yeasts as model system to study molecular and cell biology……3
3. Iron homeostasis in budding yeast *S. cerevisiae*……5
3.1. Mechanisms of iron acquisition in *S. cerevisiae*……6
3.1.1. High-affinity iron uptake: reductase-independent……6
3.1.2. High-affinity iron uptake: reductase-dependent……8
3.1.3. Low-affinity iron uptake……12
3.1.4. Storage of iron in the vacuoles……13
3.2. Regulation of iron homeostasis in budding yeast……15
3.2.1. Regulation of iron transport by Aft1 and Aft2……15
3.2.2. Regulation of iron storage by Yap5……18
3.3. Post-transcriptional regulation of iron homeostasis by Cth1 and Cth2……19
4. Iron homeostasis in *S. pombe*……21
4.1. Extracellular iron scavenging systems: high-affinity iron uptake……21
4.1.1. Reductive iron acquisition system……21
4.1.2. Non-reductive iron acquisition system……22
4.2. Intracellular iron storage system……25
4.3. Iron transport regulation: role of Fep1……28
4.4. The CCAAT binding complex (CBC) and its role in iron homeostasis……30
5. Php4, a subunit of CBC, plays a critical role in iron economy……33
5.1. Php4 subunit……33
5.2. Php4 regulon……34
5.3. Iron-dependent subcellular localization of Php4 and its post-translational regulation……35
6. Role of monothiol glutaredoxin and BolA-like proteins in iron homeostasis……37
6.1. Role of Grx3/4 and Fra2 in iron homeostasis in budding yeast……37
6.2. Role of Grx4 and Fra2 for iron homeostasis in *S. pombe*……39

7. Nucleo-cytoplasmic trafficking of proteins……41
7.1. Nuclear localization sequence (NLS) triggers nuclear import of proteins……41
7.2. Role of karyopherin α/β in transporting cargo protein bearing NLSs……42
8. Hypothesis and research objectives……45

RESULTS……46

Article: Characterization of the nuclear import mechanism of the CCAAT-regulatory subunit Php4.

Résumé……46
Contribution……47
Abstract……49
Introduction……50
Material and Methods ……53
Results……57
Discussion……66
Acknowledgments……70
Reference……70

DISCUSSION……93

1. **Role of other karyopherin β in the recognition of Php4 NLSs ……93**
2. **Validation of Php4 subcellular localization with a small tag……95**
3. **Php4 NLSs specificity for karyopherins……97**
4. **Assembly of other subunits of CBC: one-step or piggy-back mechanism? ……99**
5. **Role of phosphorylation in the nuclear localization of Php4……102**
6. **Role of Grx4 in iron sensing……105**
7. **Php4 as an antifungal therapeutic target……107**

ACKNOWLEDGMENTS……111

REFERENCES……111

LIST OF FIGURES

INTRODUCTION

Figure 1. The Fenton reaction produces free hydroxyl radicals that have potential to damage DNA, proteins and lipids in cells……2

Figure 2. Reductase-dependent iron acquisition in *S. cerevisiae*……11

Figure 3. Vacuolar iron storage and mobilization……14

Figure 4. Cth1 and Cth2 control post-transcriptional regulation of iron-using gene transcripts under iron deficiency……20

Figure 5. Ferrichrome biosynthesis pathway in the fission yeast *S. pombe*……24

Figure 6. Proposed model for iron transport in *S. pombe*……26

Figure 7. Schematic representation of Fep1……30

Figure 8. Php4 plays a significant role in the transcriptional regulation of genes encoding iron-using proteins in *S. pombe*……35

Figure 9. Schematic representation of nuclear protein import……43

RESULTS

Figure 1. Iron-regulated nucleo-cytoplasmic trafficking of Php4 is independent of Php2, Php3 and Php5 proteins……81

Figure 2. Distinct regions of Php4 are required for its nuclear localization……82

Figure 3. Two regions of Php4 encompassing amino acid residues 171 to 174 and 234 to 240 are involved in targeting Php4 to the nucleus……83

Figure 4. Php4 NLSs are required for Php4-mediated repressive function……84

Figure 5. Amino acid fragments 160-190 and 219-246 of Php4 contain nuclear import activity……85

Figure 6. Identification of two functional Php4 NLSs……86

Figure 7. Inactivation of *imp1*$^{+}$, *cut15*$^{+}$ and *sal3*$^{+}$ produced defect in nuclear import of GFP-Php4……87

Figure 8. Loss of Imp1, Cut15 or Sal3 resulted in increased expression of *isa1*$^{+}$ under low iron conditions……88

Figure 9. Php4 interacts with Imp1, Cut15, and Sal3 in *S. pombe*……89

Supplementary Figures:

Figure S1. Detection of intact GST-GFP and GST-GFP fusion proteins……90

Figure S2. Inactivation of *imp1Δ, cut15-85* or *sal3Δ* resulted in increased expression of isa1^{+} under iron starvation conditions……91

DISCUSSION

Figure 10. Iron-responsive nucleo-cytoplasmic trafficking of HA3-Php4……96

Figure 11. A) A Proposed piggy-back model in *S. pombe*……100

B) Amino acid sequence of Php2 exhibits potential NLSs……100

Figure 12. Proposed [2Fe-2S] cluster model……107

LIST OF TABLES

INTRODUCTION

Table 1. Siderophore substrates of ARN/SIT family of transporters……..…8

Table 2. Examples of genes that are up-regulated by Aft1/ Aft2 during iron deficiency……17

RESULTS:

TABLE 1. *S. pombe* strain genotypes……..80

DISCUSSION

Table 3. Possible localization of Php2-GFP, Php3-HA3 or Php5-Myc13 in wild-type, *php2Δ, php3Δ,* and *php5Δ* strains that would support a piggy-back mechanism……..102

Table 4. List of several known cargo proteins nuclear localization sequences whose nuclear importation are regulated by phosphorylation……..105

Table 5. Predicted NLSs in Php4 orthologs in pathogenic yeasts……110

LIST OF ABBREVIATIONS

ABC	ATP-binding cassette
ARE	AU-rich element
ATP	Adenosine triphosphate
BiFC	Bimolecular fluorescence complementation
CBC	CCAAT-binding complex
CBF	CCAAT-binding factor
CCC	Cation-Chloride Co-transporter
CNLS	Classical NLS
Co-IP	Co-immunoprecipitation
CRD	Cysteine-rich domain
Dip	2,2'-dipyridyl
DNA	Deoxyribonucleic acid
DUF	Domain of unknown function
ER	Endoplasmic Reticulum
FRET	Fluorescence resonance energy transfer
GFP	Green fluorescent protein
GTP	Guanosine-5'-triphosphate
GTPase	Guanosine-5'-triphosphatase
HTTP	Human tristetraprolin
IBB	Importin beta binding domain
Kap	Karyopherin
mRNA	Messenger RNA
NES	Nuclear export sequence
NLS	Nuclear localization sequence
NPC	Nuclear pore complex
Nramp	Natural-resistance-associated macrophage protein
PY-NLS	proline-tyrosine NLS
Ran	RAs-related nuclear protein
RNA	Ribonucleic acid
SIT	siderophore-iron-transporters
TCA cycle	Tricarboxylic acid cycle
TZF	Tandem zinc finger
UTR	untranslated region
UV	ultra-violet
ZF	Zinc Finger

ABSTRACT

Nuclear import mechanism of Php4 under iron deprivation in fission yeast *Schizosaccharomyces pombe.*

Md Gulam Musawwir Khan

Département de Biochimie,

Faculté de Médecine et des Sciences de la Santé,

Université de Sherbrooke, Sherbrooke, QC, Canada

Php4 is a subunit of the CCAAT-binding protein complex that has a negative regulatory function during iron deprivation in the fission yeast *Schizosaccharomyces pombe*. Under low iron conditions, Php4 fosters the repression of genes encoding iron using proteins. In contrast, under iron-replete conditions, Php4 is inactivated at both transcriptional and post-transcriptional levels. Our group has already described that Php4 is a nucleo-cytoplasmic shuttling protein, which accumulates into the nucleus during iron deficiency. On the contrary, Php4 is exported from the nucleus to the cytoplasm in response to iron abundance. Php4 possesses a leucine-rich NES (^{93}LLEQLEML^{100}) that is necessary for its nuclear export by the exportin Crm1. Our current study aims at understanding the mechanism by which Php4 is imported in the nucleus during iron starvation. Through microscopic analyses using different mutant strains, we showed that the nuclear localization of Php4 is independent of the other subunits of the CCAAT-binding core complex namely Php2, Php3 and Php5. Deletion mapping analysis of Php4 identifies two putative nuclear localization sequences (NLSs) in Php4 (^{171}KRIR^{174} and ^{234}KSVKRVR^{240}). Using chimeric proteins that consist of GFP fused to Php4, we engineered substitutions of the basic amino acid residues ^{171}AAIA^{174} and ^{234}ASVAAAA^{240} and analyzed the functionality of both NLSs. We observed that both monopartite NLSs play critical role for Php4 nuclear localization. We also observed that

mutant strains of *cut15*$^{+}$, *imp1*$^{+}$ or *sal3*$^{+}$ exhibited defects in nuclear targeting of Php4, revealing that nuclear accumulation of Php4 is dependent on two karyopherin α (Imp1 and Cut15) and one karyopherin β (Sal3) receptors. Consistently, the Php4-mediated repression activity is abolished in the absence of two functional NLSs. Moreover, loss of Imp1, Cut15 or Sal3 resulted in increased expression of *isa1*$^{+}$, which is a target gene of Php4. Co-immunoprecipitation assay (Co-IP) reveals physical interaction of Php4 with Imp1, Cut15 and Sal3 in vitro. Collectively, our results demonstrate that Php4 has two distinct NLS regions responsible for its nuclear localization. Furthermore, karyopherin α and β receptors play a role in the nuclear import of Php4. Because Php4 is essential for growth under low iron conditions, the presence of two NLSs would ensure the protein to reach its nuclear destination when cells undergo a transition from iron-sufficient to iron-limiting conditions.

INTRODUCTION

1. Iron: An essential element for living organisms

Iron is an essential microelement for almost all living eukaryotes; ranging from yeast to mammals. The capacity to freely lose and gain electrons permits iron to play a substantial role in biochemistry and cellular physiology. Due to its ability to exchange electrons, iron can be found in the ferrous form (Fe^{2+}), which is an electron donor and ferric form (Fe^{3+}), which is an electron acceptor. This property makes it a cofactor of choice for many enzymes involved in oxido-reduction reactions including oxygen transport, respiration and the tricarboxylic acid cycle. Iron can be found in various forms such as inorganic iron, oxoiron, heme and iron-sulfur cluster. These facts make this transition metal indispensable for the function of several enzymes and thus, for the viability of virtually all living organisms. Exceptionally, only few species of bacteria do not require iron (VAN HO *et al.* 2002).

Although iron is the fourth most abundant metal on earth, its bioavailability is highly restricted. Major geographical areas like ocean, lakes and other water surfaces possess very low concentrations of iron. When abundant, iron is found in various biologically inaccessible forms such as magnetite (Fe_3O_4), hematite (Fe_2O_3), goethite ($FeO(OH)$), limonite ($FeO(OH).n(H_2O)$) or siderite ($FeCO_3$). Furthermore, due to its redox chemical properties, iron is rapidly oxidized in the presence of O_2 to generate insoluble ferric hydroxides. To combat the poor bioavailability, iron must be acquired through specialized cellular transport systems which have been developed by organisms throughout their evolution.

Unfortunately, the redox property of iron could make it toxic to cells, especially when its concentration exceeds the normal requirements. In cytoplasm of cells, free iron is found in its reduced state (Fe^{2+}). Ferrous ions can easily react with hydrogen peroxide (H_2O_2) to generate both hydroxyl ion (OH^-) and hydroxyl radical ($^{\bullet}OH$), according to the Fenton reaction (Figure 1) (HALLIWELL and GUTTERIDGE 1992).

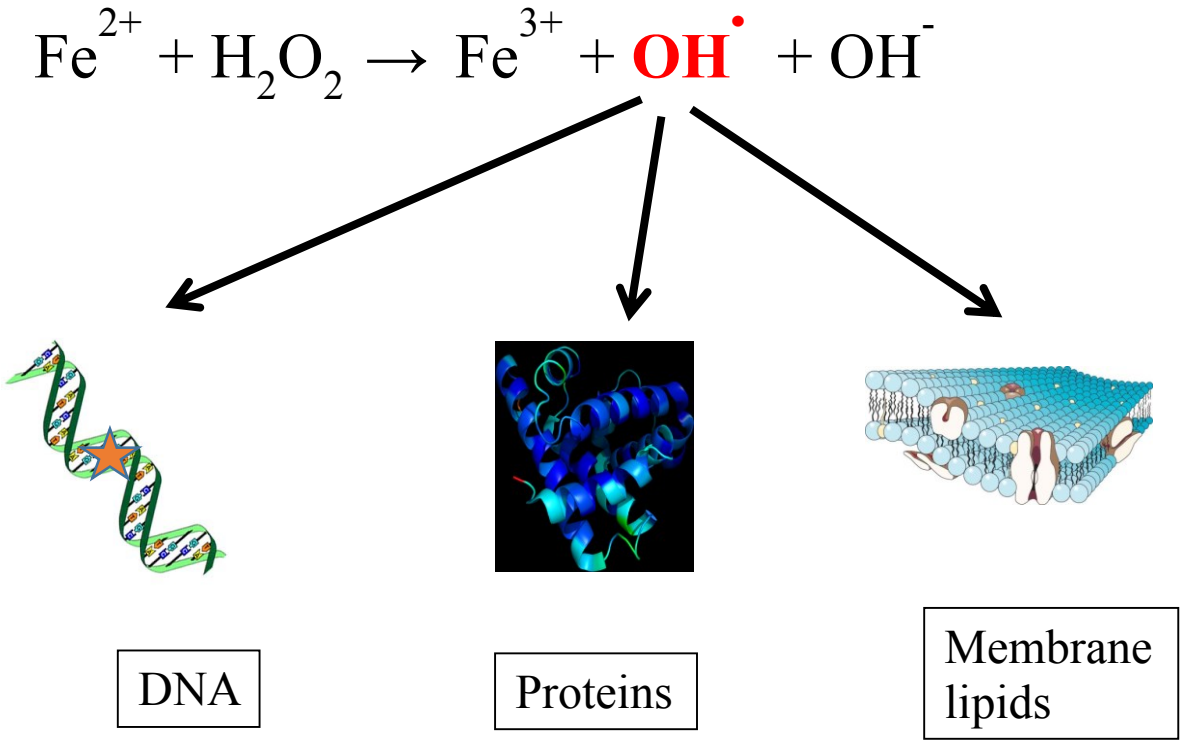

Figure 1. The Fenton reaction produces free hydroxyl radicals that have potential to damage DNA, proteins and lipids in cells.

Hydroxyl radicals produced via this reaction are part of the reactive oxygen species (ROS) family. These possess a strong oxidative power and are known for their ability to alter certain cellular components like proteins, membrane phospholipids and nucleic acids (REITER *et al.* 1995). More specifically, free radicals affect the DNA backbone by breaking the links between DNA bases at the phosphodiester bonds resulting in single and double stranded DNA breaks. Free hydroxyl radicals cause oxidative degradation of membrane lipids through

a free radical chain reaction mechanism. This sequesters electrons at polyunsaturated fatty acids and results in the damage of lipoprotein (HALLIWELL and CHIRICO 1993). Positively charged iron can directly bind to DNA and interfere with the attachment of magnesium. This results in adverse effects on DNA repair mechanisms and subsequently on DNA integrity (LI *et al.* 2009b). Iron also has the ability to substitute the zinc in "zinc finger structural motifs" resulting in the loss of stability and function of the proteins. Furthermore, iron-substituted zinc fingers may also generate free radicals and lead to adverse consequences which could be fatal for cell survival (SARKAR 1995; CONTE *et al.* 1996).

Considering iron is both essential and toxic for organisms, maintaining a delicate balance of this transition metal in the cell is vital. A tight regulation of the acquisition and distribution of iron inside the cell prevents deficiency as well as toxicity that comes with iron excess. So organisms developed mechanisms to absorb precise quantity of iron to meet their metabolic requirements. To study prevailing mechanisms at the molecular level, *Schizosaccharomyces pombe* provides us with an excellent model for understanding how eukaryotic cells regulate the acquisition of iron.

2. Yeasts as model system to study molecular and cell biology

For many years, the budding yeast *Saccharomyces cerevisiae,* commonly known as baker's yeast, has been used for baking, brewing and winemaking. Therefore, its extensive commercial applications have been observed in the food and beverage industries. For several years, the use of the budding yeast *S. cerevisiae* in biological research has greatly advanced our knowledge of several biological and cellular mechanisms. Several advantageous traits like its non-pathogenic nature, simple growth conditions, rapid proliferation, low cost

associated with its use, and conservation of several biochemical and physiological processes in higher eukaryotes make it a widely studied model organism in biochemistry, molecular and cell biology. Moreover, this is the first eukaryotic organism whose complete genome sequence has been elucidated (GOFFEAU *et al.* 1996).

In the case of *Schizosaccharomyces pombe*, it has been first isolated in 1893 from an African beer by Paul Lindner. S. pombe holds some advantages of having more genetic similarities with complex organisms. It is a single celled, rod-shaped fungus which reproduces by binary fission (that's why it is often called as 'fission yeast'), a mechanism similar to mammalian cells (CHANG and NURSE 1996). Its complete genome sequence was performed jointly by the Sanger Institute and Cold Spring Harbor Laboratory in 2002 (WOOD *et al.* 2002). By many features *S. pombe* is closer to higher eukaryotes than *S. cerevisiae.* For example *S. cerevisiae* proliferates by budding and lacks RNA-dependent RNA interference machinery, which is conserved in *S. pombe* as well as in mammals. As a laboratory model, *S. pombe* has proven its excellency in the field of cellular biology in terms of harmless nature, ease of handling, well defined internal organelles, rapid division cycle, and its constitutive haploid genetic nature (also workable in diploid state by conjugation during nutritional deficiency). Use of fission yeast has allowed many research studies to be carried out, which improved our understanding of many cellular mechanisms. Some of those are well conserved in higher eukaryotes including mammals. For example, DNA damage and repair mechanisms (ALAO and SUNNERHAGEN 2008; LIN *et al.* 2012; QU *et al.* 2012, 2013), cell death, aging and apoptosis (LOW and YANG 2008; OHTSUKA *et al.* 2013; LIN and AUSTRIACO 2013), gene silencing mechanisms (REYES-TURCU and GREWAL 2012; SMIALOWSKA *et al.* 2014), chromatin remodeling and histone dynamics (KHOROSJUTINA *et al.* 2010) and metal ion

homeostasis and transport mechanisms (LABBÉ *et al.* 2007, 2013; LABBÉ 2010; BEAUDOIN *et al.* 2013) were thoroughly studied using the fission yeast model.

In this study we have used the fission yeast to understand the regulatory mechanism of iron economy during iron deficiency. The details of these mechanisms will be described in the following sections.

3. Iron homeostasis in budding yeast *S. cerevisiae*

The budding yeast *S. cerevisiae* is a well-studied eukaryote used to understand the molecular mechanisms of iron homeostasis. Studies at the cellular level in this yeast model organism have been performed successfully, providing with important information about iron physiology and eukaryotic diseases related to iron deficiency. This is possible because many of those genes and pathways are conserved in mammals (ASKWITH and KAPLAN 1998; DE FREITAS *et al.* 2003). Furthermore, several components of iron acquisition systems operating in budding yeast are well conserved throughout many other yeasts and pathogenic fungi (RAMANAN and WANG 2000; JUNG *et al.* 2008). The following sections will focus on modes of iron acquisition, and mechanisms of regulation of iron homeostasis in budding yeast.

3.1. Mechanisms of iron acquisition in *S. cerevisiae*

S. cerevisiae possesses two well-characterized iron acquisition systems. The high affinity system is privileged under limited iron conditions (K_M < 1μM). The high affinity iron uptake system deploys two different mechanisms, one is reductase independent and the other is reductase dependent. In contrast, a low affinity system becomes active under high iron conditions (K_M > 40μM) (KOSMAN 2003). The integration of both iron acquisition systems and their roles in iron homeostasis of *S. cerevisiae* will be addressed in the following sections.

3.1.1. High-affinity iron uptake: reductase-independent

The mechanism of reductase independent iron uptake relies mainly on capturing small Fe-siderophore complexes. Siderophores are small organic molecules synthesized and secreted by many microorganisms, including Gram negative and positive bacteria, as well as several fungal species (BYERS and ARCENEAUX 1998). Siderophores are non-proteinaceous compounds of relatively low molecular weight (M_r <1500), having the characteristic of chelating ferric ion with an extraordinary high affinity. This allows them to scavenge iron from the environment where it is often present in an insoluble form (NEILANDS 1993, 1995). Unlike the majority of microorganisms, the budding yeast *S. cerevisiae* is unable to synthesize siderophores, but can assimilate those produced by other organisms (NEILANDS 1995; LESUISSE *et al.* 1998). Nevertheless, the siderophore-mediated iron uptake in *S. cerevisiae* occurs through the function of a group of siderophore-iron-transporters (SIT) that comprise the ARN/SIT subfamily of the major facilitator superfamily of transporters. In *S. cerevisiae*, there are four members of these transporters that have been designated: Sit1/Arn3,

Arn1, Taf1/Arn2, and Enb1/Arn4. These are responsible for transporting siderophore-iron chelates under iron depletion conditions (PHILPOTT 2006).

Specificity of these transporters (Table 1) for fungal or bacterial siderophores varies from specific to broad spectrum (HEYMANN *et al.* 2000; YUN *et al.* 2000; LESUISSE *et al.* 2001). Two of those siderophore transporters, Arn1 and Arn3/Sit1, are regulated post-translationally. When substrates are unavailable, both Arn1 (ferrichrome transporter) and Sit1 (ferrioxamine B transporter) are sorted in endosome-like intracellular vesicles resulting in their degradation in the vacuolar lumen. The presence of siderophore substrates, even in very low concentration, causes Arn1 and Sit3 to relocalize to the plasma membrane (KIM *et al.* 2002, 2005; FROISSARD *et al.* 2007). Curiously, Sit1 exhibits similar endosome-to-plasma membrane tafficking even in the presence of a non-specific substrate such as coprogen (FROISSARD *et al.* 2007). In contrast, the enterobactin transporter Enb1/Arn4 is consititutively localized to the plasma membrane even in the absence of its specific substrate. Thus, different intracellular trafficking responses are found with different siderophore transporters upon the iron status and substrates (FROISSARD *et al.* 2007). It has been demonstrated that intact ferrichrome-iron chelate (transported by Arn1) can be accumulated in the cytosol of *S. cerevisiae* where the iron can be recovered upon siderophore degradation. This indicates a direct role of siderophores in iron storage (MOORE *et al.* 2003).

Table 1. Siderophore substrates of ARN/SIT family of transporters

Transporter	Siderophore substrates	K_m for transport (μM)
Arn1	Ferrichromes[a] Coprogen (Triacetylfusarinine C)[b]	0.9
Arn2/Taf1	Triacetylfusarinine C	1.6
Arn3/Sit1	Ferrioxamine B Ferrichromes[a] Coprogen (Triacetylfusarinine C)[b]	0.5 2.3
Arn4/Enb1	Enterobactin	1.9

[a] Arn1 and Arn3 exhibit specificity for multiple members of the ferrichrome family of siderophores.

[b] Arn1 and Arn3 exhibit a trace amount of transport activity for triacetylfusarinine C

3.1.2 High-affinity iron uptake: reductase-dependent

S. cerevisiae uses a second mechanism for high-affinity Fe acquisition that relies on cell surface metalloreductase activity. Two metalloreductases encoded by the gene *FRE1* and *FRE2* play a major role in the exogenous iron uptake of budding yeast. These two flavocytochromes constitute the majority (>98%) of plasma membrane-associated ferric reductase activity (DANCIS *et al.* 1990, 1992; GEORGATSOU and ALEXANDRAKI 1994; GEORGATSOU *et al.* 1997). The expression of both *FRE1* and *FRE2* genes is induced under iron-depleted conditions, and double deletion of both genes shows a drastic decrease in ferrireductase activity (only 2-10%) compared to wild type cells (DANCIS *et al.* 1992; GEORGATSOU and ALEXANDRAKI 1994). Due to their broader substrate specificity, Fre1 and

Fre2 are enabled to catalyze the reduction of ferric-siderophore complexes resulting in the release of divalent iron (Fe^{2+}). Subsequently, the ferrous iron can be transported across the plasma membrane by ferrous specific transporters (Figure 2) (YUN *et al.* 2001). Transcription of the family members, *FRE1, 2, 3, 4, 5,* and *6*, is induced under iron-depleted conditions, whereas transcription of *FRE1* and *FRE7* is also found to be induced under copper limited conditions (YUN *et al.* 2001). Fre3 and Fre4 possess a weaker catalytic activity in the reduction of some ferric-siderophore complexes (YUN *et al.* 2001). Although, the function of Fre5 is still unclear, the protein exhibits a mitochondrial localization. In the case of Fre6, the protein localizes in the vacuole (SICKMANN *et al.* 2003; REES and THIELE 2007; SINGH *et al.* 2007). The *FRE* reductases mediate reduction of oxidized forms of iron and copper, as well as other non-metallic compounds which are capable of accepting one-electron (LESUISSE *et al.* 1987).

Under conditions of iron starvation, the high-affinity transport complex is activated in *S. cerevisiae* to assimilate soluble iron (Fe^{2+}) into the cell following the external reduction of Fe^{3+}. The high-affinity transport system is activated with a Km of ~0.15μM (DE SILVA *et al.* 1996) and its action is performed by the combined action of two proteins: a copper-dependent ferrous oxidase, Fet3 (ASKWITH *et al.* 1994) and an iron permease, Ftr1 (STEARMAN *et al.* 1996). In *S. cerevisiae*, *FET3* was first discovered through a genetic screen for mutants exhibiting a defect in high-affinity iron transport (ASKWITH *et al.* 1994). Moreover, defective utilization of non-fermentable carbon sources, malfunctioning respiratory systems, as well as growth retardation under iron and copper depleted conditions, were observed in *fet3Δ* mutant strains (DANCIS *et al.* 1994; ASKWITH and KAPLAN 1998). Sequence analysis suggests that Fet3 is a multi-copper oxidase which oxidizes ferrous iron to ferric iron before allowing its

transport across the plasma membrane. This mechanism of action is strictly copper dependent and requires molecular oxygen. For the function of Fet3, four copper ions are required as cofactors. They are loaded onto the protein during its maturation in the secretory pathway. Thus, an intrinsic connection has been observed between iron and copper uptake in *S. cerevisiae,* where copper depletion can lead to a secondary defect, which is iron starvation (DANCIS *et al.* 1994; YUAN *et al.* 1995, 1997; HASSETT *et al.* 1998b).

The expression of Fet3 alone is not enough to induce high-affinity iron transport. This suggests the involvement of other proteins required for the transmembrane iron transport (DE SILVA *et al.* 1996). This question was resolved when a permease encoded by the *FTR1* gene had been found to be involved in the high-affinity iron transport system along with Fet3 (STEARMAN *et al.* 1996). The expression of either one of these proteins in a mutant strain null for both genes (*fet3Δftr1Δ*) results in the retention of the "orphan" protein in the endoplasmic reticulum (ER) (STEARMAN *et al.* 1996). Thus, it is important that both proteins assemble together and mature through the secretory pathway to form a stable complex prior trafficking to the plasma membrane. The association between Fet3 and Ftr1 has also been demonstrated by FRET (fluorescence resonance energy transfer) and yeast two-hybrid analysis experiments (SINGH *et al.* 2006). Accordingly, in the high-affinity iron transport system, Fet3 catalyzes the ferroxidase reaction to convert ferrous iron into ferric iron which is transported across the plasma membrane by Ftr1 (Figure 2) (KWOK *et al.* 2006). Interestingly, a paralogous oxidase/permease complex has been found to be expressed on vacuolar membranes, encoded by *FET5* and *FTH1*, which are homologs of *FET3* and *FTR1*, respectively. The Fet5/Fth1 complex directs the transport of iron from the vacuole to the

cytosol which will be discussed in the following section (3.1.4) (URBANOWSKI and PIPER 1999).

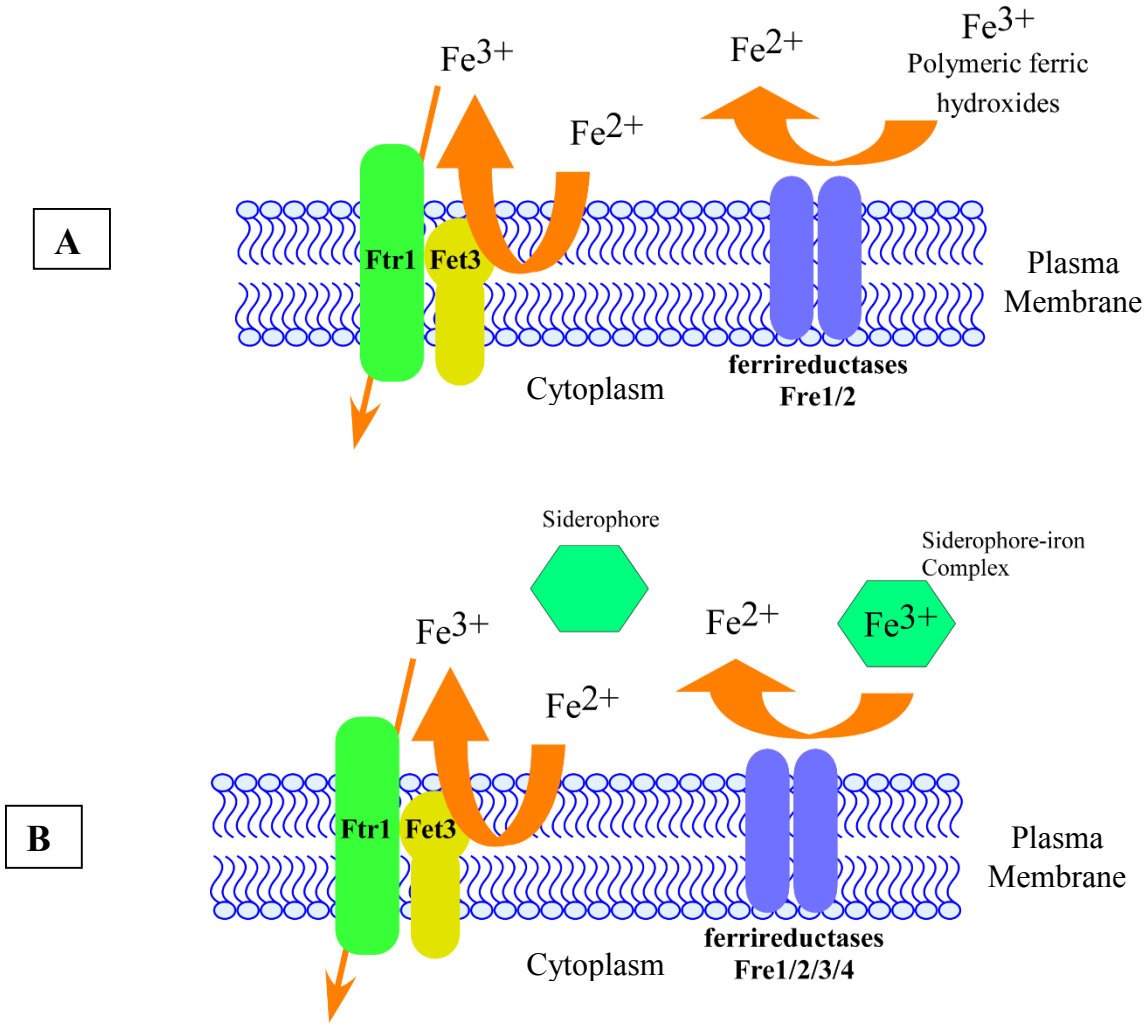

Figure 2. Reductase-dependent iron acquisition in *S. cerevisiae*. A) Uptake of inorganic Fe requires the initial reduction of Fe^{3+} to Fe^{2+} by the plasma membrane reductases Fre1/2. Subsequently, Fe^{2+} is oxidized by Fet3 before its passage across the plasma membrane via Ftr1. **B)** Fe^{3+} sequestered in siderophore chelates is reduced by the action of Fre1/2/3/4 ferrireductases. Subsequently, free reduced Fe^{2+} is re-oxidized to Fe^{3+} by the multi-copper oxidase Fet3 and then transported across the plasma membrane by the membrane permease Ftr1.

3.1.3 Low-affinity iron uptake

It is interesting that *S. cerevisiae* mutant strains defective for high-affinity iron transport are still able to grow on an iron supplemented media. A low-affinity iron transport system is activated when cells are exposed to an iron-rich environment and is functionally independent of the high-affinity iron transport systems. The low-affinity iron system prefers Fe^{2+} over Fe^{3+} and continues to work properly in the absence of oxygen. In the case of the high-affinity iron transport, the presence of oxygen is required since Fet3 is an oxygen- and Cu-dependent protein (DIX *et al.* 1994, 1997).

Fet4 is a low-affinity transporter and its function is not only limited to iron transport but is also able to transport a wide range of other divalent metals such as copper, cobalt, manganese, and zinc (DIX *et al.* 1994; LI and KAPLAN 1998). Fet4 shows relatively low-affinity to iron (Km = 30μM) as compared to an affinity of 0.15μM found in the high-affinity iron system. That is why the Fet4 function is inactive when iron concentrations are in the lower Km (<1 μM) range. Under conditions of excess iron, the expression of Fet4 is increased and low-affinity transport system plays a primary role in iron uptake, especially under anaerobic conditions (HASSETT *et al.* 1998a; JENSEN and CULOTTA 2002).

Budding yeast also expresses three proteins, Smf1, Smf2 and Smf3 that are encoded by the *SMF1*, *2* and *3* genes, respectively. These proteins also play a role in low-affinity iron transport. They are similar to members of the Nramp (natural-resistance-associated macrophage protein) family, which are involved in the iron transport in mammals (CHEN *et al.* 1999; PORTNOY *et al.* 2000; FORBES and GROS 2001). Although Smf1 and Smf2 primarily function as manganese ion transporters, they can also efficiently transport ferrous iron across the plasma membrane under iron-replete conditions. Overexpression of Smf1 results in the

accumulation of cytosolic iron (COHEN *et al.* 2000). Smf3, a paralogue of Smf1 and Smf2, is induced under oxygen depletion and is the only member of the Nramp family found in yeast that is regulated by the cellular iron status. Smf3 localizes on the vacuolar membrane (discussed in the following section 3.1.4) and is required as a means to mobilize stored iron from the vacuole to cytosol (PORTNOY *et al.* 2000).

3.1.4 Storage of iron in the vacuoles

Storage of iron in vacuoles is an important homeostatic mechanism found in *S. cerevisiae* that allows cells to maintain an adequate amount of intracellular iron. It is also known that these vacuolar reserves of iron contribute to the survival of cells when iron is scarce (PHILPOTT and PROTCHENKO 2008).

Ccc1 is the only identified vacuolar iron importer in budding yeast. The expression of *CCC1* is induced in response to high levels of iron (LAPINSKAS *et al.* 1996; LI *et al.* 2001). The transcription factor Yap5 induces expression of *CCC1* under conditions of excess iron (LI *et al.* 2008). Cells lacking *CCC1* exhibit hypersensitivity to detrimental effects of high iron and are unable to grow on iron-rich media (LI *et al.* 2001). The molecular form of iron stores in the vacuole is still poorly understood. However, it is has been shown that iron can form complexes with polyphosphates in this compartment (PHILPOTT and PROTCHENKO 2008).

In contrast, under iron-depleted conditions, the transcription of *CCC1* is shut down, thereby preventing vacuolar iron accumulation. The iron-responsive transcription factors Aft1 and Aft2 induce transcription of several genes that encode proteins involved in iron acquisition

and iron utilization. Some of these genes encode proteins that mobilize stored iron out of the vacuole (PHILPOTT and PROTCHENKO 2008). Among those proteins, Fre6 localizes on the

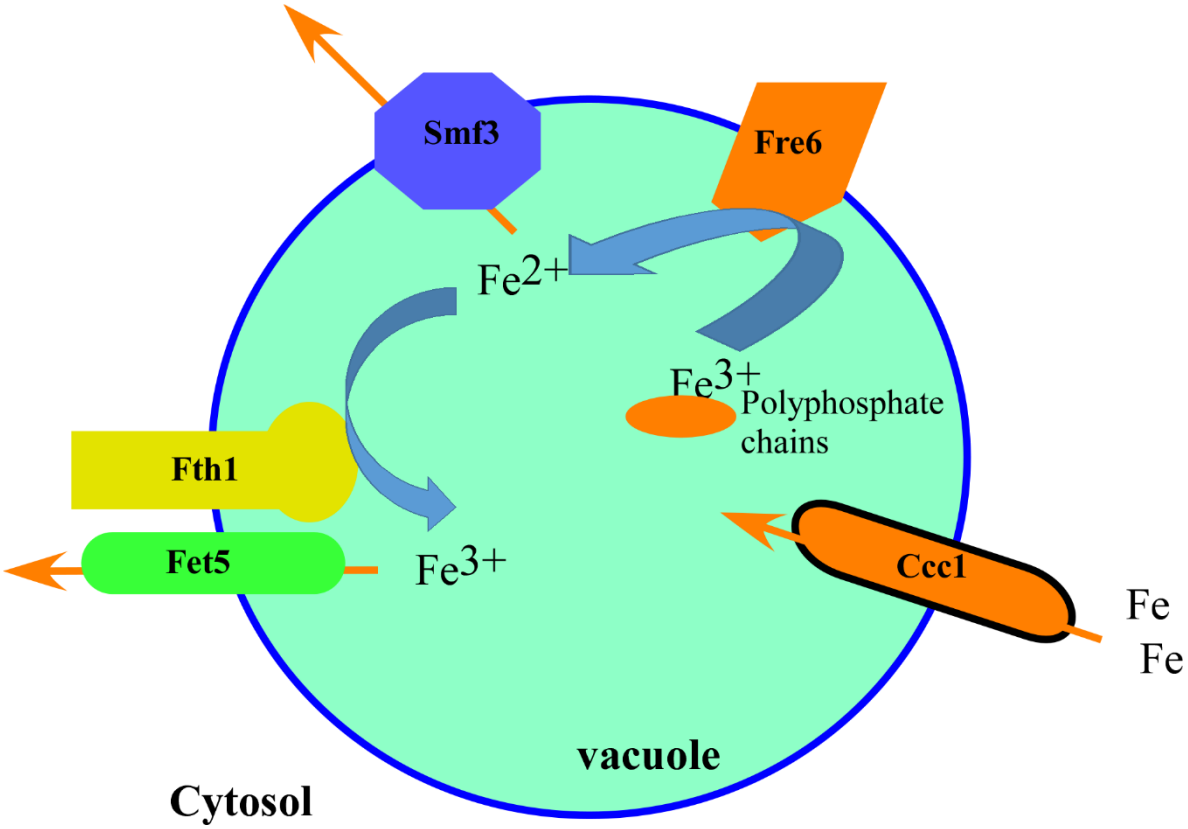

Figure 3. Vacuolar iron storage and mobilization. Excess Fe is transported into the vacuole through the Ccc1 transporter for safe storage. Vacuolar Fe can be mobilized out of the vacuole after its reduction that is carried out by Fre6. Iron transport is then mediated by Smf3 or Fet5/Fth1.

vacuolar membrane and is involved in the vacuolar iron reduction prior to its transport into the cytosol (Figure 3) (REES and THIELE 2007; SINGH *et al.* 2007). As mentioned in the previous section, the Fet5 and Fth1 are paralogues of Fet3 and Ftr1, respectively. They are

found on the vacuolar membrane under low iron conditions. Under those conditions, Fet5 and Fth1 mobilize stored iron from the vacuole to replenish the cytosol according to iron need (Figure 3) (URBANOWSKI and PIPER 1999; SINGH *et al.* 2007). Another mechanism by which the reduced iron can be exported out of the vacuole requires the action of Smf3 (Figure 3). Expression of *SMF3* is induced under iron-depleted and hypoxic growth conditions (PORTNOY *et al.* 2000). Cells lacking Smf3 accumulate iron in the vacuole, whereas overexpression of Smf3 results in the diminished retention of iron in the vacuole as compared to the wild-type cells (SINGH *et al.* 2007).

3.2. Regulation of iron homeostasis in budding yeast

3.2.1. Regulation of iron transport by Aft1 and Aft2

Iron homeostasis is sternly regulated in budding yeast so that necessary iron can carry out all the cellular processes such as respiration, while retaining the levels of free iron below toxic levels. In the iron homeostasis of *S. cerevisiae,* Aft1 and Aft2 are the major players that regulate the expression of genes encoding proteins involved in iron transport and utilization depending on the cellular iron status (YAMAGUCHI-IWAI *et al.* 1995; RUTHERFORD *et al.* 2003). Under iron limiting conditions, Aft1 localizes within the nucleus and activates transcription of target genes. In contrast, under high iron conditions, Aft1 is rapidly exported into the cytoplasm by the nuclear export receptor Msn5, resulting in the repression of target genes (UETA *et al.* 2007). *aft1Δ* mutant cells exhibit severe iron deficiency phenotype in comparison to *aft2Δ* mutant cells, signifying that Aft1 plays the major role in iron homeostasis over Aft2. Although *aft1Δ aft2Δ* double mutant cells are more vulnerable during iron scarcity than single *aft1Δ,* when *AFT2* was overexpressed in *aft1Δ* cells, it could rescue

from iron-dependent defects. This is due to increased expression of *FET3* and *FTR1* via Aft2, suggesting that Aft2 is able to compensate for the loss of Aft1. Thus, both Aft1 and Aft2 have partially overlapping roles in iron regulation, with Aft1 possessing the major regulatory function (BLAISEAU *et al.* 2001; RUTHERFORD *et al.* 2001, 2003).

Both transcription factors, Aft1 and Aft2, activate a group of genes during iron deficiency whose products are involved in the reductase-dependent iron transport, siderophore transport, and others that are involved in the modulation of cellular metabolism (RUTHERFORD *et al.* 2003; SHAKOURY-ELIZEH *et al.* 2004; COUREL *et al.* 2005) (Table 2). Although Aft1 and Aft2 recognize the same consensus sequence (GCACCC) at the promoter of target genes, Aft1 shows stronger binding affinity to TGCACCC element, whereas Aft2 prefers to bind with G/CGCACC element (COUREL *et al.* 2005).

Table 2. Examples of genes that are up-regulated by Aft1/ Aft2 during iron deficiency.

Gene	Function
Iron uptake	
FRE1 and *FRE2*	Major plasma membrane metalloreductases
FRE3 and *FRE4*	Plasma membrane metalloreductases involved in the reduction of siderophore bound Fe^{3+}
FET3	Plasma membrane multicopper oxidase
FTR1	Plasma membrane Fe^{2+} permease
FET4	Plasma membrane low affinity Fe^{2+} transporter
FIT1, FIT2 and *FIT3*	Cell wall proteins that are involved in siderophore capture
ARN1, ARN2, ARN3, and *ARN4*	Plasma membrane siderophore transporters
Vacuolar iron mobilization	
FRE6	Vacuolar metalloreductase
FET5	Vacuolar multicopper oxidase
SMF5	Low affinity vacuolar iron tansporter
FTH1	Vacuolar Fe^{2+} permease
Metabolic adaptation	
VTH1	Biotin transporter
HMX1	Heme oxygenase homologue
CTH1	mRNA regulatory protein
CTH2	mRNA regulatory protein

3.2.2. Regulation of iron storage by Yap5

Recently another iron-responsive transcription factor, Yap5, has been identified that is responsible for up-regulating a gene, which encodes the vacuolar iron transporter Ccc1 (LI *et al.* 2008). Ccc1 is required for iron import into vacuole in yeast and plants, although no mammalian homologue of Ccc1 has yet been identified (LI *et al.* 2001). In *Candida albicans,* Ccc1 is involved in multiple functions, including maintenance of cell-wall integrity, filamentous growth and virulence, mitochondrial function and drug resistance (XU *et al.* 2013). In budding yeast, Yap5 is constitutively expressed and accumulated into the nucleus where it interacts with the TTCACGA sequence of the *CCC1* promoter. The association of Yap5 with the *CCC1* promoter is not iron-dependent. However, in response to high levels of iron Yap5 transcriptionally activates *CCC1* gene expression. Two conserved cysteine-rich domains (CRDs) of Yap5 are predicted to play a critical role in iron-dependent transcriptional activation. The N-terminal CRD (composed of four cysteine) is separated by a 37 amino acids linker from C-terminal CRD (composed of three cysteine). Mutation of all the seven cysteine residues results in the loss of transcriptional induction ability of Yap5 even in the presence of iron. This occurs without affecting the nuclear localization of Yap5. Cells expressing this mutant allele are found to be more vulnerable to iron-toxicity. It has been proposed that excess iron might affect the thiol groups of cysteine residues within CRDs, which would trigger conformational changes of Yap5, conferring the protein with an ability to trans-activate gene expression (LI *et al.* 2008). Interestingly, the expression of *CCC1* is not exclusively regulated by Yap5. Under low-iron conditions, *CCC1* mRNA is degraded by Cth1 and Cth2, thus limiting iron storage through this vacuolar iron transporter. The role of Cth1 and Cth2 in iron homeostasis will be discussed in the next section.

3.3. Post-transcriptional regulation of iron homeostasis by Cth1 and Cth2

During iron deficiency, budding yeast also employs a post-transcriptional mechanism to tightly regulate several components involved in iron homeostasis. Two proteins, Cth1 and Cth2, are involved in this mechanism. Their expression is regulated under the control of Aft1 and Aft2 (Figure 4) (PUIG *et al.* 2005, 2008).

Cth1 and Cth2 belong to the family of human tristetraprolin (HTTP). They are characterized by the presence of two CCCH-type tandem zinc fingers (TZFs) in their carboxy-terminal regions. Cth1 and Cth2 possess a mRNA binding domain that binds to the AU-rich elements (AREs) within the 3'unstranslated region (3'-UTR) of their target mRNAs (THOMPSON *et al.* 1996; BLACKSHEAR 2001). The association of these proteins with AREs promotes destabilization and rapid degradation of transcripts through the recruitment of an RNA decaying enzyme (e.g. Dhh1 helicase) (LYKKE-ANDERSEN and WAGNER 2005; PEDRO-SEGURA *et al.* 2008). Under iron-limiting conditions, Cth2 appears to down-regulate 94 transcripts harboring AREs within their 3'UTR; half of those encode proteins that are involved in iron-dependent metabolic pathways. In the case of Cth1, it is responsible for down-regulation of 20 ARE-containing transcripts; most of them encode mitochondrial proteins that are involved in respiration (PUIG *et al.* 2008; PHILPOTT *et al.* 2012).

The mechanism by which Cth1/Cth2 recognize their target mRNAs is still unknown. A recent study has demonstrated that the nucleo-cytoplasmic shuttling of Cth2 is important for its role in ARE-dependent mRNA decay. A nuclear localization signal located within its TZF domain promotes its binding with target mRNAs. Interestingly, nuclear export of Cth2 is not dependent on a classical nuclear export signal (NES). Instead, nuclear export of Cth2 relies on the nuclear mRNA export machinery (VERGARA *et al.* 2011).

The action of Cth2 is indispensable for iron economy in *S. cerevisiae*. In contrast, *CTH1* can be inactivated without compromising the iron sparing response in *S. cerevisiae* (PUIG *et al.* 2005, 2008). Interestingly, when *CTH1* is expressed under control of a *CTH2* promoter, it could replace Cth2 in a double mutant cth1Δcth2Δ strain (PUIG *et al.* 2008). This suggests a redundant function for both proteins, Cth1 and Cth2.

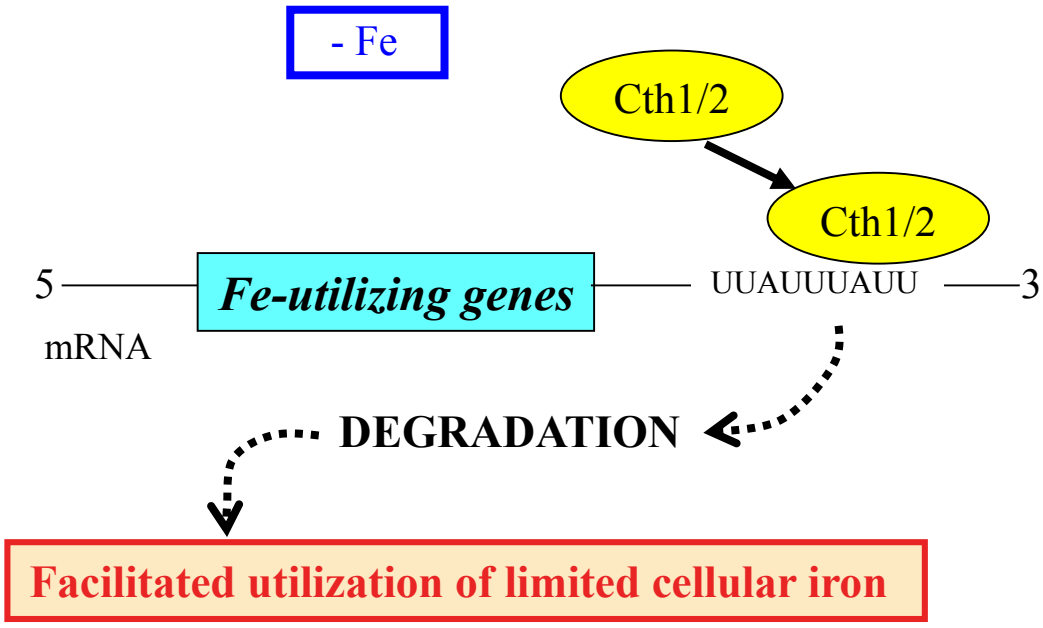

Figure 4. Cth1 and Cth2 control post-transcriptional regulation of iron-using gene transcripts under iron deficiency. Under conditions of iron-starvation (-Fe), Cth1 and Cth2 bind to specific AU-rich elements in the 3′ untranslated region of mRNAs, leading to their degradation.

4. Iron homeostasis in *S. pombe*

4.1. Extracellular iron scavenging systems: high-affinity iron uptake

4.1.1. Reductive iron acquisition system

Iron bioavailability is restricted in natural environment due to the fact that iron is oxidized into insoluble compounds such as ferric oxides. The fission yeast possesses a reductive iron scavenging system for high-affinity iron uptake. One of the components of its reductive iron acquisition system is the ferricreductase Frp1.

The function of Frp1 was first described in 1993 when it was discovered that this protein is responsible for plasma membrane reductase activity in fission yeast (ROMAN *et al.* 1993). Frp1 reduces ferric iron to its ferrous state. *frp1Δ* mutant cells show impaired ferric iron uptake, whereas ferrous iron uptake remains unaffected. Frp1 shows sequence homology with gp91-phox, a membrane component of an oxidoreductase complex that is present in human granulocytes. Furthermore, Frp1 exhibits a strong similarity with Fre1 in budding yeast (DANCIS *et al.* 1992; ROMAN *et al.* 1993; FINEGOLD *et al.* 1996). Frp1 orthologs in other fungal pathogenic species are important virulence factors (JONKERS *et al.* 2011).

The high-affinity iron transport system requires two other components, Fio1 and Fip1. Fio1 is a plasma membrane multicopper oxidase, which re-oxidizes the reduced iron by Frp1 into ferric ion (ASKWITH and KAPLAN 1997). Ferric iron is then transported across the plasma membrane by Fip1, an iron permease. *S. pombe* Fio1 and Fip1 proteins show sequence homology and share similar functions with their counterparts in *S. cerevisiae*, Fet3 and Ftr1, respectively. When both *S. pombe fio1*$^{+}$ and *fip1*$^{+}$ genes are expressed in a *S. cerevisiae fet3Δ* mutant strain, restoration of iron transport is observed. This demonstrates that both oxidase and permease activities are required for reconstitution of high-affinity iron transport in yeasts (ASKWITH and KAPLAN 1997). Interestingly, both *fio1*$^{+}$ and *fip1*$^{+}$ genes are under the control

of a common promoter in the *S. pombe* genome. Furthermore, their expression is transcriptionally regulated by the cellular iron status (ASKWITH and KAPLAN 1997).

4.1.2. Non-reductive iron acquisition system

In order to warrant a delicate supply of iron, *S. pombe* acquires iron through siderophores. Siderophores are low molecular weight chemical compounds with strong iron (ferric) chelating ability (NEILANDS 1993). Several organisms including bacteria, fungi and some plants synthesize and utilize siderophores to counteract the problem of iron bioavailability in the environment. With the exception of a novel polycarboxylate type siderophore (Rhizopherine) synthesized by zygomycetes (THIEKEN and WINKELMANN 1992), the majority of fungal species produce a particular type of siderophore that belongs to the class of hydroxamates (VAN DER HELM and WINKELMANN 1994). Fungal hydroxamates are derivatives of ornithine, an amino acid not coded by DNA (non-proteinogenic). They are divided into four structural families: (I) rhodotorulic acid, (II) fusarinines, (III) coprogens, and (IV) ferrichromes (HAAS *et al.* 2008).

Although most of the fungi produce more than one siderophores for iron acquisition and storage (HAAS *et al.* 2008), ferrichrome is the only one that is produced by *S. pombe* (SCHRETTL *et al.* 2004). Unlike *S. cerevisiae,* which is unable to produce siderophores, *S. pombe* possesses all the machinery that is required for their biosynthesis (SCHRETTL *et al.* 2004). The first enzyme of the ferrichrome synthesis pathway is the L-Ornithine N^5-oxygenase, Sib2, which catalyzes N-hydroxylation of the precursor L-orthinine to form N^5-hydroxy-L-ornithine. Sib2 protein exhibits sequence homology with *A. nidulans* SidA (EISENDLE *et al.* 2003) and was predicted to share common features of amino acid

hydroxylases, including (i) a flavine adenine dinucleotide (FAD)-binding domain, (ii) a nicotinamide adenine dinucleotide phosphate (NADP)-binding domain, and (iii) a domain anticipated to be involved in substrate binding (SCHRETTL *et al.* 2004). The next step is N^5-acylation of N^5-hydroxyornithine, which is accomplished with the attachment of an acyl group from acyl-CoA derivatives by N5-transacylases, a gene product of *SPBC17G9.06c* in the fission yeast. From here the pathway is divided depending on the choice of acyl group that produces hydroxamate siderophores (HAAS *et al.* 2008). In the final step of ferrichrome biosynthesis, the hydroxamates are covalently linked to peptides by a non-ribosomal peptide synthetase (NRPS) termed Sib1. Sib1 adds amino acid glycine to hydroxamate groups and produces ferrichrome (Figure 5) (SCHWECKE *et al.* 2006).

S. pombe mutant *sib1Δsib2Δ* strains show severe growth impairment during iron deficiency. Cellular growth can be restored by adding exogenous ferrichrome ((MERCIER and LABBÉ 2010). Therefore, ferrichrome synthesis is an important property of fission yeast in terms of extracellular iron acquisition. Ferrichrome also serves as an iron storage molecule during iron replete conditions (SCHRETTL *et al.* 2004).

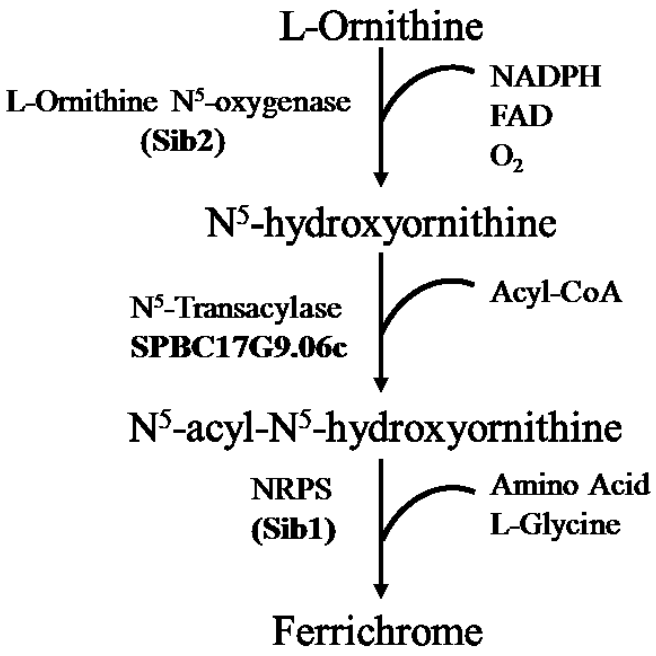

Figure 5. Ferrichrome biosynthesis pathway in the fission yeast *S. pombe*

In addition to the ability to produce and excrete ferrichrome, three siderophore transporters have been identified in *S. pombe.* They are denoted as Str1, Str2 and Str3. Moreover, they differ in their substrate preference (PELLETIER *et al.* 2003). The expression of these siderophore transporters is repressed by iron. In contrast, they are induced under low-iron conditions. The siderophore transporter Str1, a protein of 614 amino acids, contains 14 transmembrane domains. Str1 exhibits significant sequence homology and shares common structural features with four siderophore transporters that have been previously identified in *S. cerevisiae* (PELLETIER *et al.* 2003; LABBÉ *et al.* 2007). When *str1+* gene is ectopically expressed under the control of a heterologous promoter in *S. cerevisiae fet3Δ arn1-4Δ* mutant cells**,** Str1 transports ferrichrome. On the other hand, Str1 fails to transport other types of siderophores (PELLETIER *et al.* 2003). Similar experiments with *S. cerevisiae fet3Δ arn1-4Δ* mutant cells have revealed that Str2 mobilizes ferroxiamine B-iron in a highly efficient

manner, although it is able to transport ferrichrome-iron complexes in a lower magnitude (PELLETIER *et al.* 2003). In the case of Str3, its substrate specificity has not yet been defined (PELLETIER *et al.* 2003).

4.2. Intracellular iron storage system

Yeast vacuoles serve as an important storage depot for essential transitional metals such as zinc, copper and iron (RAMSAY 1997; SZCZYPKA *et al.* 1997). This is not only to supply these metal ions during deficiency, but also to prevent cells from the toxic effect of excess cytosolic metal ions (RAMSAY 1997; REES *et al.* 2004; SIMM *et al.* 2007; SINGH *et al.* 2007). In *S. pombe,* the vacuole iron transporter is Pcl1. It belongs to the DUF125 transmembrane protein family. Pcl1 possesses significant sequence homology, especially within two regions that encompass five transmembrane domains, with other members of the DUF125 family, e.g. Ccc1 from *S. cerevisiae* (MERCIER *et al.* 2006). The *pcl1*$^{+}$ gene transcription is induced in the presence of excess iron. *pcl1Δ* disrupted mutant cells show hypersensitivity to iron as compared to wild type cells. Similar observations have been reported for Ccc1 in the budding yeast (MERCIER *et al.* 2006). Consistent with the role of Pcl1 as an iron storage transporter in the vacuole, it has been observed that *pcl1Δ* mutant cells can store less iron than the wild-type cells (POULIOT *et al.* 2010).

Due to the absence of functional homologs of *S. cerevisiae* Fth1/ Fet5 proteins, *S. pombe* vacuolar iron export mechanisms seem to function in a novel way (POULIOT *et al.* 2010). In fission yeast, an active export of iron from the vacuole to the cytosol is mediated by the Abc3 protein which shares significant sequence homology with the ABCC subfamily of ATP-

binding cassette transporters (POULIOT *et al.* 2010). Expression of *abc3*$^{+}$ is induced under iron deprivation conditions. It could mobilize vacuolar iron to satisfy cytosolic iron requirements. *abc3Δ* mutant cells also exhibit a significant increase of cell surface Frp1 ferrireductase activity (POULIOT *et al.* 2010). The discovery of Abc3 in *S. pombe* opens the door to perform more detailed studies in other similar ABC-like proteins that are found in filamentous yeasts. Like Abc3 in *S. pombe,* they are regulated by iron and may play a similar role in iron homeostasis.

A summary of iron acquisition systems in fission yeast has been illustrated in Figure 6.

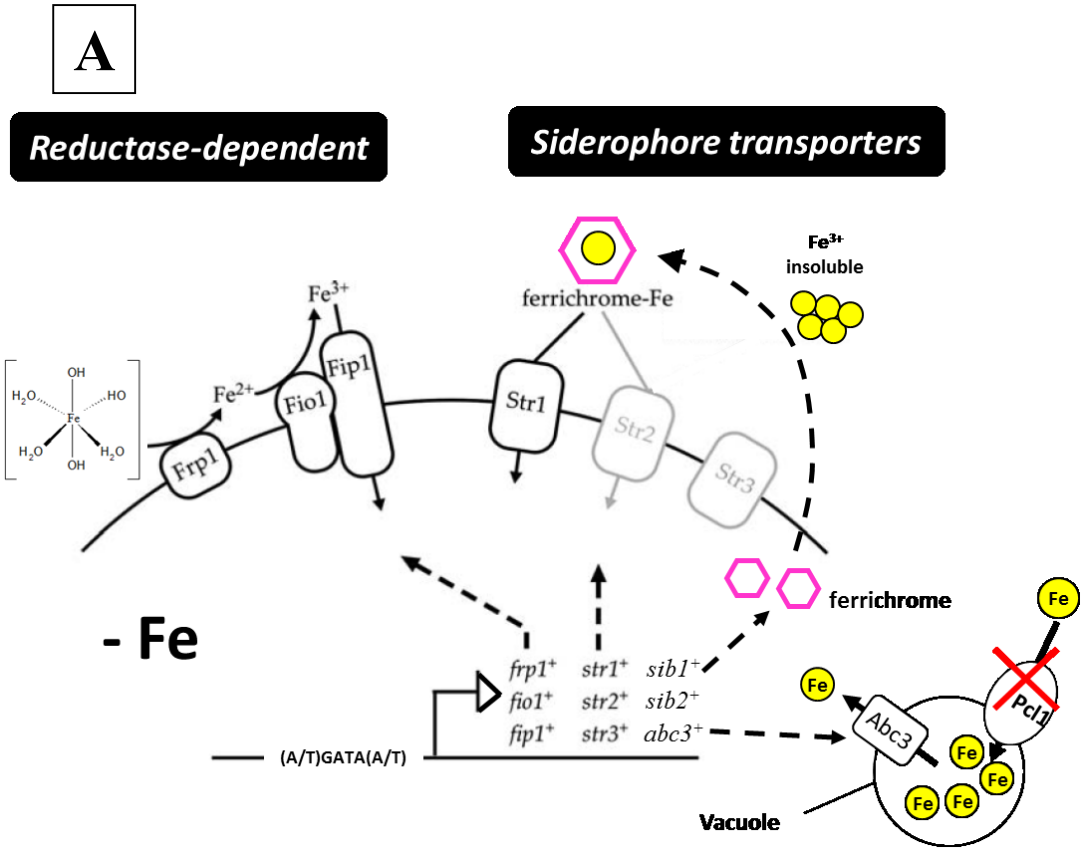

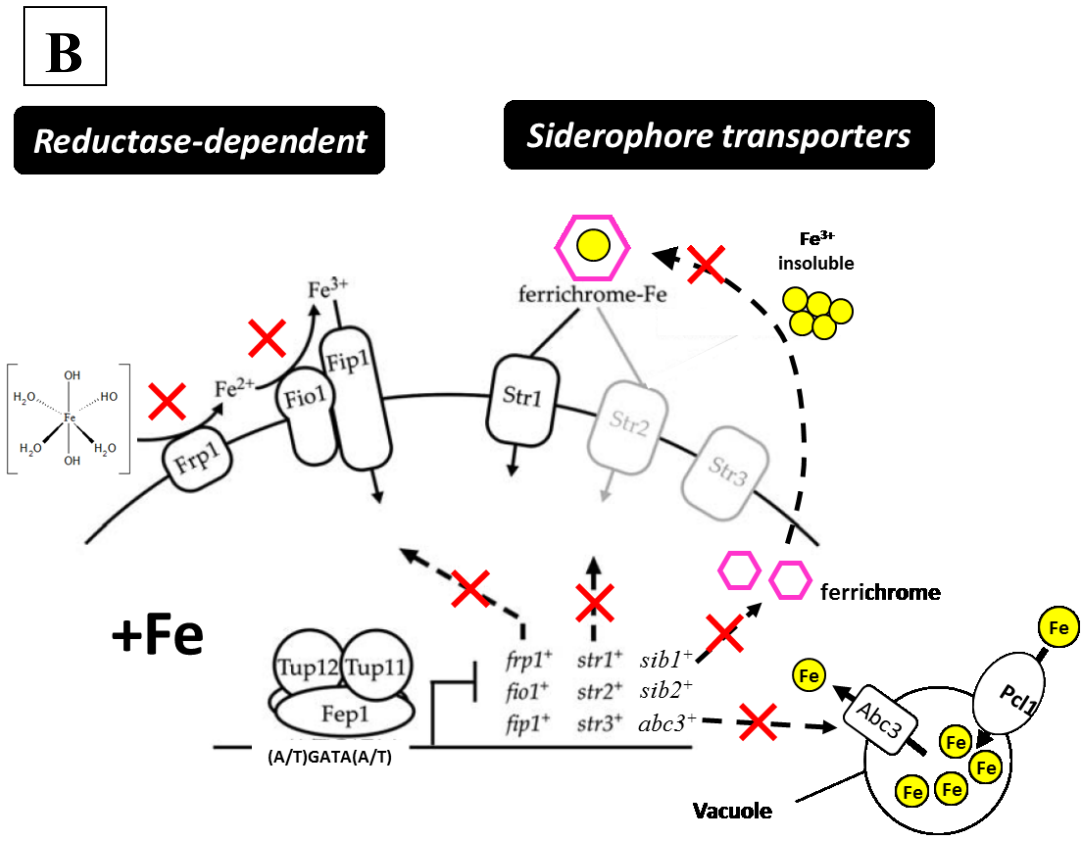

Figure 6. Proposed model for iron transport in *S. pombe*. (A) Upon iron starvation (-Fe), components of the reductive iron acquisition system (Frp1, Fio1 and Fip1) and siderophore-iron transporters (Str1, Str2 and Str3) are activated, leading to acquisition of iron from the extracellular environment. Moreover, the vacuolar iron transporter Abc3 is also activated to supply stored iron from the vacuole to the cytosol. **(B)** Under iron-replete conditions, the GATA-type transcription factor Fep1 along with co-repressors Tup11/12 (discussed in the section 4.3) bind to the DNA to repress all the components of reductive and non-reductive iron transport systems at the level of transcription. In contrast, Pcl1 that encodes for a vacuolar iron transporter is transcriptionally induced under iron-replete conditions. Figure modified from the original (LABBÉ *et al.* 2007; LABBÉ 2010).

4.3. Iron transport regulation: role of Fep1

In *S. pombe,* under iron-replete conditions, genes that encode components of reductive, non-reductive and vacuolar iron transport systems are repressed by the GATA-type transcription factor Fep1 (PELLETIER *et al.* 2002, 2003; POULIOT *et al.* 2010). Although Fep1 constitutively localizes to the nucleus (PELLETIER *et al.* 2005), its binding to the chromatin is strictly iron-dependent and is lost when iron is depleted (JBEL *et al.* 2009). Iron-mediated transcriptional repression by Fep1 is achieved through its recognition of the *cis*-acting element (A/T)GATA(A/T) in the promoter of target genes (PELLETIER *et al.* 2002, 2003). The Fep1-dependent repression appears to be stronger when the *cis*-acting DNA element is ATC(A /T) GATAA (POULIOT *et al.* 2010). The amino-terminal region of Fep1 possesses two Cys2/Cys2-type zinc fingers (ZF1 and ZF2) which are involved in its association with DNA (PELLETIER *et al.* 2005). It has been shown that ZF2 is essential to allow Fep1 to interact with the DNA sequence 5'-(A/T)GATA(A/T)-3'. Moreover, it has been shown that the amino-terminal ZF1 increases the Fep1 DNA binding activity by approximately fivefold (PELLETIER *et al.* 2005). Interestingly, the N-terminal region (1-241 amino acids) of Fep1is highly similar to other members of iron-responsive GATA-type transcriptional repressors found in filamentous fungi such as Urbs1 in *Ustaligo maydis* (AN *et al.* 1997a; b), SRE in *Neurospora crassa* (ZHOU and MARZLUF 1999), SREA in *Aspergillus nidulans* (HAAS *et al.* 1999), SREP in *Penicillium chrysogenum* (HAAS *et al.* 1997), Sre1 in *Histoplasma capsulatum* (PATHOGEN *et al.* 2008) and Sful in *Candida albicans* (LAN *et al.* 2004). A conserved N-terminal 27-amino acid fragment between the two zing fingers, bearing four highly conserved Cys residues, plays a critical role for the iron sensing by Fep1. It also participates in its DNA binding activity (Figure 7) (PELLETIER *et al.* 2005). Mutation of these four conserved cysteine

residues leads to the failure of Fep1 to repress its target genes under iron excess conditions (PELLETIER *et al.* 2005).

The C-terminal region of Fep1 is also critical for iron-dependent transcriptional repression. The 522-536 amino acid region of Fep1 contains a leucine-zipper motif that allows the formation of Fep1-Fep1 homodimers (Figure 7) (PELLETIER *et al.* 2005). Mutation in this region of Fep1 abolishes its ability to form homodimers, leading to reduced transcriptional repression by Fep1 (PELLETIER *et al.* 2005). Moreover, the function of Fep1 as a transcriptional repressor depends on two corepressors, Tup11 and Tup12 (Figure 6) (PELLETIER *et al.* 2002). Deletion of both of these genes results in the abolition of the ability of Fep1 to exert transcriptional repression even under iron-replete conditions (PELLETIER *et al.* 2002; ZNAIDI *et al.* 2004). The C-terminal region of Fep1 (405-541) is critical for its association with Tup11 (Figure 7). Tup11 harbors WD40-repeat sequence motifs, which are required for its interaction with Fep1 (ZNAIDI *et al.* 2004). The Tup12 protein also interacts with Fep1, but its minimal region that is required for physical association with Fep1 has not yet determined (LABBÉ *et al.* 2007, 2013). Interestingly, the ortholog (Tup1) of Tup11/12 that is present in the pathogenic yeast *Candida albicans,* is also involved in iron-mediated transcriptional repression of iron transport genes (KNIGHT *et al.* 2002).

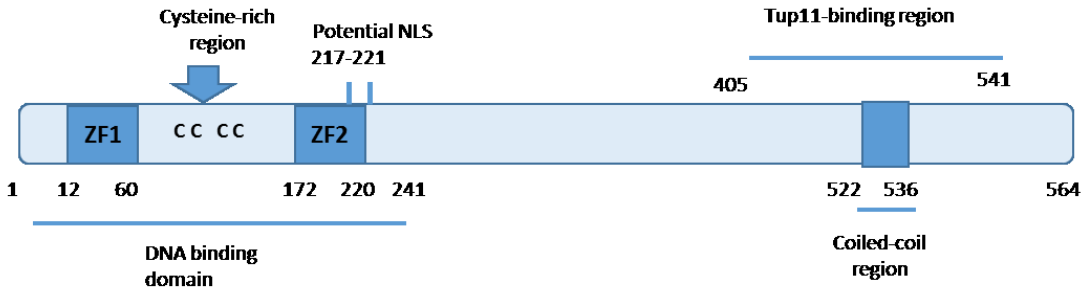

Figure 7. Schematic representation of Fep1. Two zinc finger motifs are designated as ZF1 and ZF2, four conserved cysteine residues are located within the region (68-94) between ZF1 and ZF2, a coiled-coil region (522-536) is required for the formation of Fep1 homodimer. Furthermore, a region encompassing amino acid residues 405-541 is required for the Fep1-Tup11 association.

4.4. The CCAAT binding complex (CBC) and its role in iron homeostasis

The CCAAT motif is present frequently in the eukaryotic promoter regions ranging from yeast to mammals. Statistical analysis reveals that 30% of eukaryotic promoters possess a *cis*-acting sequence CCAAT (BUCHER 1990). CCAAT sequences are bound by a variety of evolutionary conserved transcription factors, often in a heterotrimeric form, designated as the CCAAT-binding complex (CBC). In eukaryotes, CBC can modulate a variety of genes that encode for components involved in specific metabolic pathways (RAYMONDJEAN *et al.* 1988; SANTORO *et al.* 1988; JOHNSON and MCKNIGHT 1989). One of the unique features of CBC is that all three protein subunits are required for the formation of the DNA binding complex; this has been well demonstrated in budding yeast, filamentous fungi and humans (MCNABB *et al.* 1995; BELLORINI *et al.* 1997; STEIDL *et al.* 1999).

CCAAT-binding factors play a crucial role in iron homeostasis in several filamentous fungi and in fission yeast by repressing genes encoding iron-using proteins during iron deprivation, thereby conferring iron economy (LAN *et al.* 2004; MERCIER *et al.* 2006; HORTSCHANSKY *et al.* 2007). The Hap complex was first discovered in the budding yeast *S. cerevisiae* where Hap2, Hap3 and Hap5 form the core CBC to bind DNA and Hap4 is involved in the transcriptional activation of the complex (MCNABB *et al.* 1995); although in budding yeast the CBC complex has no direct implication in iron homeostasis under conditions of iron starvation.

During iron deficiency, *A. nidulans* CBC plays a critical role in the down regulation of genes encoding iron-using proteins. Under low-iron conditions, the HapX protein physically interacts with CBC, resulting in negative regulation of gene expression (HORTSCHANSKY *et al.* 2007). A mutual transcriptional control was also observed between HapX (homolog of Php4) and GATA-type transcription factor SreA in *A. nidulans* (HORTSCHANSKY *et al.* 2007). In a recent study, a similar reciprocal transcriptional regulation was reported in a soil-borne fungal pathogen *Fusarium oxysporum (LOPEZ-BERGES et al. 2012). In F. oxysporum, the CCAAT-binding factor HapX has a similar function as its counterpart (HapX) from A. nidulans*. Furthermore, its function is required for plant infection. Deletion of *hapXΔ* does not affect the iron uptake machinery, but leads to impaired growth under iron-scarce conditions (LOPEZ-BERGES *et al.* 2012). Likewise, the CCAAT-binding homologous protein HapX in *A. fumigatus* mediates transcriptional remodeling when fungal cells face iron starvation; this adaptation is crucial for yeast virulence (SCHRETTL *et al.* 2010). In *Candida albicans,* a HapX homolog is named as Hap43. It is activated under low-iron conditions. Hap43 also acts as an iron-dependent negative regulatory repressor when it is bound to CBC.

Its participation in iron sparing response is required for rendering *C. albicans* virulent and pathogenic (HSU *et al.* 2011).

In *S. pombe*, Php2/3/5 (Hap2/3/5 orthologs) compose the core CBC. Php4 (HapX ortholog) is a subunit of the CBC. It exerts a negative regulatory function on gene expression of iron-using proteins during iron scarcity (MERCIER *et al.* 2006). The expression of *php4*$^{+}$ is repressed by Fep1 when cells are grown under iron-replete conditions. When iron is sufficient, Php4 is not only inactivated at the transcriptional level, but also at the post-translational level (MERCIER *et al.* 2006, 2008). Microarray data analysis reveals that during iron deprivation, Php4 is able to repress 86 genes, including genes encoding the TCA cycle components, electron transport chain proteins, amino acid biosynthesis enzymes, and iron-sulfur cluster biogenesis proteins. Thus, Php4 plays a key regulatory role in iron economy (MERCIER *et al.* 2008). The following sections will explain in more detail the iron-mediated regulatory function of Php4, its subcellular localization and its iron-dependent inactivation mechanism.

5. Php4, a subunit of CBC, plays a critical role in iron economy

Budding yeast *S. cerevisiae* experiences a metabolic reprogramming during iron deprivation conditions. Two proteins, designated Cth1 and Cth2, promote the degradation of many mRNAs encoding proteins involved in Fe-dependent metabolic pathways, which leads to optimize iron utilization (Discussed in the section 3.3) (MARTÍNEZ-PASTOR *et al.* 2013). In bacteria, small RNAs are responsible for down-regulating mRNAs of iron-using proteins to repress iron-dependent metabolic pathways under iron deficiency (JACQUES *et al.* 2006; DESNOYERS *et al.* 2013). However, in fission yeast, regulation of iron sparing response is controlled by a regulatory subunit of the CCAAT-binding factor, denoted as Php4. The mechanism of action of Php4 and the importance of its function during iron deficiency will be described in detail in the following sections.

5.1. Php4 subunit

In *S. pombe,* a group of genes are repressed during iron deficiency and the conserved *cis*-acting regulatory sequence CCAAT has a significant role in this action (MERCIER *et al.* 2006). The CCAAT sequence is recognized by a hetero-protein complex composed of Php2, Php3 and Php5 (MCNABB *et al.* 1997). These proteins are constitutively expressed and form the core constituents of the CBC. However, they are not sufficient to exert transcriptional repression under iron deficiency. A fourth subunit, Php4, harboring a functional repression domain, triggers transcriptional repression activity when associated with Php2/3/5 subunits under iron-depleted conditions. Php4 itself is unable to bind DNA directly. Expression of *php4*$^{+}$ is induced under iron starvation, whereas it is repressed under iron-replete conditions (MERCIER *et al.* 2006, 2008).

Using computational analysis of the *S. pombe* whole genome sequence, Php4 was first predicted to be a putative *S. cerevisiae* Hap4 homolog (SYBIRNA *et al.* 2005). Php4 harbors a conserved 16-amino acid region (^{26}RVSKQWVVPPRPKPGR^{41}) that is also present in that of Hap4. This conserved motif is required for the association of Hap4 with the Hap2/3/5 heterocomplex in *S. cerevisiae*. However, the rest of Php4 protein shares a limited overall sequence homology with that of Hap4 (MCNABB and PINTO 2005; MERCIER *et al.* 2006).

5.2. Php4 regulon

Three genes encoding iron-using proteins, pcl1$^+$ (encoding an iron storage protein), sdh4$^+$ (encoding a protein involved in the TCA cycle), and isa1$^+$ (encoding a protein involved in the iron-sulfur cluster biogenesis), were primarily found to be down-regulated during iron deficiency (MERCIER *et al.* 2006). It has also been demonstrated by genetic studies that the presence of Php4 is essential for transcriptional repression of those genes under iron starvation conditions (MERCIER *et al.* 2006). Later, microarray analyses were performed and identified several additional genes that are differentially regulated by Php4 in response to iron starvation. The genome-wide picture reveals that 86 genes are down-regulated by Php4 in response to iron depletion (MERCIER *et al.* 2008). Among these 86 genes, 55 encode proteins that have been assigned a probable function in iron-related processes, including the TCA cycle, mitochondrial respiration, heme biosynthesis, amino acid biosynthesis, and oxidative stress defense. All of those Php4 target genes possess one or more potential CCAAT sequence in their promoters (MERCIER *et al.* 2008). Under iron depleted conditions, Php4 is associated with the Php2/3/5 heterotrimer on a CCAAT sequence and exerts its negative regulatory function to repress gene expressions (Figure 8).

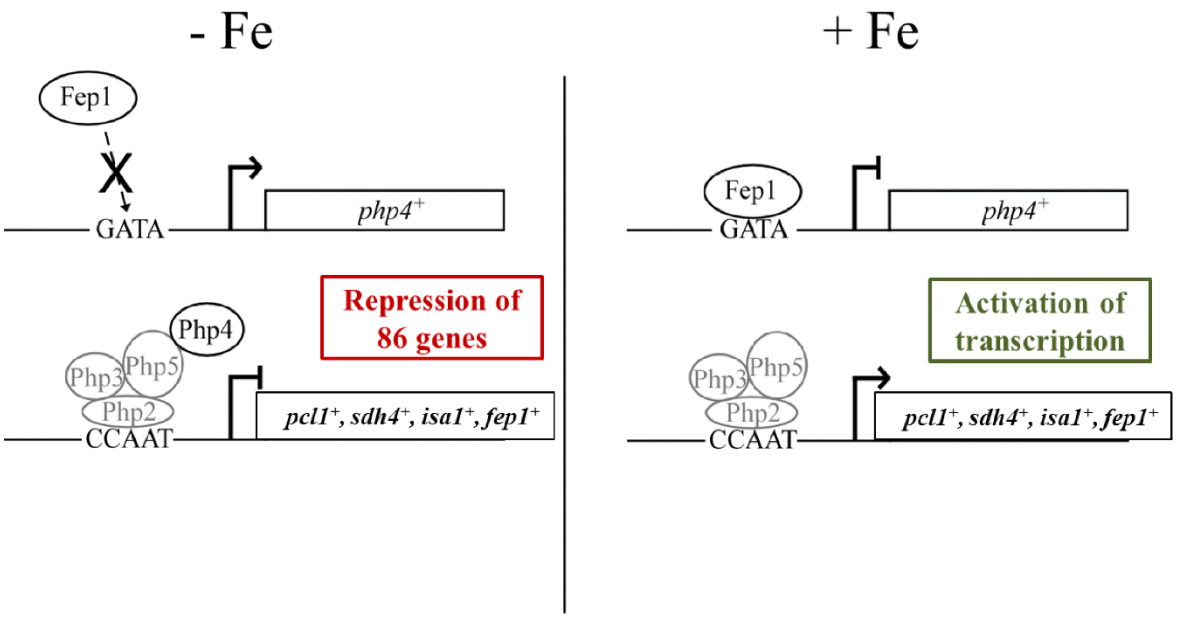

Figure 8. Php4 plays a significant role in the transcriptional regulation of genes encoding iron-using proteins in *S. pombe*. In fission yeast, the CCAAT-binding factor is a multi-subunit complex that is composed of Php2, Php3, and Php5. Under low-iron conditions, Php4 acts as a negative regulatory subunit of the CCAAT-binding factor and fosters repression of genes encoding iron-using proteins. Under conditions of iron excess, Php4 expression is turned off by GATA-type transcription factor Fep1, resulting in the de-repression of genes encoding iron-using proteins.

5.3. Iron-dependent subcellular localization of Php4 and its post-translational regulation

The function of Php4 is regulated at different levels. As already described, the expression of Php4 is transcriptionally regulated by the iron-dependent repressor Fep1(MERCIER *et al.* 2006). Moreover, Php4 also undergoes an iron-dependent post-translational regulation that requires the action of the monothiol glutaredoxin Grx4 (MERCIER *et al.* 2008; MERCIER and LABBÉ 2009). This regulation of Php4 is critical for its subcellular localization, as well as its inactivation by iron. In the presence of excess iron, Php4 is exported from the nucleus to the

cytosol, while under iron deficiency, Php4 accumulates in the nucleus (MERCIER and LABBÉ 2009).

The mechanism underlying the Php4 nuclear export in response to excess iron has been characterized (MERCIER and LABBÉ 2009). A functional leucine-rich (^{93}LLEQLEML^{100}) nuclear export sequence (NES) has been identified within Php4, which is necessary for its iron-mediated nuclear export (MERCIER and LABBÉ 2009). The export of Php4 also requires the action of two other proteins: the monothiol glutaredoxin Grx4 and the exportin Crm1. Grx4 is an interacting partner of Php4 during its nuclear export. Grx4 is also required for iron inhibition of Php4 function (MERCIER and LABBÉ 2009). In *grx4Δ* mutant cells, Php4 exhibits a constitutive nuclear localization and represses target gene expression irrespective of the cellular iron status. Further studies have revealed that the thioredoxin (TRX)-like domain of Grx4 constitutively interacts with Php4, whereas the glutaredoxin (GRX)-like domain of Grx4 associates with Php4 only under iron-replete conditions (VACHON *et al.* 2012). Site-directed mutagenesis revealed that Cys 172 of Grx4 and two conserved cysteine residues, Cys 221 and Cys 227, in Php4 are required for the iron-dependent association of GRX domain and Php4. The GRX-Php4 interaction would prevent Php4 to associate with the hetero-complex Php2/3/5, leading to its release and subsequent export from the nucleus to the cytosol by the exportin Crm1. The leucine-rich NES in Php4 is recognized by Crm1 and leads to the export of the protein from the nucleus to the cytoplasm. In the presence of the Crm1-inhibitor leptomycin B, the nuclear export mechanism is abolished and this results in a permanent nuclear accumulation of Php4 (MERCIER and LABBÉ 2009).

In contrast, when cells are exposed to iron-depleted conditions, Php4 is imported inside of the nucleus where it could exert its negative regulatory function. To date, its nuclear import

mechanism is unclear. My studies mainly focused to unveil the mechanism underlying the nuclear localization of Php4 during iron starvation conditions. My results are presented in the result section.

6. Role of monothiol glutaredoxin and BolA-like proteins in iron homeostasis

Monothiol glutaredoxins (Grxs) with a conserved CGFS active site and BolA-like proteins, have become recognized as novel players in iron homeostasis. Their functions include intracellular iron signaling, iron trafficking, and maturation of Fe−S cluster proteins. Studies on CGFS Grxs and BolA-like proteins using model organisms *S. cerevisiae* and *S. pombe* have provided a framework for understanding many aspects of iron regulation at the cellular level (LI and OUTTEN 2012). Given the widespread distribution of BolA-like proteins and CGFS Grx homologs in other prokaryotes and eukaryotes, it is of paramount importance to uncover their involvement in iron homeostasis. The following sections will address the roles of CGFS Grxs and BolA-like proteins in the regulation of iron metabolism in both budding and fission yeast.

6.1. Role of Grx3/4 and Fra2 in iron homeostasis in budding yeast

Grxs can be of single- or multi-domains, with an N-terminal thioredoxin (TRX)-like domain and a C-terminal glutaredoxin (GRX)-like domain. In *S. cerevisiae,* Grx5 plays a crucial role in mitochondrial iron-sulfur cluster synthesis. In the cases of Grx3 and Grx4, they participate in sensing of cellular iron status, cytosolic iron trafficking, and in communicating the

presence of iron to iron-responsive transcription factors (ROUHIER *et al.* 2010; MÜHLENHOFF *et al.* 2010).

Out of three subfamilies of BolA-like proteins (BolA1-, BolA2-, and BolA3-), BolA1-like proteins are found in both prokaryotes and eukaryotes, whereas the BolA2- and BolA3-like proteins are found only in eukaryotes (LI and OUTTEN 2012). In *S. cerevisiae,* a role for Fra2 (a BolA2-like protein) in iron homeostasis has been revealed based on a phenotypic analysis of *FRA*-deleted mutant cells. *fra2Δ* mutant cells exhibited aberrant regulation of iron metabolism, including accumulation of mitochondrial iron, constitutive siderophore, and ferrous iron uptake (LESUISSE *et al.* 2005). In *S. cerevisiae,* Aft1 and Aft2 are the transcription factors that regulate the expression of genes encoding proteins involved in iron transport and distribution (Discussed in the section 3.2.1). Under iron-replete conditions, Fra2 along with Grx3/4 inhibit the function of Aft1 and Aft2 through an iron-dependent mitochondrial inhibitory signal that leads to the nuclear export of Aft1/Af2 (UETA *et al.* 2007; KUMÁNOVICS *et al.* 2008). Under iron starvation conditions, due to the interruption of mitochondrial Fe−S cluster biogenesis, the Fra-Grx complex can no longer inhibit the activity of Aft1/2, resulting in their accumulation within the nucleus and subsequent activation of the iron regulon**.** The interaction between Fra2 and Grx3/4 has been characterized, revealing that Fra2 forms [2Fe-2S]$^{2+}$ -bridged heterodimers with Grx3 and Grx4 (LI *et al.* 2009a, 2011). A recent study also confirmed the nature of the Fra2−Grx3/4 heterodimer, revealing that the conserved Cys residue of the CGFS active site in Grx3/4, a conserved His in Fra2 (His103), and a Cys from GSH provide the iron ligands in the Fra2−Grx3/4 heterodimer (LI *et al.* 2011). It is indisputable that the Fra2-Grx3/Grx4 heterodimer has a significant role in the inhibition of Aft1/2, and plays a key role in regulating iron homeostasis in *S. cerevisiae*.

6.2. Role of Grx3/4 and Fra2 for iron homeostasis in *S. pombe*

Under iron starvation, the *S. pombe* CGFS monothiol glutaredoxin Grx4 exerts a negative regulatory action on Fep1 activity. Mutant cells lacking *grx4Δ* exhibit a permanent Fep1 occupancy on chromatin, leading to a constitutive repression of iron transport genes (JBEL *et al.* 2011). It has been demonstrated that the TRX-like domain of Grx4 strongly interacts with the C-terminal region of Fep1 in an iron-independent manner, whereas the GRX-like domain associates with the N-terminal region of Fep1 in an iron-dependent manner. Further analysis revealed that Cys35 of Grx4 (located within the TRX-like domain, WAAP**C**K motif) is required for the interaction between the C-terminal region of Fep1 and the TRX domain, whereas Cys172 of Grx4 (located within the conserved **C**GFS motif) is essential for the interaction between the Fep1 N-terminus and the GRX domain. The molecular mechanism underlying the cross-talk between Grx4 and Fep1 is still unknown. Protein-protein interaction assays have revealed that under low-iron conditions, the GRX domain associates with the N-terminal DNA-binding domain of Fep1. This Fep1-GRX interaction would foster conformational changes that cause interference with Fep1's ability to associate with its GATA recognition sequences. Consequently, Fep1 would be unable to trigger repression of its target genes. In contrast, under conditions of high iron levels, it is predicted that two GRX domains of Grx4 can generate [2Fe-2S]-bridged homodimers with the coordination of two cysteine ligands (from each CGFS motif) along with the aid of two cysteines from glutathione (GSH) molecules (PICCIOCCHI *et al.* 2007; BANDYOPADHYAY *et al.* 2008; IWEMA *et al.* 2009) . Thus, the N-terminal region of Fep1 would be available to bind chromatin and functions as a transcriptional repressor, shutting down gene expression.

Studies also suggest that Grx4 exerts an inhibitory effect on Php4 function in an iron-dependent manner (Discussed in the section 5.3) (MERCIER and LABBÉ 2009; VACHON *et al.* 2012). Under conditions of excess iron, the GRX domain interacts with Php4. Php4 is exported from the nucleus to the cytosol by exportin Crm1, resulting in the inactivation of Php4 function. In contrast, under iron starvation conditions, the GRX domain can no longer interact with Php4, which would lead to its association with Php2/3/5, thereby allowing Php4 to repress target gene expression of iron-using proteins.

To date, the role of BolA homologues in the regulation of iron homeostasis is poorly understood in fission yeast. A recent study has demonstrated the role of Fra2 as a co-regulator of Fep1 activity during iron deficiency (JACQUES *et al.* 2014). Results have demonstrated that Fra2 exhibits a negative regulatory action on Fep1 activity under iron starvation. Mutant cells lacking *fra2*$^{+}$ (*fra2Δ*) invariably activate Fep1 and allow Fep1 to bind promoters of target genes, resulting in their constitutive repression. Microscopic analyses reveal that Fra2 is localized throughout the cells under both iron deficient and iron-replete conditions, although a significant proportion of Fra2 is detected in nuclei. This permits Fra2 to be available for interactions with Grx4 and Fep1 in the nucleus. Coimmunoprecipation analyses have confirmed that Fra2, Grx4 and Fep1 form a heteroprotein complex in cells. Furthermore, *in vivo* BiFC experiments revealed that Fra2 associates with Fep1 in nuclei. All these findings suggest that under iron deficiency, Fra2 plays an important role to inactivate Fep1. Further investigations are required to discover the detail molecular mechanism underlying this Fra2-mediated inactivation of Fep1.

7. Nucleo-cytoplasmic trafficking of proteins

Synthesis of proteins take place in the cytoplasm, but some proteins need to be translocated into the nucleus to accomplish important cellular functions (e.g. gene control through transcriptional regulation). As like other eukaryotic cells, transport of *S. pombe* macromolecules between the cytoplasm and the nucleus occurs through the nuclear pore complex (NPC). The NPC is composed of about 30 different proteins (nucleoporins). It forms a gateway that facilitates the nucleo-cytoplasmic exchange of soluble proteins (SOROKIN *et al.* 2007; HOELZ *et al.* 2011). Several factors have been identified and found to be involved in nucleo-cytoplasmic trafficking of proteins. This includes karyopherins (transport receptors), nuclear localization signal (NLS) for nuclear import of cargo proteins, nuclear export signal (NES) for nuclear export of cargo proteins and GTPase Ran that regulates the interaction between karyopherin and cargo proteins (SOROKIN *et al.* 2007). This section will describe the detailed mechanisms underlying nuclear import of proteins.

7.1. Nuclear localization sequence (NLS) triggers nuclear import of proteins

Nuclear import of proteins is a regulated process in eukaryotes. Proteins to be imported into the nucleus often possess nuclear localization signals (NLSs) that are recognized by carrier proteins, termed importins or karyopherins. Importins can distinguish cargo proteins targeted for nuclear localization from other cellular proteins through the recognition of NLSs (LANGE *et al.* 2007). Typically, NLSs consist of one or more short basic amino acid sequences and were first described for their role in the nuclear import of simian virus 40 (SV40) T antigen and nucleoplasmin (DINGWALL *et al.* 1982; KALDERON *et al.* 1984).

Based on the NLS's recognition by the adaptor protein (importin α), there are two types of classical NLSs (cNLSs) that have been identified (LANGE *et al.* 2007). The monopartite cNLS consists of single stretches of basic amino acid residues, whereas in bipartite cNLSs two basic clusters are separated by a 10-12 short, non-conserved amino acid spacer. Monopartite NLSs can be of two types; one has at least four consecutive basic amino acids and the second type has only three basic amino acid residues present in a loose consensus sequence (K-K/R-X-K/R). A number of experimentally defined NLSs do not match the classical consensus sequence. Furthermore, some other NLSs that match consensus sequences could be found non-functional (LANGE *et al.* 2007).

Recently, a new consensus sequence called PY-NLS has been identified apart from classical NLSs. It is recognized by the Kapβ transport receptor. PY-NLS consensus sequence consists of a hydrophobic or basic region followed by an arginine (R)/lysine (K)/histidine (H), then a proline and tyrosine (R/K/H-X(2–5)-PY) (LEE *et al.* 2006). Several RNA binding proteins that shuttle between nucleus and cytoplasm have been reported to possess PY-NLS motifs (LANGE *et al.* 2008; TWYFFELS *et al.* 2013; MALLET and BACHAND 2013).

7.2. Role of karyopherin α/β in transporting cargo protein bearing NLSs

Karyopherins are a group of proteins that play a crucial role in the nuclear import of proteins that possess NLSs. There are two types of karyopherins: karyopherin-α (Kap α) and karyopherin-β (Kap β). Kap β can be further subdivided into Kap β1 and Kap β2. In nuclear import pathways, Kap β1 is involved in the recognition of cNLSs along with a Kap α adaptor, whereas Kap β2 recognizes only PY-NLSs containing cargo proteins (MARFORI *et al.* 2011).

During the nuclear transport, kap-α first binds to cargo proteins bearing NLSs. Kap α can also bind to Kap β in the cytoplasm through its N-terminal importin-beta-binding (IBB) domain. Then, Kap β interacts with the components of the NPC and, subsequently, the heterotrimer complex is transported through the NPC. Translocation is an active process involving the GTPase Ran and other accessory molecules. This multi-step process involves hydrolysis of GTP molecules. After translocation into the nucleoplasm, at some point, the cargo protein dissociates from the importins, which are recycled into the cytoplasm (Figure 9) (CHOOK and BLOBEL 2001; KUERSTEN *et al.* 2001).

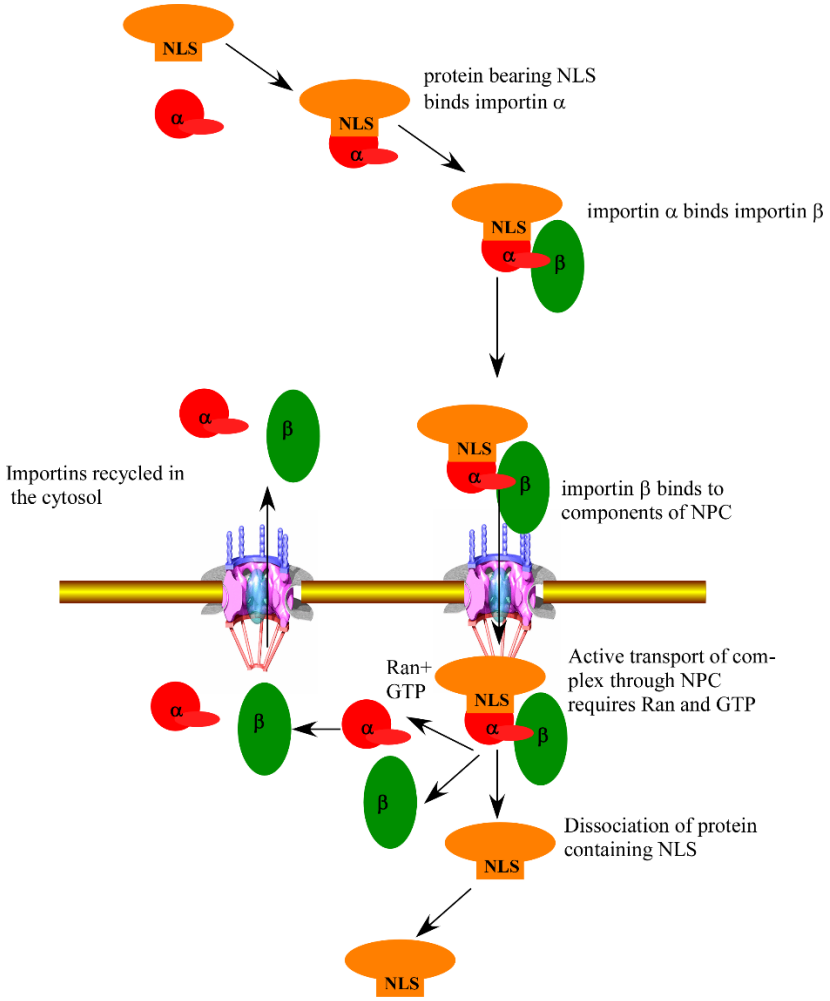

Figure 9. Schematic representation of nuclear protein import.

In *S. cerevisiae,* Srp1 is the only Kap α that can translocate NLS-bearing cargo proteins, whereas 10 out of the 14 known Kap βs are involved in nuclear import (TRAN *et al.* 2007). In contrast, two members of the Kap α family of proteins have been characterized in *S. pombe*: Cut15 and Imp1. Both proteins can efficiently import classical monopartite and bipartite NLS-containing cargo proteins (UMEDA *et al.* 2005). Moreover, there are 12 candidate Kap βs that have been identified in fission yeast through gene bank annotation, most of them are still uncharacterized (WOOD *et al.* 2002). Studies have shown that Sal3, a member of the Kap β family, is involved in the nuclear accumulation of Cdc25 (mitotic regulator phosphatase) (CHUA *et al.* 2002) as well as in the nuclear import of Clp1 (a key player for phosphatase regulation during mitotic exit and cytokinesis) (CHEN *et al.* 2013). Sal3 is also required for the nuclear import of Rdp1, a RNA-dependent RNA polymerase, which plays a critical role in the RNA interference pathway (PARK *et al.* 2012). Nuclear localization of nuclear poly(A)-binding proteins (PABPs) in fission yeast is mediated by another Kap β member, named Kap104 (a Kap β2-type receptor) (MALLET and BACHAND 2013).

8. Hypothesis and research objectives:

It is evident that the iron-responsive transcription factor Php4 plays a crucial role in iron economy in fission yeast. We already learned about the iron-dependent inactivation of Php4 and its subsequent nuclear-to-cytosolic export, which relies on Grx4 and Crm1. However, how Php4 translocates inside the nucleus under iron starvation conditions is still unknown. My studies were designed to identify the factors underlying the nuclear import of Php4. Objectives of my project were:

1. To identify the role of other CCAAT-binding subunits (Php2/3/5) in the nuclear localization of Php4.
2. To identify functional nuclear localization sequences in Php4.
3. To identify karyopherins (α/β) that can recognize NLSs and then mediate nuclear import of Php4 under iron starvation conditions.

RESULTS

Résumé

La protéine Php4 possède la propriété de se déplacer entre le cytosplasme et le noyau selon le statut cellulaire en fer. En conditions de carence en fer, Php4 est nucléaire, alors que sa localisation est cytoplasmique lorsque le fer est abondant. Lorsque qu'elle se localise au noyau, Php4 s'associe au complexe protéique liant les boîtes CCAAT afin de réprimer l'expression des gènes codant pour des protéines qui requièrent du fer comme co-facteur. Dans cette présente étude, nous montrons que l'importation nucléaire de Php4 se déroule de façon indépendante et ne requiert pas la présence des autres sous-unités protéiques qui composent le complexe CCAAT. L'importation nucléaire de Php4 requiert deux signaux de localisation nucléaire (NLSs) qui se retrouvent d'une part, entre les acides aminés 171 et 174 (KRIR) et d'autre part, entre les résidus 234 et 240 (KSVKRVR). Les substitutions spécifiques de ces acides aminés pour des résidus alanines empêchent la localisation nucléaire de Php4. Les deux NLSs sont autonomes et fonctionnellement redondants. De plus, ils sont suffisants, par eux-mêmes, pour forcer la localisation au noyau d'une protéine rapportrice. En conditions de carence en fer, la protéine de fusion GFP-Php4, qui, malgré le fait qu'elle est fonctionnelle, se localise que partiellement au noyau lorsqu'elle est exprimée dans des cellules imp1Δ ou sal3Δ mutantes. Un phénotype similaire a également été observé lorsque GFP-Php4 est exprimée chez des cellules exprimant la protéine thermosensible Cut15 à une température non permissive pour cette dernière. Des analyses d'interactions protéine-protéine ont montré l'existence d'associations protéiques entre Php4 et l'une ou l'autre des trois karyophérines : Imp1, Cut15 ou Sal3. Collectivement, les résultats indiquent que Php4 peut être reconnue et liée par différentes karyophérines, suggérant que son transport au noyau peut s'effectuer par plus d'un sentier d'importation.

CONTRIBUTION

I contribute to generate 90% of the results that are presented in the following article. Majority of molecular constructs and mutant strains are developed by me. I have the major contribution in preparation of figures. I also participate in the writing of manuscript.

All images showing cells or nuclei are representative of at least 95 % of all cells examined. For all experiments at least three independent replicates were performed and at least 1000 cells or nuclei were examined for each replicate.

Characterization of the nuclear import mechanism of the CCAAT-regulatory subunit Php4.

Md. Gulam Musawwir Khan, Jean-François Jacques, Jude Beaudoin, and Simon Labbé*

Département de Biochimie, Faculté de médecine et des sciences de la santé, Université de Sherbrooke, Sherbrooke, Québec, Canada.

*Corresponding author: Département de Biochimie, Faculté de médecine et des sciences de la santé, Université de Sherbrooke, Sherbrooke, Québec, Canada. Tel: (819) 821-8000 ext.: 75460. e-mail: Simon.Labbe@USherbrooke.ca

Keywords: Iron homeostasis, fission yeast, CCAAT-binding transcription factor, nuclear localization signal, karyopherin.

Abstract

Php4 is a nucleo-cytoplasmic shuttling protein that accumulates in the nucleus during iron deficiency. When present in the nucleus, Php4 associates with the CCAAT-binding protein complex and represses genes encoding iron-using proteins. Here, we show that nuclear import of Php4 is independent of the other subunits of the CCAAT-binding complex. Php4 nuclear import relies on two functionally independent nuclear localization sequences (NLSs) that are located between amino acid residues 171 to 174 (KRIR) and 234 to 240 (KSVKRVR). Specific substitutions of basic amino acid residues to alanines within these sequences are sufficient to abrogate nuclear targeting of Php4. The two NLSs are biologically redundant and are sufficient to target a heterologous reporter protein to the nucleus. Under low-iron conditions, a functional GFP-Php4 protein is only partly targeted to the nucleus in *imp1Δ* and *sal3Δ* mutant cells. We further found that cells expressing a temperature-sensitive mutation in *cut15* exhibit increased cytosolic accumulation of Php4 at the nonpermissive temperature. Further analysis by pull-down experiments revealed that Php4 is a cargo of the karyopherins Imp1, Cut15 and Sal3. Collectively, these results indicate that Php4 can be bound by distinct karyopherins, connecting it into more than one nuclear import pathway.

Introduction

In eukaryotic cells, the nucleus is a membrane-enclosed organelle that physically separates genetic material and transcriptional machinery from cytoplasm. Although proteins are translated in the cytoplasm, several of them play important roles in the nucleus. In order to accomplish their cellular function, they must be imported into the nucleus. The way that proteins can be transported into and out of the nucleus is through large protein assemblies denoted nuclear pore complexes (NPCs)[1]. Although some proteins smaller than ~40-60 kDa can passively diffuse through NPCs, most of the proteins with functions in the nucleus are actively transported by specific soluble carrier proteins called karyopherins (Kaps) [2,3]. The orientation of transport through NPCs is determined by short signal sequences within proteins or cargoes. The nuclear localization signal (NLS) triggers proteins into the nucleus, whereas the nuclear export signal (NES) fosters the transport of proteins into the cytoplasm [4]. Kaps are responsible for the vast majority of protein flow through NPCs. Kaps are classified in two families: Kap α (also known as importin α) and Kap β (also known as importin β) [5]. Kap α is an adaptor protein that recognizes two classes of NLSs, which are also called classical NLSs [6]. One class, denoted monopartite NLS, is composed of a single cluster of basic amino acid residues, whereas the second class, termed bipartite NLS, possesses two clusters of basic amino acid residues separated by a 10-12-amino acid spacer. Furthermore, there are two types of monopartite NLSs. The first type has at least four consecutive basic amino acid residues in its primary structure, whereas the second type possesses the degenerate consensus sequence of K(K/R)X(K/R) [6]. To be transported in the nucleus, a protein containing a classical NLS is recognized by a Kap α. Subsequently, a Kap β1 binds the Kap α-cargo-complex to mediate its transport across NPCs. Kap β1 interacts with both Kap α-cargo-complex and NPC proteins (nucleoporins), thereby targeting the cargo to the NPC for its translocation into the nucleus [6,7]. Numerous proteins contain nonclassical NLSs. These proteins bind directly and specifically to different Kap β1 homologs that constitute the Kap β family [2]. Kap β1 is unique among the Kap β family in its use of Kap α as an adaptor protein.

Other members of the Kap β family bind their substrates directly [2]. The dissociation of Kap β-cargo complexes is under the control of the GTPase Ran. Inside the nucleus, Ran-nucleotide guanine triphosphate (GTP) binds to Kap β-cargo complexes, resulting in the dissociation and release of cargoes into the nucleus [8].

In the fission yeast *Schizosaccharomyces pombe*, Imp1 and Cut15 are two members of the Kap α family [9]. In the case of Kap βs, twelve candidates have been annotated from the *S. pombe* Genome Project [10]. Although the majority of them have not yet been characterized, Kap95 is predicted to be the ortholog of *S. cerevisiae* Kap95, which is a Kap β1 [2,11]. Recent studies have also shown that Kap104 is a Kap β2-type receptor, which mediates nuclear import of proline-tyrosine (PY)-NLS cargoes [12]. Unlike classical NLSs, PY-NLS consensus sequence corresponds to [basic/hydrophobic]-X_n-[R/H/K]-$X_{2\text{-}5}$-PY [12,13].

Iron-regulatory transcription factors play fundamental roles by controlling expression of multiple genes encoding proteins involved in iron homeostasis. In the model organism *S. pombe*, regulation of iron homeostasis is mainly controlled by two iron-responsive proteins, the GATA-binding transcription factor Fep1 and the CCAAT-regulatory subunit Php4 [14]. When iron levels exceed those needed by the cells, Fep1 binds to GATA-type *cis*-acting elements and represses the expression of a number of genes involved in iron transport and intracellular iron utilization [15,16]. In contrast, Fep1 is unable to bind chromatin in response to iron deficiency [17]. This situation leads to transcriptional activation of the Fep1 regulon, which includes the *php4*$^+$ gene [18,19]. During iron starvation, Php4 is synthesized and coordinates the iron-sparing response by repressing many genes encoding iron-using proteins [19]. At the molecular level, Php4 regulates its target genes by recognition of the CCAAT-binding complex which is constituted of Php2, Php3 and Php5. The Php2/3/5 heterotrimer binds CCAAT *cis*-acting elements whereas Php4 lacks DNA-binding activity. Php4 is responsible for the ability of the Php complex to repress transcription as a consequence of its association with the heteromeric complex [18,19]. As for Fep1 orthologs, Php4-like proteins are

widely distributed in other fungal species. *Saccharomyces* species is the only group that lacks Php4 and Fep1 orthologs [20].

Studies have shown that the monothiol glutaredoxin Grx4 is a binding partner of Php4 and that it plays an essential role in inhibiting Php4 function when cells undergo a shift from iron-limiting to iron-replete conditions [21,22]. Under conditions of iron abundance, Php4 is exported from the nucleus to the cytoplasm. The nuclear export of Php4 requires both exportin Crm1 and Grx4 [21]. Consistently, disruption of the *grx4*$^{+}$ gene (*grx4Δ*) results in Php4 being constitutively active and invariably located in the nucleus. Although the mechanism by which Grx4 communicates the high concentrations of iron to Php4 remains unclear, deletion mapping analysis revealed that the thioredoxin (TRX) domain of Grx4 interacts strongly and constitutively with Php4 [22]. Further analysis has revealed that, in response to iron repletion, the glutaredoxin (GRX) domain of Grx4 associates with Php4. A putative mechanism for Grx4-mediated inhibition of Php4 function would be that the Php4-GRX domain iron-dependent association disrupts the Php4/Php2/Php3/Php5 heteromeric complex, leading to Php4 release and its subsequent export from the nucleus to the cytoplasm by Crm1.

Exported Php4 is observed in the cytosol. However, when external growth conditions change and cells are exposed to iron-poor conditions, it follows that nuclear localization of Php4 should be re-established via its import to the nucleus. To address this issue, we have characterized the mechanism of cytosolic-to-nuclear import of Php4. In response to iron deficiency, nuclear import of Php4 occurred and deletion of *php2*$^{+}$, *php3*$^{+}$ and *php5*$^{+}$ (*php2Δ php3Δ php5Δ*) did not cause any defects in its nuclear localization. Protein function analysis identified two independent and biologically redundant NLSs within Php4. Each NLSs was sufficient to target an unrelated reporter protein to the nucleus. Disruption of *imp1Δ* or *sal3Δ* gene caused GFP-Php4 to partly mislocalize to the cytoplasm under low-iron conditions. Similarly, in cells containing a temperature-sensitive mutation of *cut15*, GFP-Php4 was mistargeted to the cytoplasm at the nonpermissive temperature. Further analysis by

pull-down experiments showed that Php4 interacted with Imp1, Cut15 and Sal3 in *S. pombe*. Collectively, our findings show that Php4 possesses two nuclear targeting sequences that are used by different Kaps for its nuclear import in response to iron starvation.

Materials and methods

Strains and growth media. *S. pombe* strains used in this study are listed in Table 1. Cells were grown in yeast extract medium plus supplements (YES) containing 0.5% yeast extract, 3% glucose, and 225 mg/l of adenine, histidine, leucine, uracil and lysine. Strains for which plasmid transformation was required were grown in synthetic Edinburgh minimal medium (EMM) lacking specific amino acids required for plasmid selection and maintenance [23]. Cells constitutively expressing a *GFP-php4*$^{+}$ allele were seeded to an A_{600} of 0.2, grown to mid-logarithmic phase (A_{600} of 0.5) and then treated with either 2,2'-dipyridyl (Dip, 250 μM) or $FeCl_3$ (100 μM), or were left untreated for 3 h, unless otherwise stated. When the wild-type or mutant *php4* alleles were expressed under the control of the *nmt1*$^{+}$ promoter, induction of transcription was initiated by removal of thiamine to cells grown to an A_{600} of 0.2. After 12 h of induction, cells were incubated with Dip (250 μM) or $FeCl_3$ (100 μM) for 3 h. In contrast, to prevent expression of *php4* alleles, cells were grown in the presence of thiamine (15 μM or 45 μM), unless otherwise indicated. In the case of *cut15-85*^{ts} cells expressing a thermolabile Cut15, cells were grown at the permissive temperature (25^{o}C) to an A_{600} of ~0.4. The cells were then shifted to 36^{o}C for 1 h and then further incubated at 36^{o}C in the presence of Dip (250 μM) or $FeCl_3$ (100 μM) for an additional 3 h.

Plasmids. pJK-194*prom*php4*$^{+}$*-GFP-php4*$^{+}$ plasmid has been described previously [21]. Plasmids pJKGFP-^{1}Php4^{88}, pJKGFP-^{1}Php4^{144}, pJKGFP-^{1}Php4^{179}, pJKGFP-^{1}Php4^{218}, pJKGFP-^{152}Php4^{295}, pJKGFP-^{188}Php4^{295}, pJKGFP-^{219}Php4^{295}, and pJKGFP-^{245}Php4^{295} were created by cloning different truncated versions of the *php4*$^{+}$ gene into pJK-194*prom*php4*$^{+}$*-GFP-php4*$^{+}$. Different lengths of *php4*$^{+}$ were generated by PCR using primers that contained SalI and Asp718 restriction sites at their ends. After amplification, purified DNA fragments were digested with these two enzymes and then swapped into the corresponding sites of pJK-194*prom*php4*$^{+}$*-GFP-php4*$^{+}$, generating a series of plasmids bearing deletions within different regions of *php4*$^{+}$. To create *php4* mutant alleles K171A/R172A/I173/R174A, K214A/I215/R216A/K217A/R218A, and K234A/S235/V236/K237A/R238A/V239A/R240A, the plasmid pJK-194*prom*php4*$^{+}$*-GFP-php4*$^{+}$ was used in conjunction with the overlap extension method [24]. Primers were designed to ensure the presence of nucleotide substitutions that gave rise to the above-mentioned mutations. Using two additional oligonucleotides corresponding to the start and stop codons of the ORF of *php4*$^{+}$, overlap extension PCR allowed generation of *php4-K171A/R172A/I173/R174A, php4-K214A/I215/R216A/K217A/R218A, and php4-K234A/S235/V236/K237A/R238A/V239A/R240A* alleles. These mutant alleles were used to replace the equivalent wild-type *php4*$^{+}$ DNA segment in pJK-194*prom*php4*$^{+}$*-GFP-php4*$^{+}$. Similarly, overlap extension PCR was used to generate additional *php4* mutants that included different combinations of *K171A/R172A/I173/R174A* mutations with *K214A/I215/R216A/K217A/R218A* or/and *K234A/S235/V236/K237A/R238A/V239A/R240A* mutations. Plasmid pSP-1178nmt-GST-GFP [25] was digested with SpeI and SacI restriction enzymes and used to join annealed synthetic DNA fragments encoding wild-type versions of SV40 NLS and Pap1 NES [26-28]. Wild-type *php4*$^{+}$ coding regions corresponding to amino acid residues 160-190, 188-224, and 219-246 were isolated by PCR and cloned downstream of and in-frame to *GST-GFP* fusion genes, generating plasmids pSP-1178nmt-GST-GFP-^{160}Php4^{190}, pSP-1178nmt-GST-GFP-^{188}Php4^{224}, and pSP-1178nmt-GST-GFP-^{219}Php4^{246}, respectively. Similarly, these *php4*$^{+}$ coding regions (amino acid residues 160-190, 188-224, and 219-246) were amplified from plasmids

pJK-194*prom*php4*$^{+}$*-GFP-php4-K171A/R172A/I173/R174A,* pJK-194*prom*php4*$^{+}$*-GFP-php4-K214A/I215/R216A/K217A/R218A,* and pJK-194*prom*php4*$^{+}$*-GFP-php4-K234A/S235/V236/K237A/R238A/V239A/R240A* to create plasmids pSP-1178nmt-GST-GFP-mutant^{160}Php4^{190}, pSP-1178nmt-GST-GFP-mutant^{188}Php4^{224}, and pSP-1178nmt-GST-GFP-mutant^{219}Php4^{246}, respectively. The wild-type *php4*$^{+}$ coding region corresponding to amino acid residues 160-246 was amplified by PCR using primers designed to generate SpeI and SacI sites at each extremity of the PCR product. The DNA fragment was inserted into the corresponding sites of pSP-1178nmt-GST-GFP. The resulting plasmid, named pSP-1178nmt-GST-GFP-^{160}Php4^{246}, was subsequently used to create three additional plasmids harboring *K171A/R172A/I173/R174A*, *K234A/S235/V236/K237A/R238A/V239A/R240A* or *K171A/R172A/I173/R174A/K234A/S235/V236/K237A/R238A/V239A/R240A* substitutions.

RNase protection analysis. Total RNA was extracted using a hot phenol method as described previously [29]. In the case of RNase protection assays, RNA (15 μg per reaction) was hybridized and digested with RNase T1 as described previously [19]. Riboprobes derived from plasmids pSK*isa1*$^{+}$ and pSK*act1*$^{+}$ [18] were used to detect *isa1*$^{+}$ and *act1*$^{+}$ transcripts, respectively. Plasmids were linearized with BamHI for subsequent antisense RNA labeling with [α-^{32}P]UTP and T7 RNA polymerase. *act1*$^{+}$ mRNA was probed as an internal control for normalization during quantification of RNase protection products.

Fluorescence microscopy analysis. Fluorescence microscopy was performed as described previously [30]. Both fluorescence and differential interference contrast images (Nomarski) of cells were obtained using a Nikon Eclipse E800 epifluorescent microscope (Nikon, Melville, NY) equipped with a Hamamatsu ORCA-ER digital cooled camera (Hamamatsu, Bridgewater, NJ). Samples were

analyzed using a 1,000X magnification with the following filters: 520 to 550 nm (YFP), 465 to 495 nm (GFP), and 340 to 380 nm (Hoechst 33342). Cell fields shown in this study represent a minimum of five independent experiments.

TAP pull-down experiments. For pull-down experiments, we created *php4Δ* null strains in which the TAP coding sequence was integrated at the chromosomal locus of *imp1*$^+$, *cut15*$^+$, or *sal3*$^+$. These integrations were performed using a PCR-based gene fusion approach as described previously [31], except that pFA6a-kanMX6-CTAP2 [32] was used to amplify the TAP coding sequence. The method allowed homologous integration of TAP at the chromosomal locus of *imp1*$^+$, *cut15*$^+$, or *sal3*$^+$, thereby replacing wild-type allele by *imp1*$^+$*-TAP*, *cut15*$^+$*-TAP* or *sal3*$^+$*-TAP* allele. To determine whether Php4 interacted with Imp1, Cut15 or Sal3 in *S. pombe*, *php4Δ imp1*$^+$*-TAP*, *php4Δ cut15*$^+$*-TAP*, or *php4Δ sal3*$^+$*-TAP* cells were transformed with pBPade6$^+$-nmt41x-GFP-php4$^+$. The cells were grown to mid-logarithmic phase in a thiamine-free medium and then treated with Dip (250 μM) for 3 h. Total cell lysates were prepared as described previously [33], except that PMSF (1 mM) was directly added to cell cultures 10 min before cell lysis. Preparation of IgG-Sepharose 6 Fast-Flow beads (GE Healthcare) and coupling of proteins to beads were carried out as described previously [33]. After end-over-end mixing for 30 to 60 min at 4°C, the beads were washed four times with lysis buffer (1 ml each time) and then transferred to a fresh microtube prior to a final wash. The immunoprecipitates were resuspended in sodium dodecyl sulfate loading buffer (60 μl), heated for 5 min at 95°C and proteins resolved by electrophoresis on 9% sodium dodecyl sulfate-polyacrylamide gels. The following antibodies were used for Western blotting analysis of Imp1-TAP, Cut15-TAP, Sal3-TAP, GFP-Php4 and α-tubulin: polyclonal anti-mouse IgG antibody (1:500) (ICN Biomedicals); monoclonal anti-GFP antibody B-2 (1:500) (Santa Cruz Biotechnology) and monoclonal anti-α-tubulin antibody (1:5000) (clone B-5-1-2; Sigma-Aldrich). Following incubation with primary antibodies, membranes were washed and incubated with the appropriate horseradish peroxidase-

conjugated secondary antibodies (1:5000) (Amersham Biosciences), developed with enhanced chemiluminescence (ECL) reagents (Amersham Biosciences) and visualized by chemiluminescence.

Results

Localization of Php4 to the nucleus in a Php2/Php3/Php5-independent manner under low-iron conditions. As we have previously shown, functional GFP-Php4 localized in the cytoplasm of cells under iron-sufficient conditions (Fig. 1) [21]. Conversely, GFP-Php4 accumulated in the nucleus when cells underwent a transition from iron-sufficient to iron-limiting conditions (Fig. 1) [21]. To further investigate the mechanism by which GFP-Php4 was imported in the nucleus, we tested whether Php2, Php3, and Php5 were required for its nuclear accumulation in response to iron starvation. To perform these experiments, *php4Δ* and *php2Δ php3Δ php4Δ php5Δ* mutant strains were transformed with an integrative plasmid harboring a *GFP-php4*$^{+}$ allele constitutively expressed from a GATA-less *php4*$^{+}$ promoter. Cells expressing GFP-Php4 were grown under basal conditions to mid-logarithmic phase and then treated with the iron chelator Dip or with $FeCl_3$ for 3 h. Results showed that in the presence of Dip, GFP-Php4 accumulated in the nucleus of both *php4Δ* and *php2Δ php3Δ php4Δ php5Δ* mutant strains (Fig. 1). In contrast, when these strains were treated with $FeCl_3$, GFP-Php4 was observed primarily in the cytoplasm (Fig. 1). As we have previously observed, GFP alone displayed a pancellular-fluorescence pattern, regardless of cellular iron status (Fig. 1) [21]. Taken together, these results indicated that GFP-Php4 localizes to the nucleus in iron-starved cells in a Php2/Php3/Php5-independent manner. Conversely, in iron-replete cells, GFP-Php4 exhibits a distinct distribution pattern that is cytoplasmic.

Mapping NLSs of Php4. To begin to characterize regions within Php4 responsible for nuclear localization, we created a series of N- and C-terminal deletions and fused GFP to the N terminus of each truncated protein (Fig. 2A). *php4Δ* cells expressing these truncated versions of GFP-Php4 were analyzed by fluorescence microscopy to identify which mutants localized to the nucleus. Truncated GFP-^{1}Php4^{88}, in which the last 207 amino acid residues of Php4 were deleted exhibited a pancellular-fluorescence pattern under both low and high iron concentrations (Fig. 2B), suggesting that GFP-^{1}Php4^{88} was able to passively enter and exit the nucleus. In the case of GFP-^{1}Php4^{144}, results showed that it primarily accumulated in the cytoplasmic region of *php4Δ* cells (Fig. 2B). This finding was consistent with the presence of a NES encompassing amino acid residues 93-100 [21]. GFP-^{1}Php4^{179} and GFP-^{1}Php4^{218} were located in the nucleus under both iron-limiting and iron-replete conditions (Fig. 2B). Although their nuclear location was independent of the cellular iron status, these observations were consistent with the interpretation of the presence of at least one NLS encompassing a common minimal region composed of amino acid residues 144-179. One reason that may explain the absence of iron-mediated nuclear export of GFP-^{1}Php4^{179} and GFP-^{1}Php4^{218} is the fact that these chimeric proteins miss part of the C-terminal region (positions 152 to 254) of Php4. Previous structure-function studies have revealed that the association of the GRX domain of Grx4 and Php4 depends on the presence of this region (Php4 152-254) [22]. Furthermore, it is known that the GRX domain-Php4 association is required for the iron-mediated inhibition of Php4 that leads to its recruitment by Crm1 (via Php4 NES 93-100), and its subsequent export out of the nucleus to the cytoplasm [21]. Deletion of amino acid residues 1 to 151, 1 to 187, and 1 to 218 from the N-terminus to generate GFP-^{152}Php4^{295}, GFP-^{188}Php4^{295}, and GFP^{219}Php4^{295} did not affect nuclear localization. Due to the absence of NES, GFP-^{152}Php4^{295}, GFP-^{188}Php4^{295} and GFP^{219}Php4^{295} were located exclusively in the nucleus, regardless of cellular iron status. However, further deletion of 26 amino acid residues in GFP^{219}Php4^{295} to generate GFP^{245}Php4^{295}, nullified its ability to localize exclusively

in the nucleus. Instead, GFP^{245}Php4^{295} exhibited pancellular localization in iron-starved and iron-replete cells (Fig. 2B), revealing loss of signal to promote active entry of Php4 into the nucleus. Taken together, these results were consistent with the interpretation that regions of Php4 from amino acid residues 144 to 179, 188 to 245, and 219 to 245 are sufficient to mediate nuclear import and accumulation of Php4.

Mutation of three predicted NLSs of Php4. In light of these observations, we sought to identify amino acid residues in regions 144 to 179, 188 to 245, and 219 to 245 of Php4 that could serve as NLSs. One of the characteristic features of a classical NLS is a degenerate consensus sequence of K(K/R)X(K/R) (where X indicates any amino acid residue) [6]. Analysis of Php4 using the NLS Mapper [34] prediction program highlighted three short regions containing positively charged residues that matched or partially matched the consensus K(K/R)X(K/R) motif. The first potential NLS, ^{171}KRIR^{174} (amino acid residues 171-174) was found in region 144 to 179, whereas the second ^{214}KIRKR^{218} (amino acid residues 214-218) and the third ^{234}KSVKRVR^{240} (amino acid residues 234-240) putative NLSs were located in region 188 to 245. In the case of region 219 to 245, it contained only the ^{234}KSVKRVR^{240} motif. To determine a functional NLS within Php4 that directs nuclear localization, we first mutated three positively charged amino acids, K^{171}, R^{172}, and R^{174} to Ala in full-length Php4 to generate Php4-N1. We also examined the effect of mutating K^{214}, R^{216}, K^{217}, and R^{218} (Php4-N2) or K^{234}, K^{237}, R^{238}, V^{239}, and R^{240} (Php4-N3) to Ala on the ability of Php4 to localize to the nucleus (Fig. 3A). Results showed that Php4-N1, Php4-N2, and Php4-N3 mutants were efficiently targeted to the nucleus under iron starvation conditions, whereas their localization was predominantly cytoplasmic under high levels of iron (Fig. 3B). Iron-dependent nuclear-cytoplasmic trafficking of these mutants was similar to that of wild-type GFP-Php4 fusion protein (Fig. 3B). Subsequently, we combined the mutated residues within Php4-N3 with mutations in Php4-N2 (generating Php4-N4) or with mutations in Php4-N1 (generating Php4-N6) or with mutations in Php4-N1 and Php4-N2

(creating Php4-N7) (Fig. 3A). Similarly, mutated residues within Php4-N1 were combined with mutations in Php4-N2 to generate Php4-N5 mutant. *php4Δ* cells expressing Php4-N4 displayed nuclear accumulation following treatment with Dip. In contrast, Php4-N4 was exported out of the nucleus to the cytoplasm when cells had been treated with iron (Fig. 3B). Microscopy analysis showed that iron-starved cells expressing the *php4-N5* allele appeared to have less nuclear accumulation than wild-type protein or Php4-N1, -N2, -N3, and N4 mutants. On the other hand, cells harboring Php4-N6 and Php4-N7 did not show obvious nuclear accumulation under iron deprivation conditions (Fig. 3B). Under elevated iron levels, Php4-N5, Php4-N6, and Php4-N7 remained in the cytoplasm as observed in the case of wild-type GFP-Php4 protein. Taken together, these results revealed that Php4 harbors two functionally redundant NLSs, ^{171}KRIR^{174} and ^{234}KSVKRVR^{240}, which could mediate nuclear import of Php4 independently.

Because nuclear import is prerequisite to Php4 function, we hypothesized that mutations in Php4-N6 mutant (^{171}AAIA^{174} and ^{234}ASVAAAA^{240}) would cause loss of Php4 function as well as produce cells defective in repression of the Php4 regulon in response to iron starvation. Indeed, cells expressing mutant *php4-N6* allele exhibited elevated *isa1*$^{+}$ mRNA levels that were virtually not repressed by iron starvation (Fig. 4A). In fact, steady-state levels of *isa1*$^{+}$ mRNA under low iron conditions were increased at least ~7-fold above the levels of wild-type or a strain expressing a functional GFP-Php4 protein that was treated with Dip (Fig. 4B). In contrast, *isa1*$^{+}$ transcript levels were down-regulated under conditions of iron starvation in cells expressing the wild-type Php4 protein or Php4-N1, -N2, and -N3 mutants. In the case of the Php4-N5 mutant (^{171}AAIA^{174} and ^{214}AIAAA^{218}), its mutations resulted in a ~2-fold increase in the expression of the *isa1*$^{+}$ gene in the presence of low iron concentrations when compared to the levels observed in iron-starved cells expressing the wild-type GFP-Php4. Nonetheless, the levels of *isa1*$^{+}$ expression in the Php4-N5 mutant were still much lower under low iron than those under basal or iron-replete conditions (Fig. 4, A and B). Because the absence of Php4 led to a constitutive expression of iron-using genes, *php4Δ* mutant cells are known

to be hypersensitive to low iron conditions (lack of optimization of iron utilization when iron is limited) (Fig. 4C). Results consistently showed that *php4Δ* cells expressing the *php4-N6* allele exhibited poor growth on low iron medium in comparison to wild-type cells (Fig. 4C). In contrast, cells expressing the wild-type GFP-Php4 protein or Php4-N1, -N2, -N3, and -N5 mutants were able to grow on medium containing Dip (Fig. 4C). Taken together, these results indicated that Php4 nuclear localization is necessary for Php4-mediated repressive transcriptional regulation of gene expression.

Two NLSs trigger nuclear import by themselves. To assess whether NLS regions of Php4 had the ability to trigger nuclear import, Php4 160-190, Php4 188-224, and Php4 219-246 fragments were fused to GST-GFP, which was used as a reporter protein in sufficiency experiments [35]. In addition, we examined the effect of mutating K^{171}, R^{172}, and R^{174} to Ala in Php4 160-190 (mutant 160-190), K^{214}, R^{216}, K^{217}, and R^{218} to Ala in Php4 188-224 (mutant 188-224), and K^{234}, K^{237}, R^{238}, V^{239}, and R^{240} to Ala in Php4 219-246 (mutant 219-246) (Fig. 5A). *GST-GFP-Php4 160-190* (wild-type and mutant), *GST-GFP-Php4 188-224* (wild-type and mutant), and *GST-GFP-Php4 219-246* (wild-type and mutant) fusion alleles were expressed under the control of the thiamine-regulatable promoter [36]. This system allowed us to induce cellular pools of the above-mentioned fusion proteins and assess the effect of the presence of a given NLS (^{171}KRIR^{174}, ^{214}KIRKR^{218}, or ^{234}KSVKRVR^{240}) on their localization. Cells expressing GST-GFP-Php4 160-190 and GST-GFP-Php4 219-246 exhibited nuclear accumulation, whereas their mutant derivatives displayed a pancellular-fluorescence pattern in a manner similar to GST-GFP alone (Fig. 5B). In the case of GST-GFP-Php4 188-224, its location was cytoplasmic as well as nuclear, irrespective of the presence or absence of the basic residues K^{214}, R^{216}, K^{217}, and R^{218} (Fig. 5B). Controls for nuclear import and export were GST-GFP-SV40NLS and GST-GFP-Pap1NES, respectively. Results showed that reporter proteins tested in sufficiency experiments were unaffected by cellular iron status (Fig. 5B). Furthermore, immunoblot analyses revealed that reporter proteins were stable and intact under the conditions analyzed (Figure S1). Taken

together, the data revealed that Php4 contains intrinsic determinants involved in nuclear import of the protein. Indeed, the Php4 160-190-(^{171}KRIR^{174}) and Php4 219-246-(^{234}KSVKRVR^{240}) regions function as transferable NLS sequence when fused with a reporter protein.

To further validate the observation that Php4 contained two functionally redundant NLSs, we expressed and analyzed a segment of Php4 comprising amino acid residues 160 to 246 using the GST-GFP reporter system (Fig. 6A). Amino acids K^{171}, R^{172}, and R^{174} were substituted by Ala in Php4 160-246 to generate Php4-N8. We converted the K^{234}, K^{237}, R^{238}, V^{239}, and R^{240} residues to Ala to generate Php4-N9. We also combined the mutated residues within Php4-N8 with those in Php4-N9 to generate the Php4-N10 mutant (Fig. 6A). Fluorescence microscopy analysis showed that *php4Δ* cells expressing mutant *GST-GFP-php4-N8* and *GST-GFP-php4-N9* alleles accumulated Php4 in the nucleus in a manner comparable to that of the wild-type GST-GFP-^{160}Php4^{246} fusion protein (Fig. 6B). When both clusters of mutated residues were combined, GST-GFP-php4-N10 was not efficiently targeted to the nucleus, showing primarily cytosolic fluorescence and to less extent some pancellular distribution (Fig. 6B). Western blot analysis of cell extracts showed that the chimeric proteins were present at their expected size (Fig. 6C). Collectively, the results showed that the two NLS regions of Php4 (^{171}KRIR^{174} and ^{234}KSVKRVR^{240}) are functionally redundant in the context of the truncated protein comprising amino acid residues 160 to 246. However, while the ^{234}KSVKRVR^{240} element is fully functional in the truncated protein, this element is not fully competent to mediate nuclear import in the context of the full protein.

Involvement of α- and β-karyopherins in import of Php4. Due to the fact that the two NLSs found in Php4 contained the degenerate consensus sequence of K(K/R)X(K/R), we concluded that both represented short basic classical NLSs [6]. To be transported in the nucleus, a protein containing a classical NLS is recognized by an importin α (karyopherin α or Kapα) protein, which serves as an adaptor. Subsequently, a karyopherin β1 (Kapβ1 or importin β1) binds the importin-α-cargo-complex

to mediate its transport across the nuclear pore. Imp1 and Cut15 are the two importin α proteins in *S. pombe*. These two import adaptors have both unique and common binding cargoes [9]. To test whether the nuclear import of Php4 required Imp1, we disrupted the *imp1*$^+$ gene (*imp1Δ*) and determined the effect on the localization of GFP-Php4. Results showed that under conditions of iron starvation, the absence of Imp1 caused a partial mislocalization of GFP-Php4 to the cytoplasm, although a nuclear accumulation of GFP-Php4 was still observed to some extent (Fig. 7A). *cut15*$^+$ is essential for cell growth and our approach was to used *cut15-85* cells expressing a thermolabile Cut15 in which a *GFP-php4*$^+$ allele was previously integrated. At the permissive temperature (25ºC) in which case Cut15 is functional, GFP-Php4 accumulated in the nuclei of iron-starved cells (Fig. 7B). However, incubation of iron-starved cells at the nonpermissive temperature (36ºC) resulted in an alteration of GFP-Php4 nuclear localization and the GFP-Php4 signal was detected to both the cytoplasm and nucleus (Fig. 7B). Control experiments showed that GFP-Php4 was localized exclusively in the cytoplasm of wild-type and *cut15-85* strains when these transformed cells were incubated in the presence of iron under both temperature conditions (Fig. 7).

S. cerevisiae iron-responsive regulator Aft1 undergoes nucleo-cytoplasmic shuttling in response to changes in intracellular iron concentration in a manner analogous to Php4 [37,38]. Aft1 accumulates in the nucleus upon iron starvation, whereas high iron concentrations result in nuclear export. Nuclear import of Aft1 is mediated by the Kapβ1 Pse1, which is a putative ortholog of *S. pombe* Sal3 [11,38]. Based on this fact, we deleted the *sal3*$^+$ gene (*sal3Δ*). Results showed that disruption of Sal3 caused a partial mislocalization of GFP-Php4 to the cytoplasm under low levels of iron, suggesting that Sal3 also participated in nuclear import (Fig. 7A). As expected, when *sal3Δ* deletion cells were treated with iron, GFP-Php4 was primarily distributed in the cytoplasm (Fig. 7A). Nuclear accumulation of GFP-Php4 in response to iron starvation appeared to rely on more than one karyopherins. Thus, we investigated whether a *imp1Δ sal3Δ* double deletion would favor increased mislocalization of Php4 under low-iron conditions. Results showed that a double deletion of *imp1*$^+$ and *sal3*$^+$ exhibited a

greater cytoplasmic accumulation of GFP-Php4, suggesting that Imp1 and Sal3 may use distinct nuclear import mechanisms for targeting Php4 to the nucleus (Fig. 7A). As a control, we tested whether the absence of Kap104 influenced Php4 localization. Kap104 is a Kapβ2 that specifically binds proline-tyrosine-NLS (PY-NLS) rather than classical NLS [12]. In this case, GFP-Php4 was properly localized in the nucleus in iron-starved *kap104Δ* cells, supporting the interpretation that the negative effect of the absence of Imp1, Cut15, or Sal3 on Php4 nuclear import was specific (Fig. 7A). When wild-type and mutant karyopherin strains were incubated in the presence of exogenous iron, GFP-Php4 was distributed in the cytoplasm of cells (Fig. 7). Taken together, the results revealed that Imp1, Cut15 or Sal3 could participate in nuclear accumulation of Php4 when cells are grown under low iron conditions.

Given the involvement of Imp1, Cut15 and Sal3 in nuclear import of Php4, we tested whether the repression of *isa1*$^+$ expression was affected in *imp1Δ*, *cut15-85* and *sal3Δ* mutant cells. Deletion of *imp1*$^+$ (*imp1Δ*) resulted in steady-state levels of *isa1*$^+$ that were increased (~30%) in cells treated with Dip in comparison with iron-starved control cells (Fig. 8). In the case of disruption of *sal3*$^+$ (*sal3Δ*) that resulted in a modest upregulation (~10%) of *isa1*$^+$ transcription under low iron conditions. Similarly to *imp1Δ* cells, mRNA levels of *isa1*$^+$ were upregulated (~40%) in *imp1Δ sal3Δ* cells, especially in the case of iron-starved control cells (Fig. 8). Similar increases in *isa1*$^+$ mRNA levels were observed in *imp1Δ*, *sal3Δ* and *imp1Δ sal3Δ* cells expressing an endogenous Php4 protein (Figure S2). We also examined steady-state mRNA levels of *isa1*$^+$ in *cut15-85* cells expressing a thermolabile Cut15. *php4Δ* and *php4Δ cut15-85* cells expressing GFP-Php4 were grown at the permissive temperature (25ºC). At mid-logarithmic phase, cells were divided in aliquots which were then incubated at permissive (25ºC) or nonpermissive (36ºC) temperature in the presence of Dip (250 μM), $FeCl_3$ (100 μM), or left without treatment. At 25ºC, a temperature where Cut15 was functional, cells displayed very low *isa1*$^+$ transcript levels under low iron conditions (Dip). In contrast, *isa1*$^+$ mRNA levels were up-regulated under basal and iron-replete conditions (Fig. 8). At nonpermissive

temperature (36ºC), inactivation of Cut15 resulted in a 34% increase in *isa1*$^+$ transcription under low iron conditions compared to levels of *isa1*$^+$ observed in a *cut15*$^+$ strain under the same conditions (Fig. 8). In *cut15-85* cells expressing an endogenous Php4 protein, inactivation of Cut15 resulted in a 20% increase in *isa1*$^+$ transcription under iron starvation conditions (Figure S2). As expected, *isa1*$^+$ mRNA levels in both untreated and iron-treated *php4Δ cut15-85 GFP-php4*$^+$ or *cut15-85* cells were induced as compared to iron-starved cells (Fig. 8 and Figure S2). Collectively, these results indicated that Php4 is less competent to repress gene expression under low iron conditions in the absence of Imp1, Cut15 or Sal3.

Imp1, Cut15 and Sal3 are interacting partners of Php4. Given the fact that inactivation of *imp1*$^+$, *cut15*$^+$ or *sal3*$^+$ negatively altered import of Php4 to a different extent, we examined whether Php4 could form complexes with Imp1, Cut15 or Sal3 *in vivo*. To address this possibility, we investigated Php4 capacity to interact with these proteins using TAP pull-down experiments. In these assays, we used iron-starved cells co-expressing distinct pairs of fusion proteins, including GFP-Php4 and Imp1-TAP, GFP-Php4 and Cut15-TAP, GFP-Php4 and Sal3-TAP or GFP-Php4 and TAP (Fig. 9). Total cell extracts were incubated in the presence of IgG-Sepharose beads that selectively bound unfused TAP or TAP-tagged proteins. This strategy allowed an enrichment of Imp1, Cut15 or Sal3 and detection of their potential interacting partners. Western blot analysis of proteins retained by the beads using an anti-GFP antibody revealed that GFP-Php4 was present in the immunoprecipitate fraction of cells expressing Imp1-TAP, Cut15-TAP or Sal3-TAP (Fig. 9). In contrast, GFP-Php4 was absent in the bound fraction of cells expressing TAP alone (Fig. 9). Whole-cell extract fractionation was confirmed using an antibody directed against α-tubulin. Results showed that α-tubulin was present in total cell extracts but not in the retained protein fractions (Fig. 9). To ascertain the steady-state protein levels of Imp1-TAP, Cut15-TAP, or Sal3-TAP, Western blot analyses of both whole cell protein preparations and bound fractions were performed using an anti-IgG antibody (Fig. 9). Taken together,

these results showed the existence of Php4-Imp1, Php4-Cut15 and Php4-Sal3 interactions in *S. pombe*.

Discussion

Php4-like proteins are widely distributed among fungal species [20,39]. These proteins include Hap43 (from *Candida albicans*), AnHapX (from *Aspergillus nidulans*), AfHapX (from *Aspergillus fumigatus*) and CnHapX (from *Cryptococcus neoformans*) [40-43] [44]. Of note, *Saccharomyces* species are one of the rare groups that lack Php4 orthologs. Although Php4-like proteins are key nuclear regulators for preventing futile expression of genes encoding iron-using proteins under low-iron conditions, the nature of their NLSs and the mechanisms responsible for triggering their nuclear import have remained poorly characterized. In this study, we have identified two functionally independent and redundant NLSs that are responsible for delivery of Php4 into the nucleus. The first NLS (^{171}KRIR^{174}) possessed a sequence that matched the degenerate consensus K(K/R)X(K/R) motif, which represents one of the two types of conventional monopartite NLSs. Furthermore, classical monopartite NLSs are known to specifically bind Kap α proteins. The second NLS (^{234}KSVKRVR^{240}) is a modified version of the first one. It has ^{237}KRVR^{240} [K(K/R)X(K/R)] as a basic core motif and few flanking residues (^{234}KSV^{236}) immediately upstream of the core basic residues. These properties represent a modified pattern of classical monopartite NLS that has been previously shown to be competent for binding with Kap α proteins [27]. Indeed, a previous study has shown that the RVSKRPR motif, which is highly reminiscent to KSVKRVR found in Php4, is specifically recognized by Kap α [27]. When we examined the effect of mutating ^{234}K to Ala on the ability of GST-GFP-^{219}Php4^{246} protein to localize to the nucleus, we observed only a weak mislocalization of the protein to the cytoplasm (in comparison with an unmodified GST-GFP-^{219}Php4^{246}). Yet, most GST-GFP-^{219}Php4^{246} ^{234}K→A signal was detected in the nucleus in response to iron starvation (unpublished data). When ^{237}KRVR^{240} were mutated to Ala residues in GST-GFP-^{219}Php4^{246}, the

mutant exhibited a pancellular distribution pattern, revealing that the basic core amino acid residues were essential for nuclear import (unpublished data).

Consistent with the amino acid composition of the two Php4 NLSs, we found that the two *S. pombe* Kap α proteins, Imp1 and Cut15, were involved in nuclear import of Php4. This observation meant that Php4 is a common cargo for Imp1 and Cut15. This situation has been reported before. SV40 NLS is functional in *S. pombe* and has been used to assess nuclear protein import competence. As observed in the case of Php4, both *cut15-85* and *imp1Δ* mutant cells were less efficient at accumulating a SV40 NLS fusion protein in the nucleus than wild type cells [9], revealing that Imp1 and Cut15 have overlapping functions for the import of an SV40 NLS-containing protein. Similarly to Php4, it has been reported that *S. pombe* transcription factor Pap1 interacts with both Imp1 and Cut15 [9]. Neither *imp1Δ* nor *cut15-85* mutant cells were competent to efficiently import Pap1 into the nucleus as compared to wild-type cells. This observation suggested an overlapping function of Imp1 and Cut15 for nuclear import of Pap1. In *S. cerevisiae*, Kap95 is a Kapβ1 involved in the nuclear import of proteins with classical NLSs. One pathway by which Kap95 mediates nuclear import of cargo proteins involves its association with a Kap α protein. One could envision that *S. pombe* Kap95, which is essential for cell viability, is required for the Imp1- or Cut15-mediated nuclear import of Php4. However, the potential involvement of Kap95 remains speculative at this time and needs further investigation.

In general, protein containing NLSs that are recognized by Kap α proteins are transported as a trimeric complex with Kapβ1 proteins. However, it has been shown in the case of some proteins that their nuclear import can be mediated by distinct Kaps or groups of Kaps. These proteins include histones, ribosomal proteins and stress-responsive transcription factors such as Asr1 and AlcR [45,46]. These findings led us to examine whether some nonessential members of the Kap β family could be required for nuclear import of Php4. Results showed that the inactivation of Sal3 caused a mislocalization of Php4 to the cytoplasm (although a significant proportion of Php4 could still be seen into the nucleus).

In *S. pombe*, Sal3 is the ortholog of *S. cerevisiae* Pse1. Interestingly, Pse1 is required for the nuclear localization of the iron-responsive transcription factor Aft1 in *S. cerevisiae*. Although Aft1 is a transcriptional activator and in contrast, Php4 is a transcriptional repressor, both are active and accumulate in the nucleus under conditions of iron starvation. Similarly to Php4, Aft1 possesses two functionally independent NLSs. Although their amino acid composition (KPKKKR and RKPK) is different than those of Php4 (KRIR and KSVKRVR), each of these NLSs is monopartite and is closely related to the consensus sequence K(K/R)X(K/R). However, as opposed to Kap α proteins that are required for nuclear import of Php4, *S. cerevisiae* Kap α (Srp1) is not involved in nuclear import of Aft1. Furthermore, it has been shown that nuclear translocation of Aft1 is exclusively dependent on Pse1 in *S. cerevisiae* and does not depend on other Kap β family members [38].

In contrast, some proteins in *S. cerevisiae* are import substrates of more than one Kaps. For instance, Kap114, Kap95, Kap123, Pse1, and Kap104 recognize NLSs present in histones H2A and H2B, whereas these Kaps mediate nuclear transport of Asr1 [46]. Based on these data, it is likely that *S. pombe* Php4 interacts with more than one type of nucleo-cytoplasmic factors, thereby leaving more options for its nuclear import when iron levels are low. However, the question whether one Php4 NLS is more specific than the others in being recognized by either Kaps α (Imp1 and Cut15) or Kap β1 (Sal3) awaits further studies.

In *A. nidulans*, the CCAAT-binding factor is composed of the HapB, HapC, HapE and HapX subunits [40,47]. Whereas HapC and HapE lack NLSs, HapB contains one functional NLS. In the case of HapX, the presence of functional NLS has not been reported. Under iron sufficient conditions, while the *HAPX* gene is repressed, HapB, HapC and HapE are expressed and assembled as a heterotrimeric complex. To enable cells to provide equimolar concentrations of HapB/C/E subunits to the nucleus, HapB subunit acts as a primary cargo for nuclear import of HapC and HapE. According to a proposed model, HapC and HapE have first to form a heterodimer that is transported into the nucleus only in complex with HapB by way of a piggy-back mechanism [47]. Although the nuclear import

mechanism of *S. pombe* CCAAT-binding Php2/3/5 subunits is unknown, we investigated whether nuclear import of Php4 was dependent of the presence of these subunits. Under iron-limiting conditions, disruption of *php2*$^{+}$, *php3*$^{+}$ and *php5*$^{+}$ had no effect on the nuclear import of Php4. Results showed that Php4 accumulated within the nucleus of iron-starved *php2Δ php3Δ php5Δ* triple mutant cells. In the presence of iron, Php4 exhibited a steady-state distribution in the cytoplasm of both *php2*$^{+}$/*3*$^{+}$/*5*$^{+}$ and *php2Δ/3Δ/5Δ* strains. We concluded that nucleocytoplasmic trafficking of Php4 was Php2/3/5-independent. This mechanism is different in comparison with the piggy-back nuclear import mechanism that occurs for the heterotrimeric CCAAT-binding complex in *A. nidulans*.

Our findings suggest that NLS-mediated import of Php4 is not iron-regulated, as we found that the presence of iron did not affect the nuclear localization of the three GST-GFP-Php4 NLS fusion proteins (GST-GFP-^{160}Php4^{190}, GST-GFP-^{219}Php4^{246}, and GST-GFP-^{160}Php4^{246}) (Figs 5 and 6). Furthermore, in the context of full-length protein, when nuclear export sequence (NES) of Php4 was mutated, Php4 exhibited a constitutive nuclear localization under both iron-depleted and iron-replete conditions [21]. This observation suggested that the recognition of Php4 NLSs by Imp1, Cut15 or Sal3 occurred regardless of iron conditions. Nevertheless, it is intriguing to note that Php4 NLSs (positions 171 to 174 and 234 to 240) are included in a region of Php4 from residues 152 to 254 that is known to be required for interaction with the GRX domain of Grx4 [22]. As opposed to the TRX domain, the GRX domain of Grx4 interacts in an iron-dependent manner with Php4. Under high-iron conditions, the GRX domain interacts with the region 152 to 254 of Php4, which may induce conformational changes that negatively affect interactions between NLSs and their import receptors. This may contribute in cytoplasmic accumulation of Php4 under iron-replete conditions. In contrast, under iron-limiting conditions, the GRX domain is no longer able to interact with Php4, which may favor associations between Php4 NLSs and Kaps, therefore contributing in nuclear accumulation of Php4. Although this dynamic interplay may occur in the context of the full-length Php4 protein, further investigation is needed to address this possibility.

Acknowledgments

We are grateful to Dr. Gilles Dupuis for critically reading the manuscript and for his valuable comments. We are indebted to Alexandre Mercier, Pierre-Luc Mallet, François Bachand and the Japanese Yeast Genetic Resource Center (NRBP/YGRC) for yeast strains. Md.G.M.K. was recipient of a Studentship from the Faculté de médecine et des sciences de la santé of the Université de Sherbrooke.

References

1. Hoelz A, Debler EW, Blobel G (2011) The structure of the nuclear pore complex. Annu Rev Biochem 80: 613-643.

2. Chook YM, Suel KE (2011) Nuclear import by karyopherin-βs: Recognition and inhibition. Biochim Biophys Acta 1813: 1593-1606.

3. Chook YM, Blobel G (2001) Karyopherins and nuclear import. Curr Opin Struct Biol 11: 703-715.

4. Hoelz A, Blobel G (2004) Cell biology: Popping out of the nucleus. Nature 432: 815-816.

5. Pemberton LF, Paschal BM (2005) Mechanisms of receptor-mediated nuclear import and nuclear export. Traffic 6: 187-198.

6. Lange A, Mills RE, Lange CJ, Stewart M, Devine SE, et al. (2007) Classical nuclear localization signals: Definition, function, and interaction with importin alpha. J Biol Chem 282: 5101-5105.

7. Xu D, Farmer A, Chook YM (2010) Recognition of nuclear targeting signals by karyopherin-β proteins. Curr Opin Struct Biol 20: 782-790.

8. Kuersten S, Ohno M, Mattaj IW (2001) Nucleocytoplasmic transport: Ran, beta and beyond. Trends Cell Biol 11: 497-503.

9. Umeda M, Izaddoost S, Cushman I, Moore MS, Sazer S (2005) The fission yeast *Schizosaccharomyces pombe* has two importin-alpha proteins, Imp1p and Cut15p, which have common and unique functions in nucleocytoplasmic transport and cell cycle progression. Genetics 171: 7-21.

10. Wood V, Gwilliam R, Rajandream MA, Lyne M, Lyne R, et al. (2002) The genome sequence of *Schizosaccharomyces pombe*. Nature 415: 871-880.

11. Chen XQ, Du X, Liu J, Balasubramanian MK, Balasundaram D (2004) Identification of genes encoding putative nucleoporins and transport factors in the fission yeast *Schizosaccharomyces pombe*: A deletion analysis. Yeast 21: 495-509.

12. Mallet PL, Bachand F (2013) A proline-tyrosine nuclear localization signal (PY-NLS) is required for the nuclear import of fission yeast PAB2, but not of human PABPN1. Traffic 14: 282-294.

13. Lee BJ, Cansizoglu AE, Suel KE, Louis TH, Zhang Z, et al. (2006) Rules for nuclear localization sequence recognition by karyopherin β 2. Cell 126: 543-558.

14. Labbé S, Khan MG, Jacques JF (2013) Iron uptake and regulation in *Schizosaccharomyces pombe*. Curr Opin Microbiol 16: 669-676.

15. Rustici G, van Bakel H, Lackner DH, Holstege FC, Wijmenga C, et al. (2007) Global transcriptional responses of fission and budding yeast to changes in copper and iron levels: A comparative study. Genome Biol 8: R73.

16. Labbé S, Pelletier B, Mercier A (2007) Iron homeostasis in the fission yeast *Schizosaccharomyces pombe*. Biometals 20: 523-537.

17. Jbel M, Mercier A, Pelletier B, Beaudoin J, Labbé S (2009) Iron activates in vivo DNA binding of *Schizosaccharomyces pombe* transcription factor Fep1 through its amino-terminal region. Eukaryot Cell 8: 649-664.

18. Mercier A, Pelletier B, Labbé S (2006) A transcription factor cascade involving Fep1 and the CCAAT-binding factor Php4 regulates gene expression in response to iron deficiency in the fission yeast *Schizosaccharomyces pombe*. Eukaryot Cell 5: 1866-1881.

19. Mercier A, Watt S, Bahler J, Labbé S (2008) Key function for the CCAAT-binding factor Php4 to regulate gene expression in response to iron deficiency in fission yeast. Eukaryot Cell 7: 493-508.

20. Haas H, Eisendle M, Turgeon BG (2008) Siderophores in fungal physiology and virulence. Annu Rev Phytopathol 46: 149-187.

21. Mercier A, Labbé S (2009) Both Php4 function and subcellular localization are regulated by iron via a multistep mechanism involving the glutaredoxin Grx4 and the exportin Crm1. J Biol Chem 284: 20249-20262.

22. Vachon P, Mercier A, Jbel M, Labbé S (2012) The monothiol glutaredoxin Grx4 exerts an iron-dependent inhibitory effect on php4 function. Eukaryot Cell 11: 806-819.

23. Sabatinos SA, Forsburg SL (2010) Molecular genetics of *Schizosaccharomyces pombe*. Methods Enzymol 470: 759-795.

24. Ho SN, Hunt HD, Horton RM, Pullen JK, Pease LR (1989) Site-directed mutagenesis by overlap extension using the polymerase chain reaction. Gene 77: 51-59.

25. Beaudoin J, Labbé S (2007) Crm1-mediated nuclear export of the *Schizosaccharomyces pombe* transcription factor Cuf1 during a shift from low to high copper concentrations. Eukaryot Cell 6: 764-775.

26. Kalderon D, Roberts BL, Richardson WD, Smith AE (1984) A short amino acid sequence able to specify nuclear location. Cell 39: 499-509.

27. Kosugi S, Hasebe M, Matsumura N, Takashima H, Miyamoto-Sato E, et al. (2009) Six classes of nuclear localization signals specific to different binding grooves of importin alpha. J Biol Chem 284: 478-485.

28. Kudo N, Taoka H, Toda T, Yoshida M, Horinouchi S (1999) A novel nuclear export signal sensitive to oxidative stress in the fission yeast transcription factor Pap1. J Biol Chem 274: 15151-15158.

29. Chen D, Toone WM, Mata J, Lyne R, Burns G, et al. (2003) Global transcriptional responses of fission yeast to environmental stress. Mol Biol Cell 14: 214-229.

30. Pelletier B, Trott A, Morano KA, Labbé S (2005) Functional characterization of the iron-regulatory transcription factor Fep1 from *Schizosaccharomyces pombe*. J Biol Chem 280: 25146-25161.

31. Bahler J, Wu JQ, Longtine MS, Shah NG, McKenzie A, et al. (1998) Heterologous modules for efficient and versatile PCR-based gene targeting in *Schizosaccharomyces pombe*. Yeast 14: 943-951.

32. Tasto JJ, Carnahan RH, McDonald WH, Gould KL (2001) Vectors and gene targeting modules for tandem affinity purification in *Schizosaccharomyces pombe*. Yeast 18: 657-662.

33. Jacques JF, Mercier A, Brault A, Mourer T, Labbé S (2014) Fra2 is a co-regulator of Fep1 inhibition in response to iron starvation. PLoS One 9: e98959.

34. Kosugi S, Hasebe M, Tomita M, Yanagawa H (2009) Systematic identification of cell cycle-dependent yeast nucleocytoplasmic shuttling proteins by prediction of composite motifs. Proc Natl Acad Sci USA 106: 10171-10176.

35. Saydam N, Georgiev O, Nakano MY, Greber UF, Schaffner W (2001) Nucleo-cytoplasmic trafficking of metal-regulatory transcription factor 1 is regulated by diverse stress signals. J Biol Chem 276: 25487-25495.

36. Moreno MB, Duran A, Ribas JC (2000) A family of multifunctional thiamine-repressible expression vectors for fission yeast. Yeast 16: 861-872.

37. Yamaguchi-Iwai Y, Ueta R, Fukunaka A, Sasaki R (2002) Subcellular localization of Aft1 transcription factor responds to iron status in *Saccharomyces cerevisiae*. J Biol Chem 277: 18914-18918.

38. Ueta R, Fukunaka A, Yamaguchi-Iwai Y (2003) Pse1p mediates the nuclear import of the iron-responsive transcription factor Aft1p in *Saccharomyces cerevisiae*. J Biol Chem 278: 50120-50127.

39. Kronstad JW (2013) Iron in eukaryotic microbes: Regulation, trafficking and theft. Curr Opin Microbiol 16: 659-661.

40. Hortschansky P, Eisendle M, Al-Abdallah Q, Schmidt AD, Bergmann S, et al. (2007) Interaction of HapX with the CCAAT-binding complex-a novel mechanism of gene regulation by iron. EMBO J 26: 3157-3168.

41. Hsu PC, Yang CY, Lan CY (2011) Candida albicans Hap43 is a repressor induced under low-iron conditions and is essential for iron-responsive transcriptional regulation and virulence. Eukaryot Cell 10: 207-225.

42. Jung WH, Saikia S, Hu G, Wang J, Fung CK, et al. (2010) HapX positively and negatively regulates the transcriptional response to iron deprivation in *Cryptococcus neoformans*. PLoS Pathog 6: e1001209.

43. Schrettl M, Beckmann N, Varga J, Heinekamp T, Jacobsen ID, et al. (2010) HapX-mediated adaption to iron starvation is crucial for virulence of *Aspergillus fumigatus*. PLoS Pathog 6: e1001124.

44. Gsaller F, Hortschansky P, Beattie SR, Klammer V, Tuppatsch K, et al. (2014) The janus transcription factor HapX controls fungal adaptation to both iron starvation and iron excess. EMBO J Aug 4 Epub ahead of print.

45. Nikolaev I, Cochet MF, Felenbok B (2003) Nuclear import of zinc binuclear cluster proteins proceeds through multiple, overlapping transport pathways. Eukaryot Cell 2: 209-221.

46. Fries T, Betz C, Sohn K, Caesar S, Schlenstedt G, et al. (2007) A novel conserved nuclear localization signal is recognized by a group of yeast importins. J Biol Chem 282: 19292-19301.

47. Steidl S, Tuncher A, Goda H, Guder C, Papadopoulou N, et al. (2004) A single subunit of a heterotrimeric CCAAT-binding complex carries a nuclear localization signal: Piggy back transport of the pre-assembled complex to the nucleus. J Mol Biol 342: 515-524.

48. Pelletier B, Beaudoin J, Mukai Y, Labbé S (2002) Fep1, an iron sensor regulating iron transporter gene expression in *Schizosaccharomyces pombe*. J Biol Chem 277: 22950-22958.

Figure legends

Fig. 1. *Iron-regulated nucleo-cytoplasmic trafficking of Php4 is independent of Php2, Php3 and Php5 proteins*. *php4Δ* or *php2Δ php3Δ php4Δ php5Δ* mutant cells were transformed with an integrative vector expressing GFP alone or a *GFP-php4*$^{+}$ allele under the control of a GATA-less *php4*$^{+}$ promoter. Transformed cells were treated with either Dip (250 μM) or $FeCl_3$ (Fe) (100 μM) for 3 h. Nuclear DNA was visualized by Hoechst staining whereas Nomarski optics (Nomarski) was used to reveal cell morphology. For simplicity, only *php4Δ* cells transformed with GFP alone are shown because fluorescent images of *php2Δ php3Δ php4Δ php5Δ* cells were identical. The results shown are representative of five independent experiments.

Fig. 2. *Distinct regions of Php4 are required for its nuclear localization*. *A*, Schematic representation of the GFP-Php4 fusion protein and different GFP-Php4 fusion derivatives. The red box indicates the nuclear export signal (NES) found in Php4 (residues 93-100). Blue boxes represent putative nuclear localization signals (NLSs) that were identified in Php4 (residues 171-174, residues 214-218 and residues 234-240). The segment encompassing residues 152-254 (light-grey box) is a C-terminal region of Php4 required for interaction with the GRX domain of Grx4, which is required for iron-mediated exportation of Php4. The green box represents the GFP coding sequence. The amino acid sequence numbers refer to the positions relative to the first amino acid of Php4. *B*, *php4Δ* cells expressing the indicated fusion alleles under the control of a GATA-less *php4*$^{+}$ promoter were incubated in the presence of Dip (250 μM) or $FeCl_3$ (Fe) (100 μM). After 3 h, cells were examined by fluorescence microscopy to visualize GFP-Php4 and its different fusion derivatives. Hoechst staining revealed nuclear DNA whereas Nomarski optics was used to monitor cell morphology. The results shown are representative of five independent experiments.

Fig. 3. *Two regions of Php4 encompassing amino acid residues 171 to 174 and 234 to 240 are involved in targeting Php4 to the nucleus*. *A*, Schematic illustration of wild-type (WT) and mutant versions (N1 to N7) of GFP-Php4 fusion protein. Green, red and blue boxes represent GFP coding sequence, NES, and putative NLS, respectively. Black boxes (marked with an asterisk) indicate mutated NLS. The amino acid residues of Php4 are numbered relative to its initiator codon. *B*, Fluorescence microscopy was used to visualize cellular location of GFP-Php4 and its mutant derivatives that were expressed in *php4Δ* cells. When indicated, cultures were treated with Dip (250 μM) or $FeCl_3$ (Fe) (100 μM) for 3 h. Cells were stained using Hoechst to visualize nuclear DNA, whereas Nomarski optics was used to monitor cell morphology. The results shown are representative of five independent experiments.

Fig. 4. *Php4 NLSs are required for Php4-mediated repressive function. A*, Cells carrying a disrupted *php4Δ* allele were transformed with an empty plasmid (vector alone) or plasmids expressing *GFP-php4*$^+$, *GFP-php4*$^+$*-N1*, *GFP-php4*$^+$*-N2*, *GFP-php4*$^+$*-N3*, *GFP-php4*$^+$*-N5*, and *GFP-php4*$^+$*-N6*. Transformed cells were grown under basal (-), iron-deficient conditions (250 μM Dip) or excess iron (100 μM $FeCl_3$) (Fe). After total RNA extraction, *isa1*$^+$ and *act1*$^+$ steady-state mRNA levels were analyzed by RNase protection assays. Results shown are representative of three independent experiments. *B*, Quantification of *isa1*$^+$ levels after treatments shown in panel A. Data are shown as the mean of triplicate ± standard deviations. *C*, Wild-type (*WT*) and *php4Δ* cells expressing the indicated wild-type or mutant *GFP-php4* allele were spotted onto YES medium containing none (-) or 140 μM Dip and incubated at 30^{o}C for 5 days. A *php4Δ* mutant containing an empty vector (vector alone) was used as a control strain known to be hypersensitive to Dip.

Fig. 5. *Amino acid fragments 160-190 and 219-246 of Php4 contain nuclear import activity*. *A*, Schematic representation of Php4 and several GST-GFP fusion reporter proteins containing NES or NLS regions of different proteins such as Pap1, SV40, and Php4. Color codes are, orange (GST), green (GFP), blue (putative Php4 NLS) and black (mutated NLS). *B*, Shown are representative *php4Δ* cells expressing GST-GFP, GST-GFP-Pap1NES, GST-GFP-SV40NLS, GST-GFP-Php4^{160}NLS^{190}, GST-GFP-Php4^{160}mutantNLS^{190}, GST-GFP-Php4^{188}NLS^{224}, GST-GFP-Php4^{188}mutantNLS^{224}, GST-GFP-Php4^{219}NLS^{246}, and GST-GFP-Php4^{219}mutantNLS^{246}, respectively. Cultures were grown in thiamine-free media for 12 h. After 3 h treatment in the presence of Dip (250 μM) or $FeCl_3$ (Fe) (100 μM), cells were analyzed by fluorescence microscopy for GFP. As controls, nuclear DNA was visualized by Hoechst staining and cell morphology by Nomarski optics. The results shown are representative of five independent experiments.

Fig. 6. *Identification of two functional Php4 NLSs*. *A,* Schematic representation of Php4 that shows relative locations of NLSs (blue boxes). The left bottom panel shows GST-GFP fusion proteins containing the amino acid fragment 160-246 of Php4, including wild-type (WT) and mutant (N8 to N10) versions. Color codes are, orange (GST), green (GFP), blue (NLS) and black (mutated NLS). Amino acid sequence numbers refer to the position relative to the first amino acid of Php4. *B*, Cells harboring a *php4Δ* deletion were transformed with the indicated integrative constructs. Cells were grown to early-logarithmic phase and then thiamine was withdrawn from cell cultures. Thiamine-free cultures were grown for 12 h, and then incubated in the presence of Dip (250 μM) or $FeCl_3$ (Fe) (100 μM) for 3 h. Subsequently, cells were subjected to fluorescence microscopy for GFP detection. Cell morphology was examined through Nomarski optics (Nomarski) and nuclear DNA was detected by Hoechst staining. The results shown are representative of five independent experiments. *C*, Cell extracts were prepared from strains observed in panel B, and analyzed by immunoblotting. GST-GFP-^{160}Php4^{246} (WT) and its mutant (N8 to N10) versions were detected using anti-GFP antibody. As an

internal control, extracts preparations were probed with anti-α-tubulin antibody. The positions of the molecular weight standards are indicated to the left.

Fig. 7. *Inactivation of imp1$^+$, cut15$^+$ and sal3$^+$ produced defect in nuclear import of GFP-Php4*. *A,* An integrative plasmid expressing a functional GFP-tagged *php4$^+$* allele was transformed into *php4Δ*, *php4Δ kap104Δ*, *php4Δ imp1Δ*, *php4Δ sal3Δ*, and *php4Δ sal3Δ imp1Δ* mutant strains. Mid-logarithmic phase cultures were treated with Dip (250 μM) or $FeCl_3$ (Fe, 100 μM) for 3 h. Fluorescence microscopy was used to visualize cellular location of GFP-Php4. Cells were treated with Hoechst dye for nuclear DNA staining. Cell morphology was examined using Nomarski optics. *B,* Mid-logarithmic phase cultures of the indicated strains were grown at either the permissive (25^{o}C) or nonpermissive (36^{o}C) temperature for 1 h. Cultures were subsequently divided into four separate aliquots which were treated with Dip (250 μM) or $FeCl_3$ (Fe, 100 μM) at permissive (25^{o}C) or non-permissive (36^{o}C) temperature. After 3 h treatment, cells were analyzed by fluorescence microscopy for GFP detection. The results shown are representative of five independent experiments.

Fig. 8. *Loss of Imp1, Cut15 or Sal3 resulted in increased expression of isa1$^+$ under low iron conditions. A*, Strains harboring insertionally inactivated *php4Δ*, *php4Δ imp1Δ*, *php4Δ sal3Δ*, or *php4Δ imp1Δ sal3Δ* genes were transformed with the *GFP*-tagged *php4$^+$* allele. The indicated strains were assessed for their ability to repress *isa1$^+$* gene expression in the presence of Dip (250 μM) versus basal (-) or iron-replete (Fe, 100 μM) conditions. After 3 h of treatment, total RNA was prepared and then analyzed by RNase protection assays. Steady-state levels of *isa1$^+$* and *act1$^+$* mRNAs are shown with arrows. *B*, Quantification of three independent RNase protection assays, including the experiment shown in panel A. *C*, *php4Δ* and *php4Δ cut15-85* strains were transformed with an integrative plasmid expressing a functional GFP-Php4 protein. Mid-logarithmic phase cultures were

divided into four aliquots which were treated with Dip (250 μM) or $FeCl_3$ (100 μM) at permissive (25°C) or nonpermissive (36°C) temperature. After 3 h, total RNA was extracted and used in RNase protection protocol to determine *isa1*$^+$ and *act1*$^+$ mRNA levels. *D*, Quantification of *isa1*$^+$ transcript levels after treatments. Data are shown as the mean values of triplicate ± standard deviations.

Fig. 9. *Php4 interacts with Imp1, Cut15, and Sal3 in S. pombe*. *php4Δ* cells expressing GFP-tagged Php4 and TAP alone (*A*), GFP-tagged Php4 and TAP-tagged Imp1 (*B*), GFP-tagged Php4 and TAP-tagged Sal3 (*C*), or GFP-tagged Php4 and TAP-tagged Cut15 (*D*) were grown to mid-logarithmic phase in EMM without thiamine in the presence of Dip (250 μM). Extracts (Total) were subjected to immunoprecipitation (IP) using IgG-Sepharose beads. The bound proteins were eluted and analyzed by immunoblot assays using a mouse anti-GFP antibody (α-GFP). A portion of the total cell extracts (~2%) was included to ascertain the presence of proteins prior to chromatography. As additional controls, aliquots of whole-cell extracts and bound fractions were probed with an anti-mouse IgG antibody (α-IgG) and an anti-tubulin antibody (α-tubulin). The positions of the molecular weight of protein standards (in kDa) are indicated on the left-hand side.

TABLE 1. *S. pombe* strain genotypes.

Strain	Genotype	Source or reference
FY435	h^+ his7-366 leu1-32 ura4-Δ18 ade6-M210	[48]
AMY17	h^+ his7-366 leu1-32 ura4-Δ18 ade6-M210 php4Δ::loxP	[21]
GKY1	h^+ his7-366 leu1-32 ura4-Δ18 ade6-M210 php4Δ::loxP php2Δ::loxP php3Δ::loxP php5Δ::loxP	This study
GKY2	h^+ his7::loxP leu1-32 ura4-Δ18 ade6-M210 kap104Δ::natMX6 php4Δ::KAN^r	This study
GKY3	h^+ his7-366 leu1-32 ura4-Δ18 ade6-M210 imp1Δ::loxP php4Δ::KAN^r	This study
GKY4	h^+ his7-366 leu1-32 ura4-Δ18 ade6-M210 sal3Δ::loxP php4Δ::KAN^r	This study
GKY5	h^+ his7-366 leu1-32 ura4-Δ18 ade6-M210 imp1Δ::loxP sal3Δ::loxP php4Δ::KAN^r	This study
GKY6	h^+ his7Δ::loxP leu1-32 ura4Δ::loxP ade6Δ::loxP php4Δ::KAN^r	This study
GKY7	h^+ his7Δ::loxP leu1-32 ura4Δ::loxP ade6Δ::loxP cut15-85 php4Δ::KAN^r	This study
GKY8	h^+ his7-366 leu1-32 ura4-Δ18 ade6-M210 php4Δ::loxP $imp1^+$-TAP::KAN^r	This study
GKY9	h^+ his7-366 leu1-32 ura4-Δ18 ade6-M210 php4Δ::loxP $sal3^+$-TAP::KAN^r	This study
GKY10	h^+ his7-366 leu1-32 ura4-Δ18 ade6-M210 php4Δ::loxP $cut15^+$-TAP::KAN^r	This study

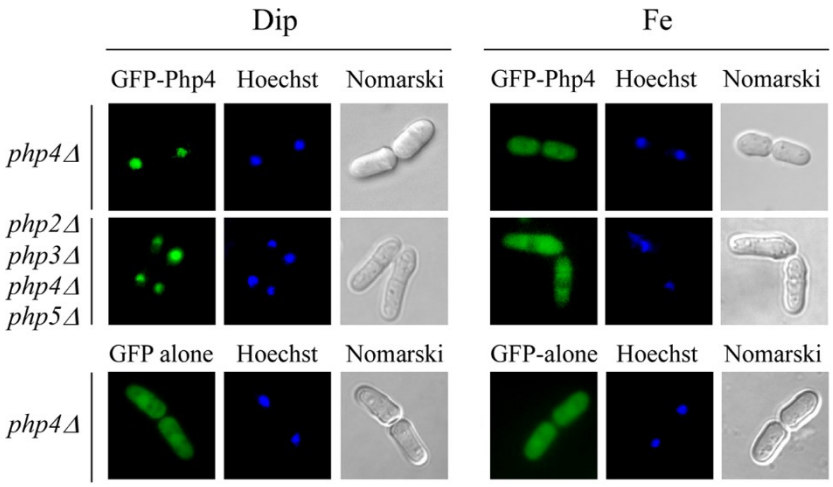

Figure 1 – Khan *et al.*

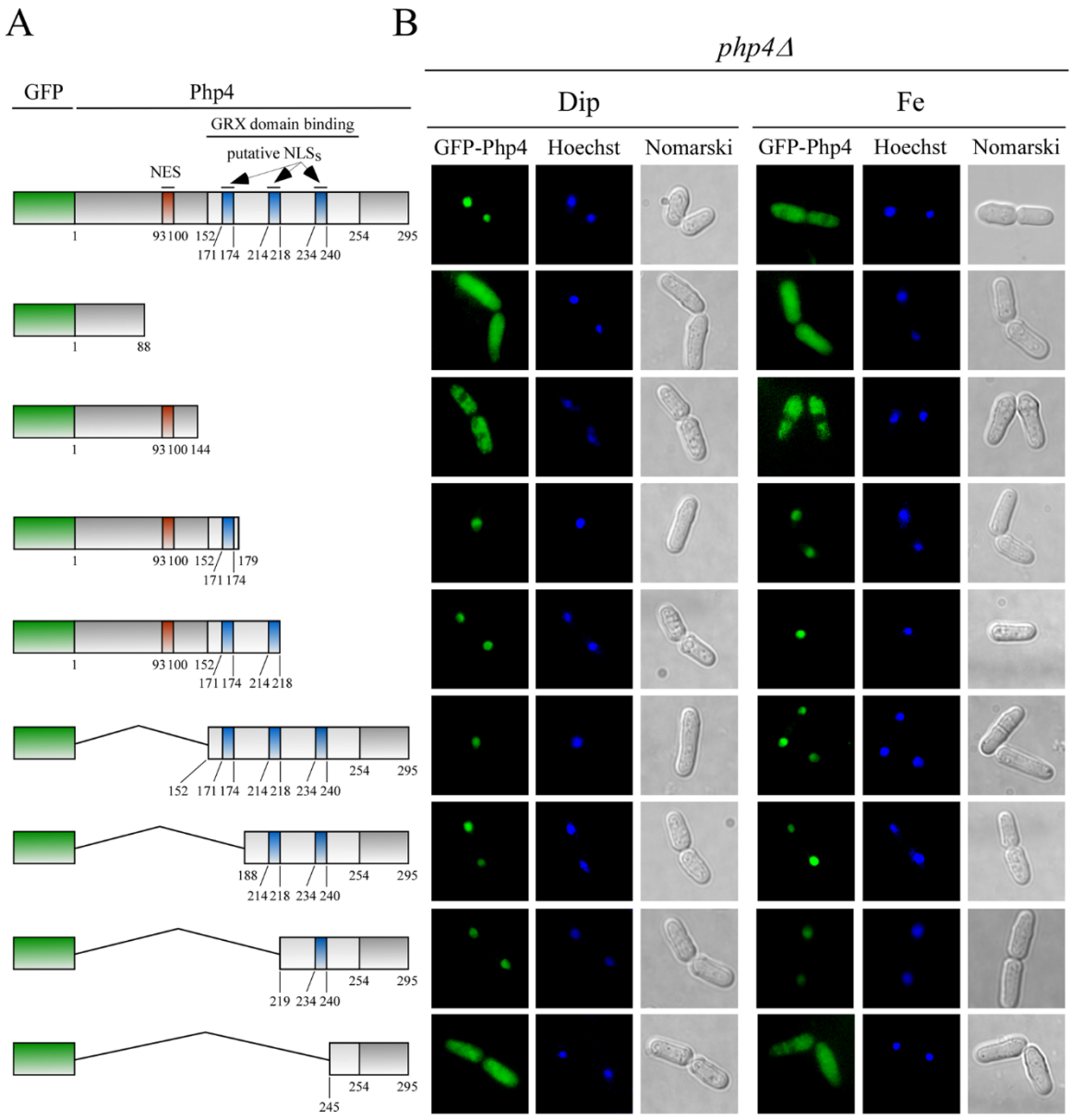

Figure 2 – Khan *et al.*

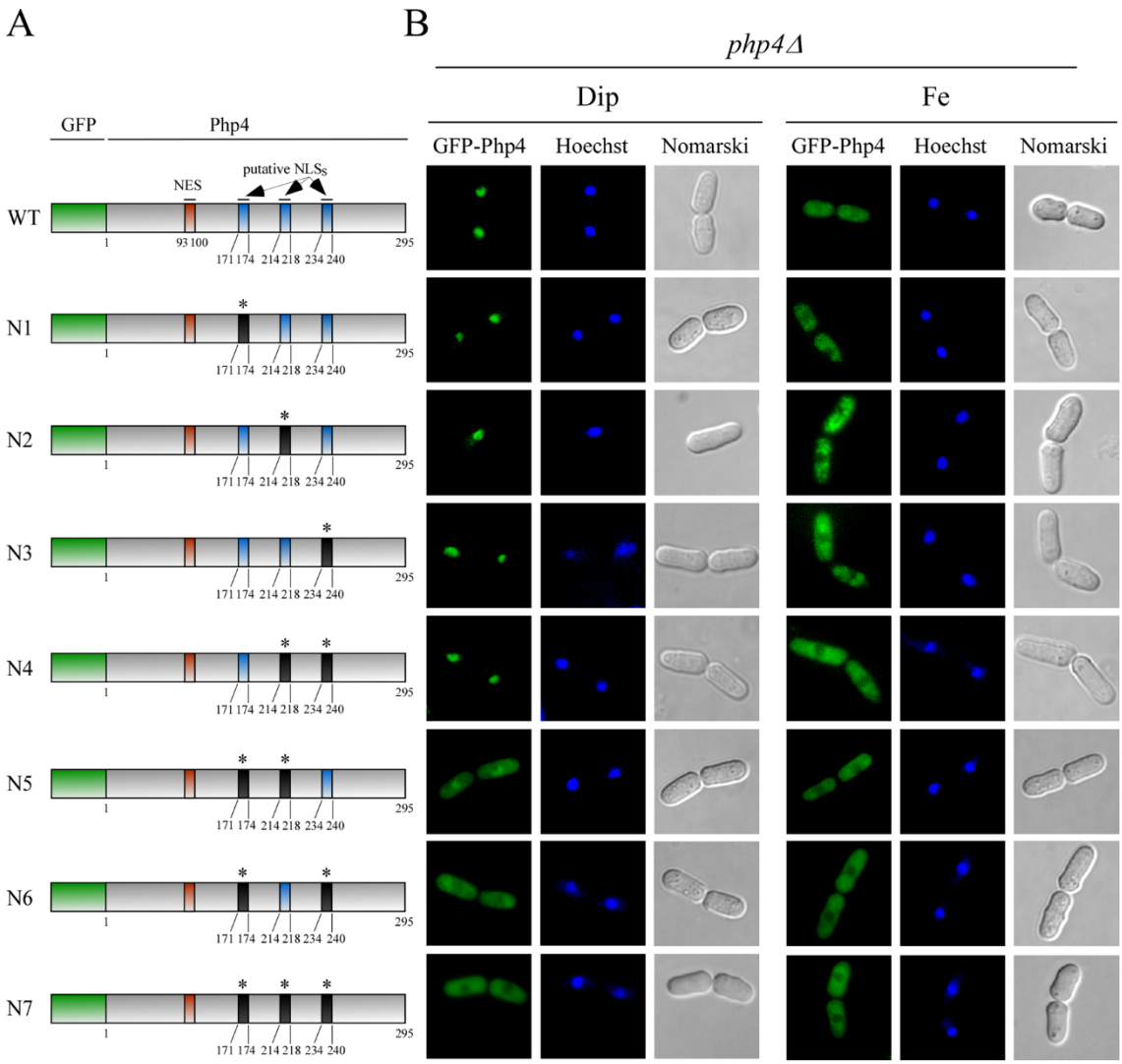

Figure 3 – Khan *et al.*

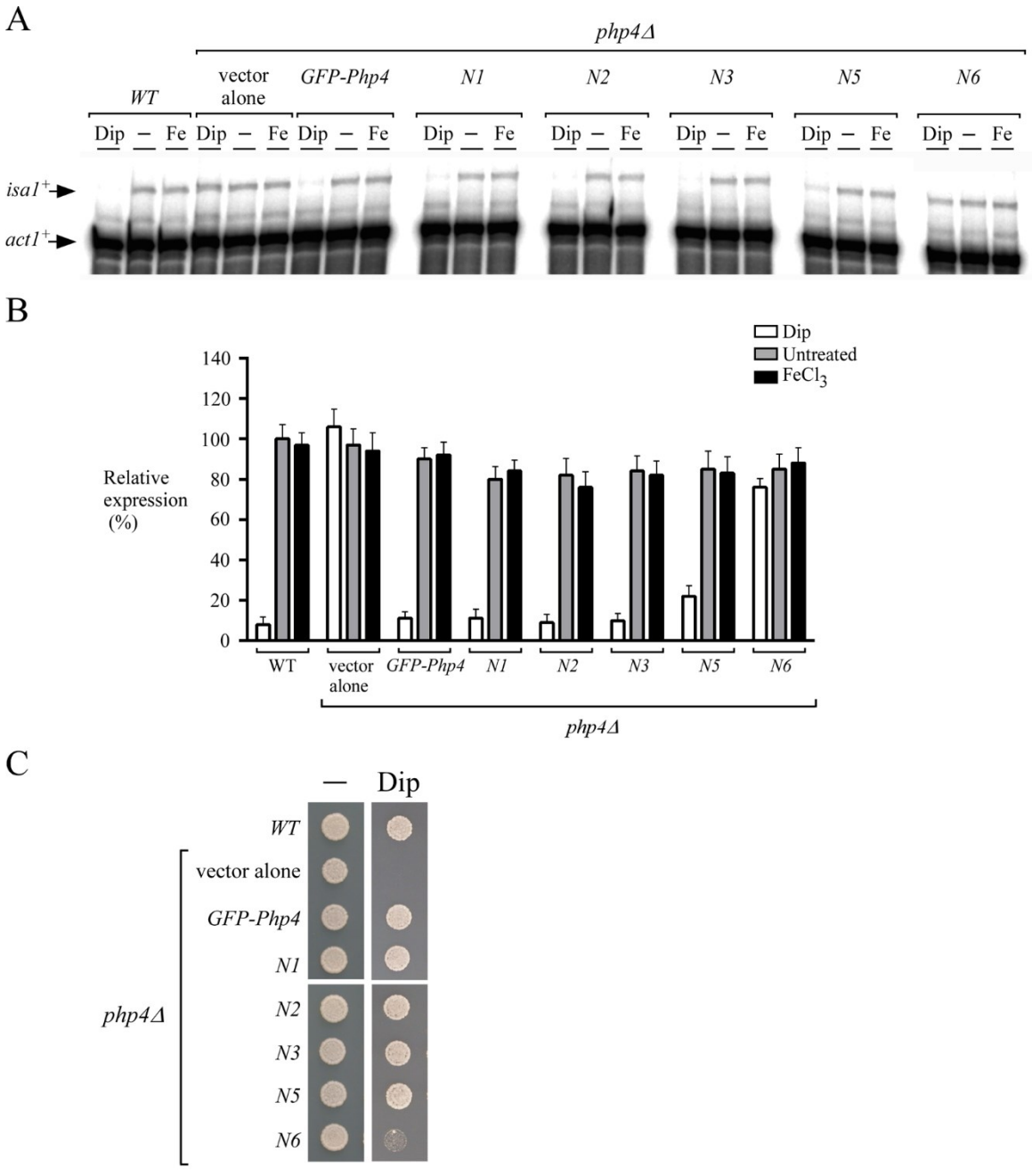

Figure 4 – Khan *et al.*

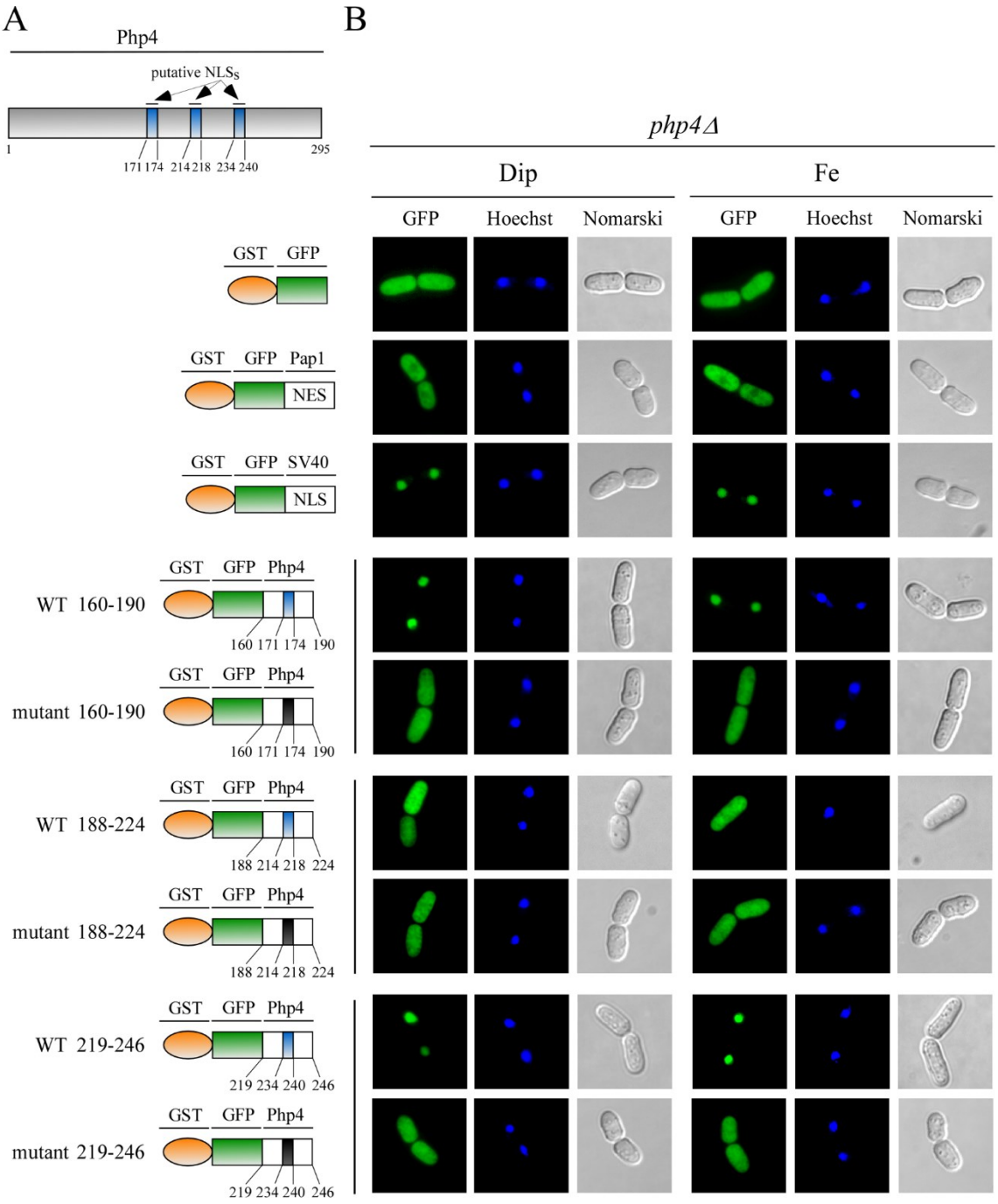

Figure 5 – Khan *et al.*

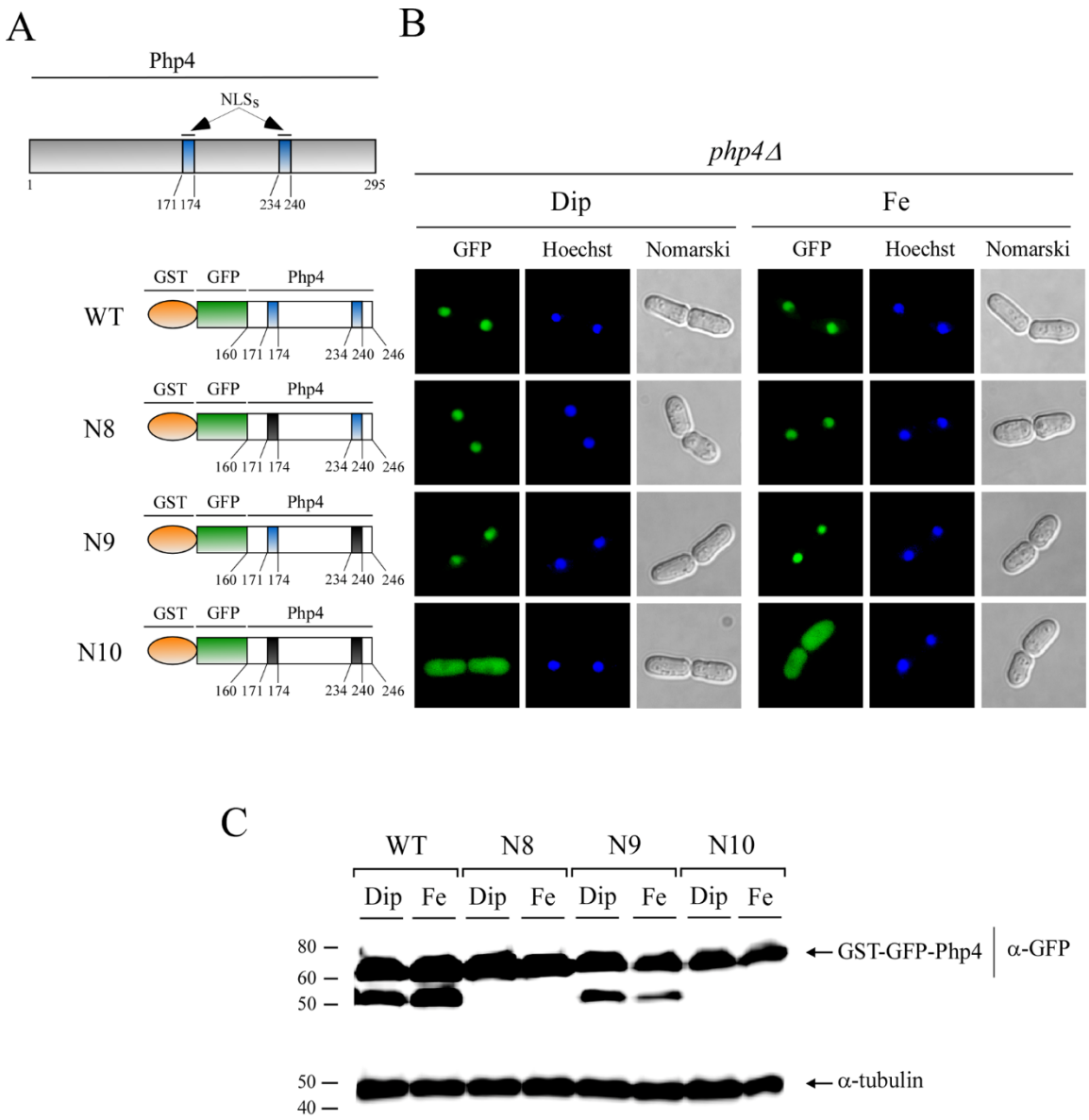

Figure 6 – Khan *et al.*

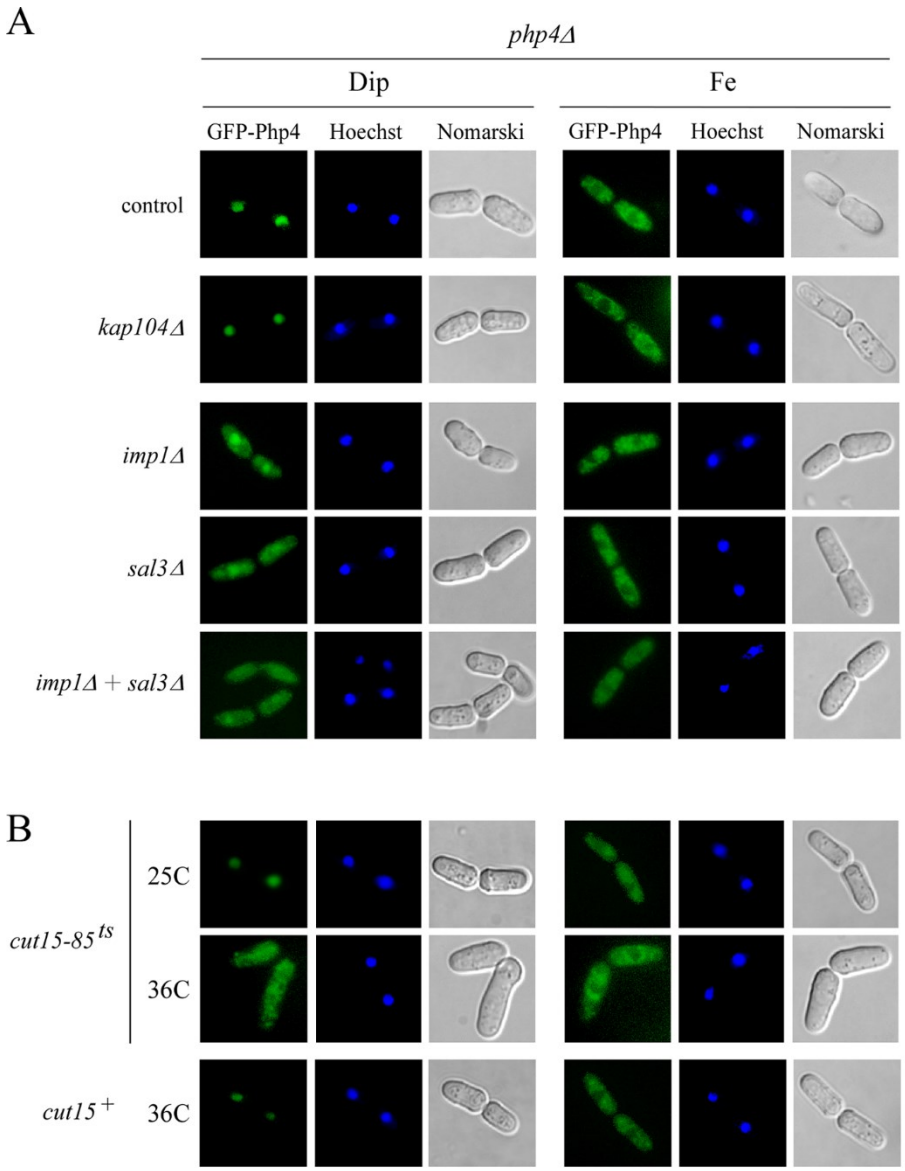

Figure 7 – Khan *et al.*

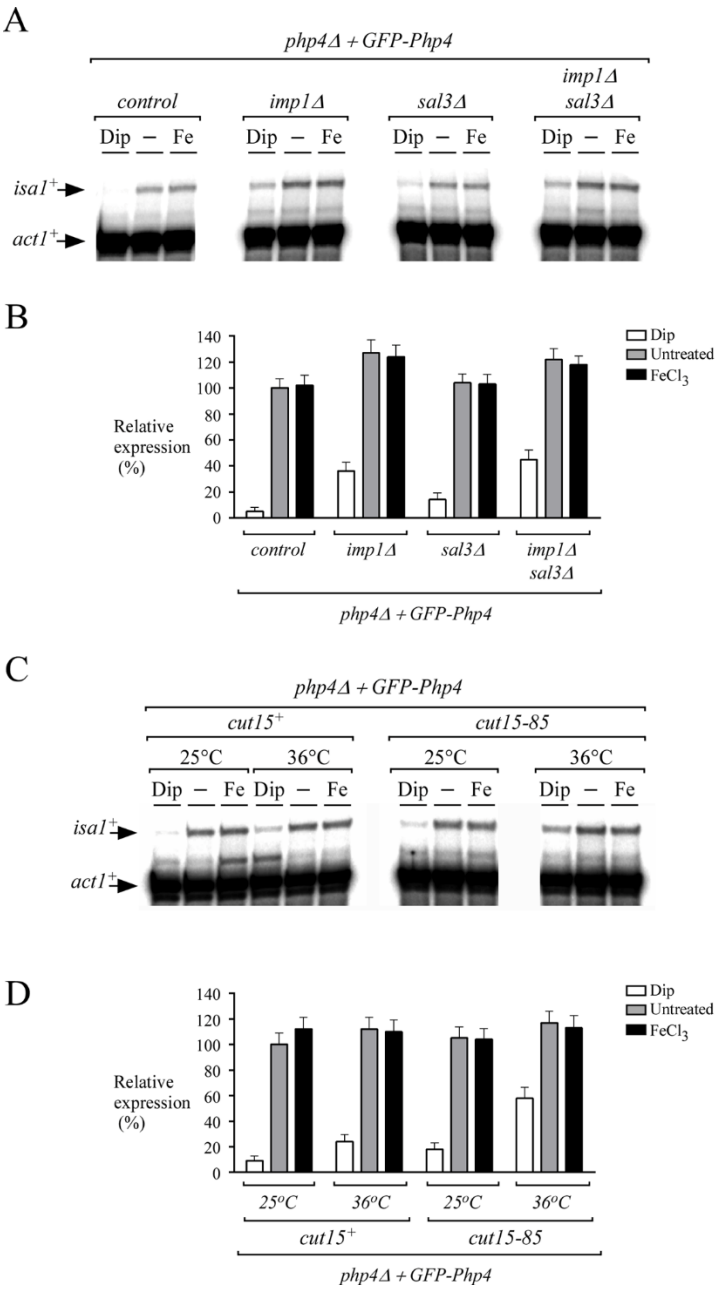

Figure 8 – Khan *et al.*

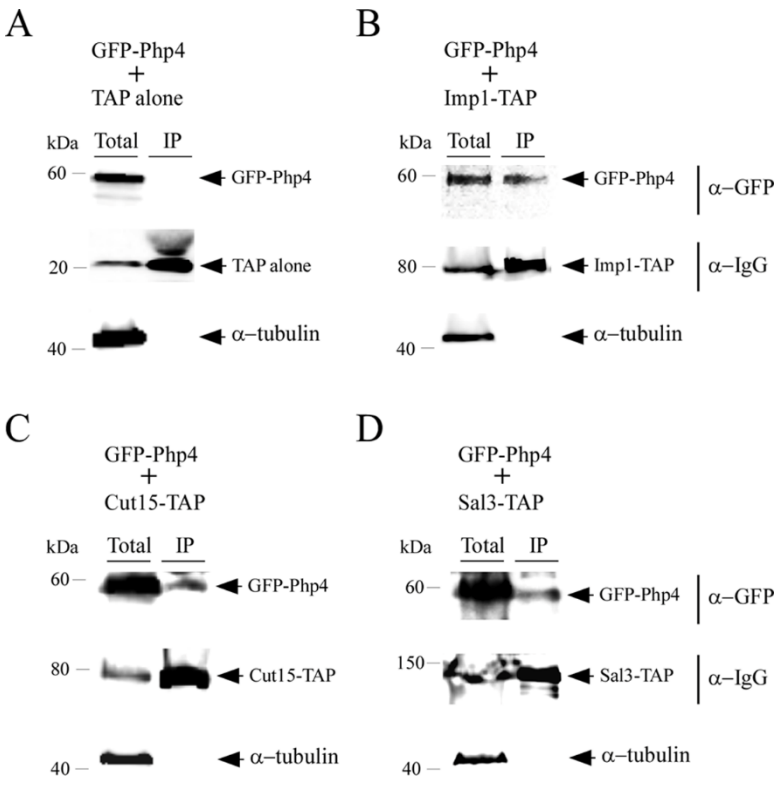

Figure 9 – Khan *et al.*

SUPPLEMENTAL DATA

Khan *et al.*

Figure S1. *Detection of intact GST-GFP and GST-GFP fusion proteins*.

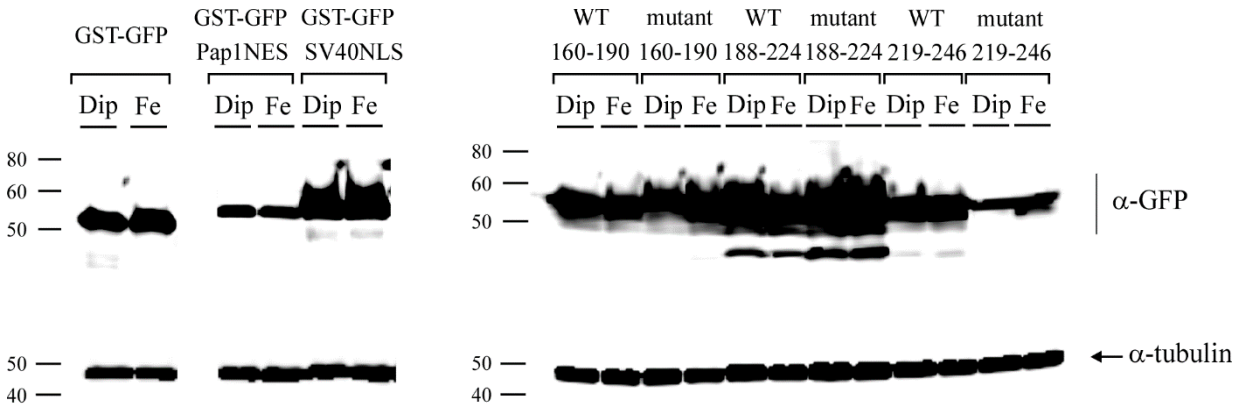

Figure S1. *Detection of intact GST-GFP and GST-GFP fusion proteins*. Cell lysates from aliquots of the cultures described in figure 5 were analyzed by immunoblotting using either anti-GFP or anti-α-tubulin (as an internal control) antibody. The positions of the molecular weight of protein standards (in kDa) are indicated on the left-hand side.

Figure S2. *Inactivation of imp1Δ, cut15-85 or sal3Δ resulted in increased expression of isa1*$^{+}$ *under iron starvation conditions.*

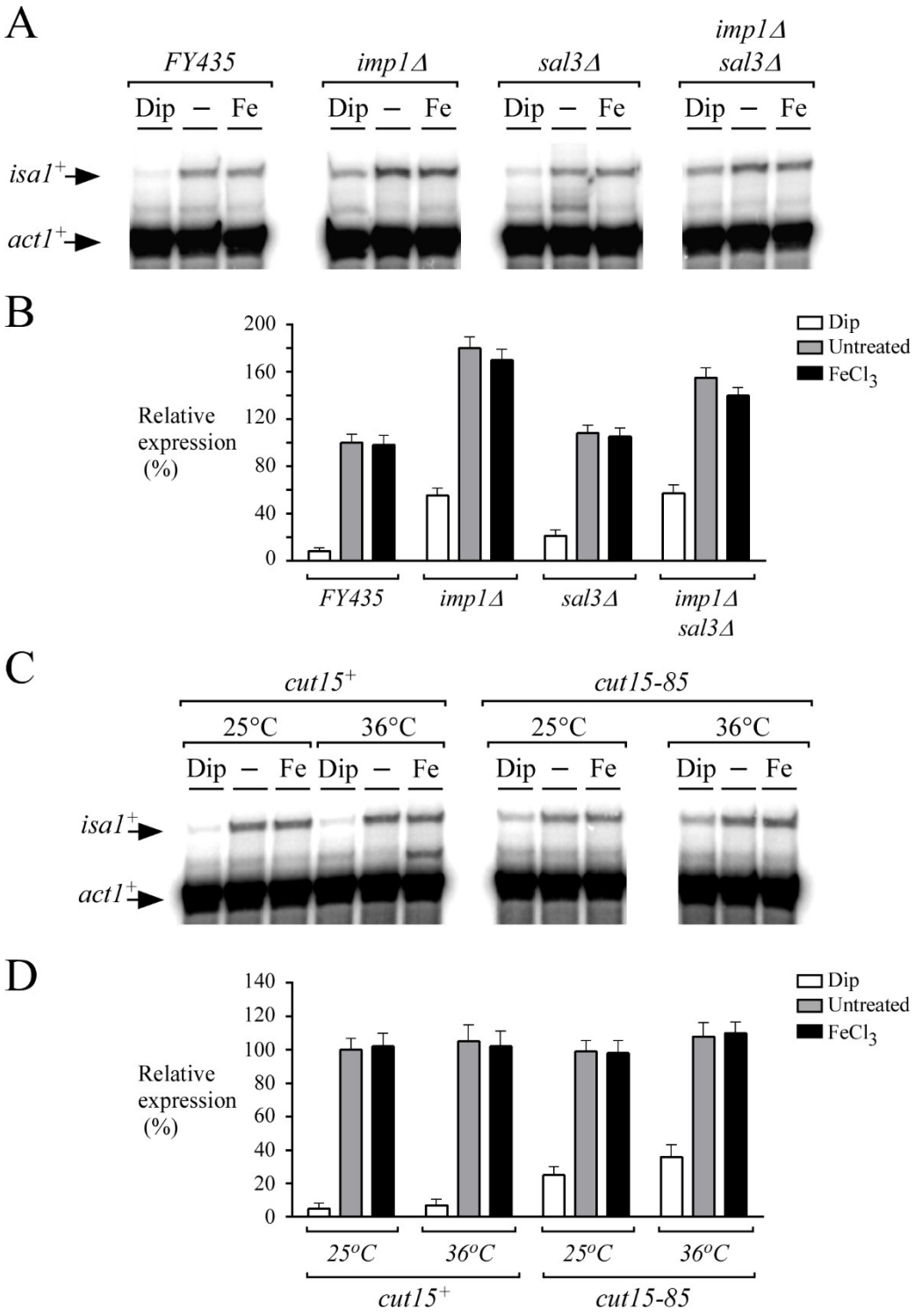

Figure S2. *Inactivation of imp1Δ, cut15-85 or sal3Δ resulted in increased expression of isa1*$^{+}$ *under iron starvation conditions. A*, The indicated strains containing an endogenous Php4 were assessed for their ability to repress *isa1*$^{+}$ gene expression in the presence of Dip (250 μM) versus basal (-) or iron-replete (Fe, 100 μM) conditions. After 90 min of treatment, total RNA was prepared and then analyzed by RNase protection assays. Steady-state levels of *isa1*$^{+}$ and *act1*$^{+}$ mRNAs are shown with arrows. *B*, Quantification of three independent RNase protection assays, including the experiment shown in panel A. *C*, *cut15*$^{+}$ and *cut15-85* strains expressing an endogenous Php4 were grown to mid-logarithmic phase and then were divided into four aliquots which were treated with Dip (250 μM) or $FeCl_3$ (100 μM) at permissive (25ºC) or nonpermissive (36ºC) temperature. After 3 h, total RNA was extracted and used in RNase protection protocol to determine *isa1*$^{+}$ and *act1*$^{+}$ mRNA levels. When indicated (-), cells were left untreated. *D*, Quantification of *isa1*$^{+}$ transcript levels after treatments. Data are shown as the mean values of triplicate ± standard deviations.

DISCUSSION

In the previous section, I described the results of my study that I have generated during my tenure of master research. During this time, I have also generated other results that raise important research questions regarding iron homeostasis in the fission yeast. In the following sections, I will focus on those issues regarding my observations and some other research perspectives. Given these observations into consideration, it could open new doors for future research that would resolve some unanswered questions in the field of iron homeostasis.

1. Role of other karyopherin β in the recognition of Php4 NLSs

In this study, we have determined that nuclear import of the iron-responsive transcription factor Php4 depends on two kap α (Cut15 and Imp1) and one kap β (Sal3) (KHAN *et al.* 2014). In fission yeast, 12 kap β have been acknowledged through the *S. pombe* genome (WOOD *et al.* 2002); thus far, a majority of them are uncharacterized. In the result section, we have shown that another kap β, Kap104, has no implication in Php4 import as it has a strong affinity for PY-NLS. Therefore, we cannot rule out the possibility of other kap β could contribute to the efficient nuclear import of Php4.

Generally, β karyopherins directly recognize NLSs in cargo proteins. In a classical mechanism, importin α acts as an adaptor that can recognize NLSs in the cargo proteins as well as facilitates binding of importin β through its importin beta-binding domain (IBB). Importin β then functions in the docking on NPC, thus mediating nuclear import of cargo protein through the NPC (GÖRLICH *et al.* 1995). Structural analysis reveals that Importin α contains several tandem armadillo repeats (ARMs) which produce a curving structure, therefore facilitating binding to classical NLSs (cNLSs) bearing cargos. Conversely, the N-

teminus of importin α contains a flexible arginine-rich IBB domain that is responsible for binding importin β, generating the importin α/β heterodimer (GÖRLICH *et al.* 1996; GOLDFARB *et al.* 2004). Interestingly, Cut15 and Imp1 also possess a conserved IBB domain and are known to be the only ones IBB-containing proteins in *S. pombe* (UMEDA *et al.* 2005). This infers a strong possibility that other kap βs might interact with the two importin αs through their IBB-domain and contribute to the Php4 nuclear import.

Kap95 is a potential kap β candidate that might participate in the nuclear import of Php4. Its ortholog in *S. cerevisiae*, Kap95, can import a set of cargo proteins bearing cNLSs through NPC with the aid of importin α: importin α/β heterodimer (MACKINNON *et al.* 2009; TABERNER and IGUAL 2010; PELÁEZ *et al.* 2012). Studies on the role of Kap95 in *S. pombe* are still in its infancy. However, the presence of IBB domains in Cut15 and Imp1 implies a strong possibility for their association with Kap95 during nuclear import of cargo proteins. Another possibility is that Kap95 can directly recognize NLSs without using kaps α as adaptor molecules like it has been found in budding yeast (YOSHIDA and BLOBEL 2001; FERNÁNDEZ-CID *et al.* 2012). Consistent with a role of Kap95 in nuclear import of many transcription factors in *S. cerevisiae*, we cannot exclude the participation of *S. pombe* Kap95 in the nuclear import of Php4.

In this study, if we could observe a complete abolishment of Php4 nuclear import in mutant cells lacking Imp1, Sal3 and Cut15 (*imp1Δ cut15 Δ sal3Δ*), it would be easy to rule out the participation of other karyopherins. Unfortunately, it is not possible to generate such a mutant, as simultaneous mutation in *imp1* and *cut15* is synthetically lethal for *S. pombe* cells (UMEDA *et al.* 2005). However, we could construct different *kap β* null mutant cells and through florescence microscopy, we could track the effect of knocking out other *kap β*s on

the nuclear import of Php4. Some kap βs in *S. pombe* are essential for its survival (e.g. Kap 95). In those cases, we could generate mutant cells by replacing essential *kap β* genes with their corresponding temperature sensitive alleles or use an inducible/repressible promoter for shutting down expression of essential *kap β* genes for only few hours.

2. Validation of Php4 subcellular localization with a small tag

Cargo proteins larger than 40 kDa are unable to shuttle through NPC without an active nuclear transport receptor (LIM *et al.* 2006). In contrast, a majority of smaller proteins (<40 kDa) can passively diffuse through the NPC (BREEUWER and GOLDFARB 1990; MARFORI *et al.* 2011). Php4 itself is a small protein (~27 kDa) consisting of only 295 amino acids. In this study, we have always used the GFP-Php4 fusion protein or its mutant derivatives for tracking subcellular localization of Php4. The predicted mass of the GFP-Php4 fusion protein is around 59.8 kDa, which is larger than NPC cut-off. Moreover, we have shown that other subunits of CCAAT-binding complex (CBC) are not responsible for Php4 nuclear import. Despite having NLSs, we cannot rule out the possibility that a smaller form of Php4 (untagged) could passively diffuse through the NPC even under iron-replete conditions. So, we have done further experiments to confirm results with a smaller tag (HA3) for which the molecular size issue will not apply.

To assess whether a smaller tag (HA3) fused with Php4 had the ability to trigger nuclear import as like GFP-Php4, *php4Δ* mutant cells were transformed with an integrative plasmid harboring a *HA3-php4*$^{+}$ allele constitutively expressed from a GATA-less *php4*$^{+}$ promoter. Cells expressing HA3-Php4 were grown under basal conditions to mid-logarithmic phase and

then treated with the iron chelator Dip or with $FeCl_3$ for 3 hours. Indirect fluorescence microscopy showed that in the presence of Dip, HA3-Php4 efficiently accumulated in the nucleus of cells. In contrast, in the case of cells treated with $FeCl_3$, HA3-Php4 was observed primarily in the cytoplasm (Figure 10). These results correlate with identical observations found for subcellular localization of GFP-Php4 (see Figure 1 in result section). Furthermore, no passive diffusion of HA3-Php4 was observed in the presence of iron. The levels of *isa1*$^+$ expression (a Php4 target gene) were regulated as a function of iron availability in an identical manner as observed in a wild-type strain or a *php4Δ* mutant strain expressing GFP-Php4 (unpublished data). These results suggest that a smaller tag does not influence the ability of Php4 to be imported in the nucleus in response to iron deficiency.

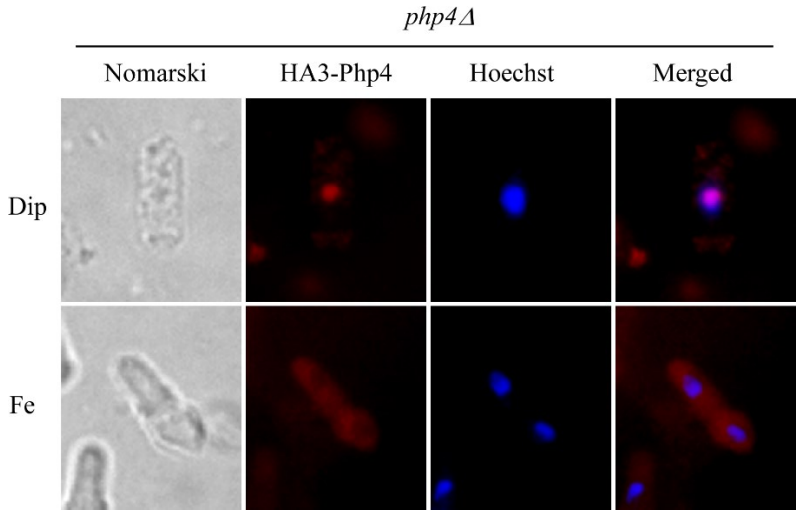

Figure 10. Iron-responsive nucleo-cytoplasmic trafficking of HA3-Php4. *php4Δ* mutant cells were transformed with an integrative vector expressing *HA3-php4*$^+$allele under the control of a GATA-less *php4*$^+$ promoter. Transformed cells were treated with either Dip (250 μM) or $FeCl_3$ (Fe) (100 μM) for 3 h. Cells were analyzed by indirect immunofluorescence microscopy for subcellular localization of a functional HA3-Php4 fusion protein. Nuclear DNA was visualized by Hoechst staining whereas Nomarski optics (Nomarski) was used to reveal cell morphology. Merged images are shown in the far right column of the panels.

3. Php4 NLSs specificity for karyopherins

Nuclear import of protein requires the interaction of karyopherins β directly or indirectly where importin α recognizes and binds cargos, and then recruits karyopherins β. In both cases, nuclear localization sequences (NLSs) are required for the import process by karyopherins. In this study, we have shown that three karyopherins are responsible to recognize two NLSs of Php4. However, at this point, we do not know if these karyopherins exhibit a preference for the first NLS or the second NLS found in Php4. Further studies are required to determine the karyopherin specificity or recognition preference for the two identified NLSs that are involved in the nuclear import of Php4. It is possible that the presence of two NLSs might allow more precise control of Php4 nuclear import, ensuring its proper nuclear localization in response to iron starvation conditions.

We already observe that the two NLSs in Php4 (^{171}KRIR^{174} and ^{234}KSVKRVR^{240}) possess high sequence homology with one of the six identified classes of NLSs (KOSUGI *et al.* 2009), especially those recognized by importin α. Furthermore, it is already known that Cut15 and Imp1 could recognize common NLSs in cargo proteins (UMEDA *et al.* 2005). So, we could envision that both NLSs in Php4 are recognized simultaneously by Cut15 and Imp1. Now, it would raise a question that how Sal3 participates in the nuclear import of Php4? Does it bind to both NLSs directly or does it associates with one importin α through its IBB domain? In the result section, we have shown that in *sal3Δ* mutant cells, Php4 is still able to accumulate within the nucleus, which implies a possibility that Sal3 is not required for Cut15 and Imp1 in the nuclear import process of Php4. This reinforce the possibility of a participation of other kaps β in the import of Php4. To gain more insight regarding a NLS preference in Php4 by a given karyopherin, experiments could be designed to assess if one NLS region of Php4 has

the ability to be imported within the nucleus by a specific karyopherin mutant. For this, Php4 160–190 (bearing the NLS ^{171}KRIR^{174}) and Php4 219–246 (bearing the NLS ^{234}KSVKRVR^{240}) regions will be fused with GST-GFP and express under the control of the thiamine-regulated promoter. Each construct will be separately express in different mutant cells: *imp1Δ, sal3Δ* or *cut15-85^{ts}*. If we observe an abolishment in the nuclear accumulation in any of the mutant strain expressing GST-GFP-Php4 160-190 or GST-GFP-Php4 219– 246, it would mean that a given karyopherin specifically recognizes a particular NLS. If inactivation of *imp1^{+}, cut15^{+}* or *sal3^{+}* alter nuclear import of Php4 160–190 or Php4 219–246 fragment, we would further examine whether GFP-Php4 160-190 or GFP-Php4219– 246 could form complexes with Imp1, Cut15 or Sal3 *in vitro*. To test this possibility, we would investigate the capacity of each NLS in Php4 to interact with either one of the three karyopherins using TAP pull-down experiments. In these assays, we will use *imp1, sal3* and *cut15-85^{ts}* mutant cells in which we would co- express distinct pairs of fusion proteins, including GFP-Php4 160-190 or 219-246 and Imp1-TAP, GFP-Php4 160-190 or 219-246 and Cut15-TAP, GFP-Php4 160-190 or 219-246 and Sal3- TAP. Total cell extracts would be incubated with IgG-Sepharose beads that selectively bind with TAP-tagged proteins. Finally, Western blot analysis using an anti-GFP antibody would reveal the presence of GFP-Php4 160-190 or 219-246 in the immunoprecipitate fraction of cells expressing Imp1-TAP, Cut15-TAP or Sal3-TAP. These results would help to elucidate if there is any preference between a given NLS in Php4 and a particular karyopherin.

4. Assembly of other subunits of CBC: one-step or piggy-back mechanism?

Although we have learnt about iron-mediated subcellular localization of Php4 in *S. pombe* and the mechanism underlying its nuclear importation and exportation, it is still unknown how the other subunits of CBC (Php2, Php3 and Php5) assemble to form a heterocomplex in the nucleus. In budding yeast, the subunits of Hap-complex (Hap2, Hap3 and Hap5) assemble in a one-step pathway to form a DNA-binding heterotrimer (Hap2/Hap3/Hap4) (MCNABB and PINTO 2005). In other organisms, it has been found that Hap-complex assembly employs a two-step assembly mechanism as that of mammalian counterparts, termed CBF-A (Hap3p), CBF-B (Hap2p), and CBF-C (Hap5p) in rats or NFY-A (Hap2p), NFY-B (Hap3p), and NFY-C (Hap5p) in human (SINHA *et al.* 1995; MANTOVANI 1999). This mechanism was well demonstrated for filamentous fungi, including *A. nidulans* Hap complex where HapC and HapE form a heterodimer in a first step and then, HapB, which possesses a functional NLS imports the heterodimer into the nucleus in a piggy-back manner (STEIDL *et al.* 2004). In the case of CBC from *Aspergillus oryzae,* similar results support a two-step transport mechanism (GODA *et al.* 2005). As the fission yeast is evolutionary more connected to filamentous fungi, we also predict the presence of a similar piggy-back mechanism for the assembly of Php2, Php3 and Php5. The proposed model for piggy-back mechanism has been illustrated in Figure 11-A.

A

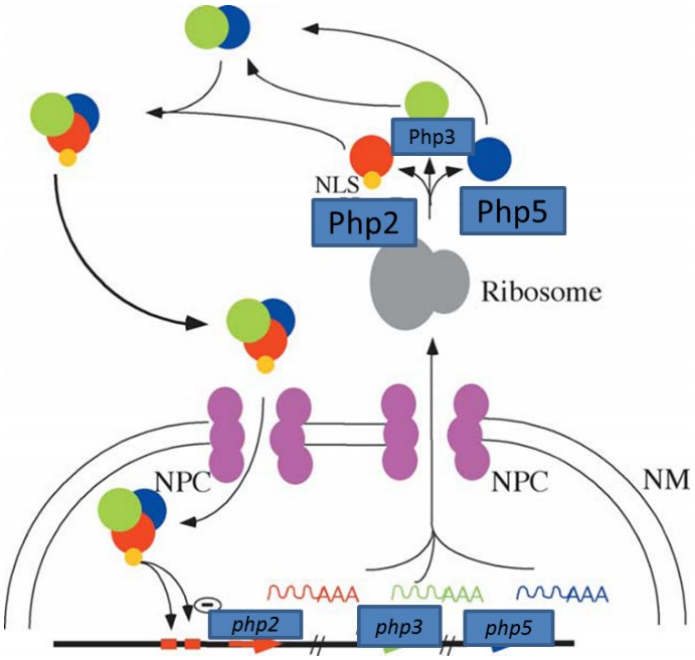

B

MNPYEPVEGLYVNAKQYHRILKRREARAKLEERLRGVQTTKKPYLHESRH	50
KHAMRRPRGPGGRFLTADKVSKLRAQEAAEAAANGGSTGDDVNATNANDA	100
TVPATVSSEVTHTSEGYADSNDSRPSSISNSSESPAPINSATASMSPANN	150
TSGNNITSPNVRGELDMSGNIAMSGGPTNTASTSGPVPHDMTVLPQTDSN	200
TSNLMSSGSQLGSFATASTNGNNSTTTTTSSAAHPGSFHKGTNDYSSTLA	250
GNEHSAFPGLDVYHDDSVSAGAAFIPHNPMDSIDHLDVNDPTATGLPVLP	300
ASDIDPLNLTGNTQDSMIIGQQTYPSHGSSGTMK	334

Figure 11. A) A proposed piggy-back model in *S. pombe:* A two-step mechanism may be employed for the assembly of Php2, Php3 and Php5 in which Php3 and Php5 form a heterodimeric complex in the first step and then, Php2 binds with Php3/5 subunits (assemble together) to mediate their nuclear import. **B) Amino acid sequence of Php2 exhibits potential NLSs.** Basic residue-rich regions are highlighted (red) and two predicted NLSs are underlined.

To test the proposed model we could design an experiment to determine the localization of Php2, Php3 and Php5 in each of the mutant strains *php2Δ, php3Δ,* and *php5Δ,* and compare

the localization pattern against a wild-type strain (Table 3). The cNLS mapper software predicts the presence of potential NLSs in Php2 (Figure 11-B), but not in Php3 and Php5. Therefore, it seems that Php3 and Php5 themselves cannot be transported within nucleus without Php2. Furthermore, *S. pombe* ORFeome database reveals a predominantly nuclear localization of Php2 (fused with YFP), although a small fraction of fluorescent signals were detected in microtubules. On the other hand, scattered fluorescence dots (mostly cytosolic, some in the nucleus) were observed for Php5-YFP, implying that this fusion protein was most likely non-functional. Unfortunately, no subcellular localization has been found for Php3 in the ORFeome database. The reason might be is low molecular weight of ~12.9, which makes the protein (Php3) very difficult to engineer with a fusion without affecting its function. To gain more insights about the localization of each of the subunit, we could fuse each of the three subunit with different reporter proteins (for example, Php2-GFP, Php3-HA3 and Php5-Myc13) and check the functionality of each fusion protein. Functionality of each of the fusion protein could be ascertained by tracking the down-regulation of *isa1*$^{+}$ at the mRNA level in response to iron depletion. The possible localization pattern for each of the subunit in different mutant strains has been hypothesized in Table-3. Given the fact that Php3 may associate with Php5 to form a heterodimer in the first step of a putative piggy-back mechanism, we could further investigate their capacity to interact *in vivo* by using a BiFC approach in fission yeast. In these experiments, Venus N-terminal fragment (VN) and Venus C-terminal fragment (VC) will be fused to the N- and C- terminal portions of Php3 and Php5, respectively. The functionality of VN-Php4 or Php5-VC fusion proteins would be verified by tracking the down-regulation of *isa1*$^{+}$ at the mRNA level in response to iron deficiency. Association between VN-tagged Php3 and VC-tagged Php5 will produce BiFC signal, indicating that formation of Php3-Php5 heterodimer. In *php2Δ* mutant cells, this BiFC signal

should be predominantly found in the cytosol due to the absence of the nuclear importer Php2. Finally, *in vitro* protein-protein interaction assays could be carried out to investigate the possibility that Php2 physically associated with Php3 and Php5 in *S. pombe.* Co-immunoprecipitation experiments could be performed in cells co-expressing *TAP-php2*$^{+}$*, php3*$^{+}$*-HA3* and *php5*$^{+}$*-Myc13*. In the case of piggy-back mechanism, TAP pull-down experiments will reveal that TAP-Php2 interacts with both Php3-HA3 and Php5-Myc13 to form a stable heteroprotein complex.

Table 3. Possible localization of Php2-GFP, Php3-HA3 or Php5-Myc13 in wild-type, *php2Δ, php3Δ,* and *php5Δ* strains that would support a piggy-back mechanism.

Strains	Php2-GFP	Php3-HA3	Php5-Myc13
Wild-type	Nuclear	Nuclear	Nuclear
php2Δ	Nuclear	Cytoplasmic	Cytoplasmic
php3Δ	Nuclear	Nuclear	Cytoplasmic
php5Δ	Nuclear	Cytoplasmic	Nuclear

5. Role of phosphorylation in the nuclear localization of Php4

Phosphorylation is one of the most frequent post-translational modification in cellular biology. It is involved in the regulation of many cellular processes, including control of nuclear trafficking of many cargo proteins. Phosphorylation either enhances the cargo binding affinities to Kaps or masks an NLS or NES, preventing their recognition by Kaps. Based on recent literature reviews, six different strategies have been defined by which phosphorylation of residues close to NLSs can up-regulate nuclear import of proteins (NARDOZZI *et al.* 2010). The mechanisms are as follows:

1) Phosphorylation within the NLS increases the binding affinity for importin α.
2) Phosphorylation facilitates docking of cargo proteins to the NPC.
3) Phosphorylation of serine residues upstream of cNLS enhances its recognition affinity by importin α.
4) Phosphorylation triggers conformational changes that expose a dimer-specific NLS (an unconventional NLS that only functions in the context of phosphorylation of STAT1 protein) thus facilitating nuclear importation.
5) Phosphorylation enhances nuclear import by unmasking a NLS as well as by masking a NES.
6) Phosphorylation can promote nuclear import by activating non-canonical NLS.

Phosphorylation of amino acid residues (mostly serine/threonine) adjacent to NLSs can modulate nucleo-cytoplasmic trafficking of a number of proteins (Table 4) (HARREMAN *et al.* 2004; NARDOZZI *et al.* 2010; RÓNA *et al.* 2013). In the case of Php4, its nuclear localization has been observed only under iron deficiency, whereas under iron-replete conditions, Php4 is inhibited by Grx4 and exported from the nucleus to the cytosol by Crm1 (MERCIER and LABBÉ 2009; KHAN *et al.* 2014). The presence of several serine residues adjacent to both functional NLSs in Php4 (Table 4) suggests a possibility that serine-phosphorylation might play a role in the nuclear import of Php4. NLS1 (^{171}KRIR^{174}) is located near three serine residues, which are at positions 169, 177 and 179. In the case of NLS2 (^{234}KSVKRVR^{240}), three serine residues at positions 231, 233 and 241 are found (Table 5). It can be envisioned that those serine residues in Php4 are potential candidates for phosphorylation. This phosphorylation event may be induced under low-iron conditions, which would subsequently facilitate the enhanced recognition of Php4 NLSs by karyopherins

α and β. To test this hypothesis, site-directed mutagenesis could be performed to substitute serine for alanine residues. Then mutated versions of Php4 could be fused to the reporter GFP and we could determine the effects of serine mutation in the nuclear import of Php4 under low-iron conditions. It will require further studies on the effect of serine phosphorylation (adjacent to both NLSs) of Php4 to learn how this modification may affect the docking of Php4 with karyopherins or its role in unmasking NLS. To address this possibility, we could design *in vitro* co-immunoprecipitation experiments to investigate the capacity of Php4 with serine mutation (near NLSs) to interact with three karyopherins (Sal3, Imp1 and Cut15) using TAP pull-down experiments. In these assays, we will use iron-starved cells co- expressing distinct pairs of fusion proteins, including GFP-Php4 (serine mutated) and Imp1-TAP, GFP-Php4 (serine mutated) and Cut15-TAP, GFP-Php4 (serine mutated) and Sal3- TAP or GFP-Php4 and TAP. Total cell extracts will be incubated in the presence of IgG-Sepharose beads that selectively bind unfused TAP or TAP-tagged proteins. If serine mutation near the NLSs of Php4 negatively modulate the interaction of Php4 with karyopherins, GFP-Php4 (serine mutation) will not be retained by the beads which would be confirmed by Western blot assays.

Table 4. List of several known cargo proteins nuclear localization sequences whose nuclear importation are regulated by phosphorylation

Cargo proteins bearing NLSs	Amino acid sequence of NLS including adjacent phosphorylation sites [a]	Nuclear importation regulation
EBNA-1 NLS	379 KRPRSPSS 386	Up-regulation
HBV core	149 VRRRDR…X(17)…SPRRRR 180	Up-regulation
SV40 T antigen	110 PSS…X(7)…S…X(5) …PKKKRKV 132	Up-regulation
STAT1-dsNLS	378 RK…X(30) …KEQKNAGTR…X(283) …Y 701	Up-regulation
DRAK2	344 EDDSLLSKRFRDDSLPSPHE 363	Up-regulation
Php4 NLS1	169SAKRIRVDSDS179	??
Php4 NLS2	230SGSPKSVKRVRES242	??
Msn2p	575 SSLRRKS…X(34)…RRPSYRRKSMTSRRSS 633	Down-regulation
NFATc1	241 RSSRPASPCNKRKYS 641	Down-regulation
Pho4-NLS	140 SANKVTKNKSNSSPYLNKRKGKPGPDS 166	Down-regulation
PTHrP-ncNLS	66 RYLTQETNKVETYKEQPLKTPGKKKKGKP 94	Down-regulation

[a] Basic amino acid sequences are colored in blue and phosphorylation sites are colored in red. In the case of Php4, potential serine residues are colored in green.

6. Role of Grx4 in iron sensing

We already addressed in the introduction that Php4 is inhibited by Grx4 at the post translational level under conditions of excess iron (MERCIER and LABBÉ 2009; VACHON *et al.* 2012). However, the molecular mechanism underlying the Grx4-mediated inhibition of Php4 is still unknown. It has been experimentally established that the GRX-like domain of Grx4 associates with Php4 in an iron-dependent manner. The 152-254 amino acid region of Php4 is required to coordinate this interaction under iron-replete conditions. Interestingly, two conserved cysteine residues (Cys 221 and Cys 227) located within Php4 (152-254) region are required for this iron-dependent interaction with the GRX-like domain of Grx4. Similarly,

it has been demonstrated that Cys 172 in the CGFS active site of the GRX-like domain is required for the interaction with Php4. Mutation of either of these three cysteine residues results in complete annihilation of the Php4-GRX domain interaction. Based on the previous findings, it can be hypothesized that under iron-replete conditions, Php4 might form an [2Fe-2S] cluster (Figure 12) with the GRX domain of Grx4, which would inhibit Php4 activity. This hypothetical [2Fe-2S] cluster is predicted to be coordinated by Cys 172 of Grx4, Cys 221 and 227 of Php4 and a fourth cysteine residues from glutathione (GSH). According to this proposed model, it is possible that in the presence of iron, Grx4 ligated with a [2Fe-2S] cluster leads to its association with Php4 through the GRX-like domain. This interaction would induce conformational changes that subsequently inhibit the ability of Php4 to suppress the transcription.

It is worth to test the predicted [2Fe-2S] cluster coordinated by Grx4 and Php4. For this, an experiment can be designed to determine the ability of purified, bacterially expressed forms of both proteins if they could physically associate in an *in vitro* system. Co-expression and co-purification of Grx4 with Php4 will be accomplished based on the procedures described previously (LI *et al.* 2009a). *In vitro* Fe-S reconstitution of Grx4 and Php4 protein will be done anaerobically after treating them with different concentration of dithionate, which maintains Fe-S cluster. UV-visible absorption spectra will be recorded under anaerobic conditions using a spectrophotometer. UV-visible absorption will also reveal differences in the cluster coordination environment for Grx4 co expressed with Php4 with Cys residues mutants. This will validate the role of Cys 221 and Cys 227 of Php4 and Cys 172 of Grx4 in the coordination of [2Fe-2S] cluster.

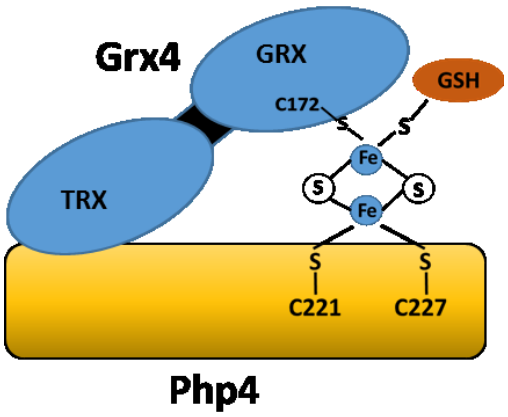

Figure 12. Proposed [2Fe-2S] cluster model. The putative [2Fe-2S] cluster is coordinated by Cys172 of Grx4, Cys221 and Cys227 of Php4, and the cysteine residue of one molecule of glutathione (GSH).

7. Php4 as an antifungal therapeutic target

The *cis*-acting regulatory sequence CCAAT is a very common regulatory element found upstream of 30% of eukaryotic genes, ranging from yeast to mammals (BUCHER 1990; MANTOVANI 1999). An evolutionary conserved transcription factor complex, the CCAAT-binding complex (CBC), specifically recognizes the CCAAT motif and modulates transcription directly or along with other transcription factors (MANTOVANI 1999). Depending on the organism, a positive or negative regulation of the CBC target genes has been observed. The CBC is designated under different names in different organisms. These include the Hap complex in *S. cerevisiae, Aspergillus nidulans, Candida albicans, Cryptococcus neoformans,* and *Arabidopsis thaliana* (PINKHAM and GUARENTE 1985; EDWARDS *et al.* 1998; BRAKHAGE *et al.* 1999; JOHNSON *et al.* 2005; JUNG *et al.* 2010), the Php complex in *S. pombe* (MCNABB *et al.* 1997), and the NF-Y complex in mammals (MAITY *et al.* 1990). In pathogenic yeasts, an exclusive connection between CBC and the regulation of virulence traits has been established in the last decade. On the other hand, due to the limited

availability of current antifungal therapeutic agents, CCAAT binding factors are considered as a lucrative target for future research for developing novel antifungal drugs.

The model organism S. pombe shares many cellular features with filamentous pathogenic yeasts. The availability of genomic resources of S. pombe as well as advanced molecular approaches make fission yeast an excellent model for the investigation of novel antifungal drugs. Iron homeostasis in S. pombe has been extensively studied over the last decade. Interestingly, optimized utilization of iron and lack of bioavailable iron in hosts represent the important virulence attributes for most pathogenic yeasts. As addressed in the introduction section, all four subunits of the CBC in S. pombe, including the iron-responsive transcription factor Php4, are well conserved in some pathogenic yeasts. Interestingly, we have shown that Php4 is obligatory for the survival of S. pombe under iron-depleted conditions (Figure 4C in the Result section). php4Δ mutant cells cannot grow under low-iron conditions. Similar observations have been found for other filamentous and pathogenic yeasts under low-iron conditions where Php4 orthologs are conserved. In fact, Php4 ortholog HapX (A. fumigatus) and Hap43 (C. albicans) are important virulence factors (BAEK et al. 2008; SCHRETTL et al. 2010). Due to the high sequence homology and functional similarities, inhibition of Php4 orthologs in pathogenic yeasts could be an important strategy for future antifungal drug developments. Furthermore, Php4 possesses a conserved region encompassing amino acids 28-42 that would be critical for its association to the Php2/3/5 heterocomplex (MCNABB and PINTO 2005; LABBÉ et al. 2007). This motif is highly conserved across other Php4 orthologs present in filamentous and pathogenic fungi (Alex Mercier PhD Thesis). This strong sequence homology offers promising prospects for designing antagonistic molecules (small peptides) that could prevent the binding of Php4 orthologs in pathogenic yeast to other

components of CBC. Thus, the failure of Php4 orthologs to interact with the DNA-binding CBC complex results in the loss of target gene expression as well as virulence properties. Moreover, absence of Php4 orthologs in other eukaryotes and mammals represents it as a unique, potential and specific fungal target for antifungal drug development.

Inhibition of nuclear import of Php4 orthologs could be another strategy for antifungal drug design. For example, introducing small peptides resembling NLS sequences could be an effective strategy to compete with karyopherins receptors and inhibit the nuclear import of Php4 orthologs. In this study, we characterize the NLSs of Php4, which are crucial for its nuclear import and subsequent triggering of iron-mediated transcriptional repression under iron-depleted conditions. Although nuclear import mechanism of other Php4 orthologs in pathogenic yeasts has not yet characterized, cNLS mapper software indicates the presence of potential NLSs in Php4 orthologs of pathogenic yeasts (Table 5). This may suggest the presence of a similar nuclear import mechanism in pathogenic yeasts as that of S. pombe. So, it deserves further studies to determine the functionality of the predicted NLSs as well as to understand detail molecular mechanism underlying the nuclear import of Php4 orthologs in pathogenic yeasts. It is of paramount importance to determine crystallographic structure of Php4, which could provide deep insights in designing potential antifungal drugs.

Table 5. Predicted NLSs in Php4 orthologs in pathogenic yeasts

Pathogenic yeast/fungi	Php4 orthologs	Potential NLSs
C. albicans	Hap43 (CaO19.681)	^{85}PAS**KRK**AQN**R**^{94}(monopartite) ^{315}LS**RKRK**I**K**ST^{324}(monopartite)
A. oryzae	HapX (BAB47239)	^{61}PPT**KRK**AQN**R**^{70}(monopartite) ^{48}**R**P**K**PG**RK**PATDTPPT**KRK**A^{67}(bipartite)
A. nidulans	HapX (XM_676428.1)	^{60}PPT**KRK**AQN**R**^{69}(monopartite) ^{47}P**R**P**K**PG**RK**PATDTPPT**KRK**A^{66}(bipartite)
A. fumigatus	HapX (XM742859.1)	^{57}PPT**KRK**AQN**R**^{66}(monopartite) ^{44}P**R**P**K**PG**RK**PATDTPPT**KRK**A^{63}(bipartite)
C. neoformans	HapX (CNAG_01242	^{706}D**R**ES**KRRR**IE^{715}(monopartite)

*Basic residues of potential NLSs are indicated in bold font.

ACKNOWLEDGEMENTS

My first and sincere gratitude goes to my supervisor, Professor Simon Labbe for welcoming me in his laboratory. His constant encouragement, scientific guidance, rigorous scientific training and stimulating discussions help me to sustain my interest and effort throughout the entire course of my research project. I am also indebted to Jean-Francois Jacques and Jude Beaudoin for their supportive discussions and constructive suggestions in improving my research work. I would like to express my gratitude to all the past and present members in the lab, in particular, Philippe Vachon, for teaching me all the techniques when I joined the lab, Raphael Ioannoni (wine specialist), for his extensive valuable discussions and suggestions to my project. Thanks to Thierry Mourer, Ariane Brault, Samuel Plante and Vincent Normant because my everyday interactions with them contributed immensely to the development of my scientific self-confidence. I would like to thank Professor Xavier Roucou for mentoring my M.Sc. I am thankful to Steve Mcdonald for critically reading this manuscript and giving valuable suggestions. Again, I want to mention the name of Professor Xavier Roucou with Professor Jean-Luc Parent for their efforts in reviewing my work and memory. I also want to thank La Faculté de médecine et des sciences de la santé of the Université de Sherbrooke selecting me for faculty studentship. Finally, special thanks go to my parents, my wife, my son and all my family members for their love, guidance, patience and for supporting me in any respect throughout my life.

REFERENCES

ALAO J. P., SUNNERHAGEN P., 2008 Rad3 and Sty1 function in Schizosaccharomyces pombe: an integrated response to DNA damage and environmental stress? Mol. Microbiol. **68**: 246–54.

AN Z., MEI B., YUAN W. M., LEONG S. A., 1997a The distal GATA sequences of the sid1 promoter of Ustilago maydis mediate iron repression of siderophore production and interact directly with Urbs1, a GATA family transcription factor. EMBO J. **16**: 1742–50.

AN Z., ZHAO Q., MCEVOY J., YUAN W. M., MARKLEY J. L., LEONG S. A., 1997b The second finger of Urbs1 is required for iron-mediated repression of sid1 in Ustilago maydis. Proc. Natl. Acad. Sci. U. S. A. **94**: 5882–7.

ASKWITH C., EIDE D., HO A. VAN, BERNARD P. S., LI L., DAVIS-KAPLAN S., SIPE D. M., KAPLAN J., 1994 The FET3 gene of S. cerevisiae encodes a multicopper oxidase required for ferrous iron uptake. Cell **76**: 403–10.

ASKWITH C., KAPLAN J., 1997 An Oxidase-Permease-based Iron Transport System in Schizosaccharomyces pombe and Its Expression in Saccharomyces cerevisiae. J. Biol. Chem. **272**: 401–405.

ASKWITH C., KAPLAN J., 1998 Iron and copper transport in yeast and its relevance to human disease. Trends Biochem. Sci. **23**: 135–8.

BAEK Y.-U., LI M., DAVIS D. A., 2008 Candida albicans ferric reductases are differentially regulated in response to distinct forms of iron limitation by the Rim101 and CBF transcription factors. Eukaryot. Cell **7**: 1168–79.

BANDYOPADHYAY S., GAMA F., MOLINA-NAVARRO M. M., GUALBERTO J. M., CLAXTON R., NAIK S. G., HUYNH B. H., HERRERO E., JACQUOT J. P., JOHNSON M. K., ROUHIER N., 2008 Chloroplast monothiol glutaredoxins as scaffold proteins for the assembly and delivery of [2Fe-2S] clusters. EMBO J. **27**: 1122–33.

BEAUDOIN J., EKICI S., DALDAL F., AIT-MOHAND S., GUÉRIN B., LABBÉ S., 2013 Copper transport and regulation in Schizosaccharomyces pombe. Biochem. Soc. Trans. **41**: 1679–86.

BELLORINI M., ZEMZOUMI K., FARINA A., BERTHELSEN J., PIAGGIO G., MANTOVANI R., 1997 Cloning and expression of human NF-YC. Gene **193**: 119–25.

BLACKSHEAR P., 2001 Tristetraprolin and other CCCH tandem zinc-finger proteins in the regulation of mRNA turnover.

BLAISEAU P. L., LESUISSE E., CAMADRO J. M., 2001 Aft2p, a novel iron-regulated transcription activator that modulates, with Aft1p, intracellular iron use and resistance to oxidative stress in yeast. J. Biol. Chem. **276**: 34221–6.

BRAKHAGE A. A., ANDRIANOPOULOS A., KATO M., STEIDL S., DAVIS M. A., TSUKAGOSHI N., HYNES M. J., 1999 HAP-Like CCAAT-binding complexes in filamentous fungi: implications for biotechnology. Fungal Genet. Biol. **27**: 243–52.

BREEUWER M., GOLDFARB D. S., 1990 Facilitated nuclear transport of histone H1 and other small nucleophilic proteins. Cell **60**: 999–1008.

BUCHER P., 1990 Weight matrix descriptions of four eukaryotic RNA polymerase II promoter elements derived from 502 unrelated promoter sequences. J. Mol. Biol. **212**: 563–78.

BYERS B. R., ARCENEAUX J. E., 1998 Microbial iron transport: iron acquisition by pathogenic microorganisms. Met. Ions Biol. Syst. **35**: 37–66.

CHANG F., NURSE P., 1996 How fission yeast fission in the middle. Cell **84**: 191–4.

CHEN J.-S., BROADUS M. R., MCLEAN J. R., FEOKTISTOVA A., REN L., GOULD K. L., 2013 Comprehensive proteomics analysis reveals new substrates and regulators of the fission yeast clp1/cdc14 phosphatase. Mol. Cell. Proteomics **12**: 1074–86.

CHEN X. Z., PENG J. B., COHEN A., NELSON H., NELSON N., HEDIGER M. A., 1999 Yeast SMF1 mediates H(+)-coupled iron uptake with concomitant uncoupled cation currents. J. Biol. Chem. **274**: 35089–94.

CHOOK Y. M., BLOBEL G., 2001 Karyopherins and nuclear import. Curr. Opin. Struct. Biol. **11**: 703–15.

CHUA G., LINGNER C., FRAZER C., YOUNG P. G., 2002 The sal3(+) gene encodes an importin-beta implicated in the nuclear import of Cdc25 in Schizosaccharomyces pombe. Genetics **162**: 689–703.

COHEN A., NELSON H., NELSON N., 2000 The family of SMF metal ion transporters in yeast cells. J. Biol. Chem. **275**: 33388–94.

CONTE D., NARINDRASORASAK S., SARKAR B., 1996 In vivo and in vitro iron-replaced zinc finger generates free radicals and causes DNA damage. J. Biol. Chem. **271**: 5125–30.

COUREL M., LALLET S., CAMADRO J.-M., BLAISEAU P.-L., 2005 Direct activation of genes involved in intracellular iron use by the yeast iron-responsive transcription factor Aft2 without its paralog Aft1. Mol. Cell. Biol. **25**: 6760–71.

DANCIS A., KLAUSNER R. D., HINNEBUSCH A. G., BARRIOCANAL J. G., 1990 Genetic evidence that ferric reductase is required for iron uptake in Saccharomyces cerevisiae. Mol. Cell. Biol. **10**: 2294–301.

DANCIS A., ROMAN D. G., ANDERSON G. J., HINNEBUSCH A. G., KLAUSNER R. D., 1992 Ferric reductase of Saccharomyces cerevisiae: molecular characterization, role in iron uptake, and transcriptional control by iron. Proc. Natl. Acad. Sci. U. S. A. **89**: 3869–73.

DANCIS A., YUAN D. S., HAILE D., ASKWITH C., EIDE D., MOEHLE C., KAPLAN J., KLAUSNER R. D., 1994 Molecular characterization of a copper transport protein in S. cerevisiae: an unexpected role for copper in iron transport. Cell **76**: 393–402.

DESNOYERS G., BOUCHARD M.-P., MASSÉ E., 2013 New insights into small RNA-dependent translational regulation in prokaryotes. Trends Genet. **29**: 92–8.

DINGWALL C., SHARNICK S. V, LASKEY R. A., 1982 A polypeptide domain that specifies migration of nucleoplasmin into the nucleus. Cell **30**: 449–58.

DIX D. R., BRIDGHAM J. T., BRODERIUS M. A., BYERSDORFER C. A., EIDE D. J., 1994 The FET4 gene encodes the low affinity Fe(II) transport protein of Saccharomyces cerevisiae. J. Biol. Chem. **269**: 26092–9.

DIX D., BRIDGHAM J., BRODERIUS M., EIDE D., 1997 Characterization of the FET4 protein of yeast. Evidence for a direct role in the transport of iron. J. Biol. Chem. **272**: 11770–7.

EDWARDS D., MURRAY J. A., SMITH A. G., 1998 Multiple genes encoding the conserved CCAAT-box transcription factor complex are expressed in Arabidopsis. Plant Physiol. **117**: 1015–22.

EISENDLE M., OBEREGGER H., ZADRA I., HAAS H., 2003 The siderophore system is essential for viability of Aspergillus nidulans: functional analysis of two genes encoding l-ornithine N 5-monooxygenase (sidA) and a non-ribosomal peptide synthetase (sidC). Mol. Microbiol. **49**: 359–75.

FERNÁNDEZ-CID A., VEGA M., HERRERO P., MORENO F., 2012 Yeast importin-β is required for nuclear import of the Mig2 repressor. BMC Cell Biol. **13**: 31.

FINEGOLD A. A., SHATWELL K. P., SEGAL A. W., KLAUSNER R. D., DANCIS A., 1996 Intramembrane bis-heme motif for transmembrane electron transport conserved in a yeast iron reductase and the human NADPH oxidase. J. Biol. Chem. **271**: 31021–4.

FORBES J. R., GROS P., 2001 Divalent-metal transport by NRAMP proteins at the interface of host-pathogen interactions. Trends Microbiol. **9**: 397–403.

FREITAS J. DE, WINTZ H., KIM J. H., POYNTON H., FOX T., VULPE C., 2003 Yeast, a model organism for iron and copper metabolism studies. Biometals **16**: 185–97.

FROISSARD M., BELGAREH-TOUZÉ N., DIAS M., BUISSON N., CAMADRO J.-M., HAGUENAUER-TSAPIS R., LESUISSE E., 2007 Trafficking of siderophore transporters in Saccharomyces cerevisiae and intracellular fate of ferrioxamine B conjugates. Traffic **8**: 1601–16.

GEORGATSOU E., ALEXANDRAKI D., 1994 Two distinctly regulated genes are required for ferric reduction, the first step of iron uptake in Saccharomyces cerevisiae. Mol. Cell. Biol. **14**: 3065–73.

GEORGATSOU E., MAVROGIANNIS L. A., FRAGIADAKIS G. S., ALEXANDRAKI D., 1997 The yeast Fre1p/Fre2p cupric reductases facilitate copper uptake and are regulated by the copper-modulated Mac1p activator. J. Biol. Chem. **272**: 13786–92.

GODA H., NAGASE T., TANOUE S., SUGIYAMA J., STEIDL S., TÜNCHER A., KOBAYASHI T., TSUKAGOSHI N., BRAKHAGE A. a, KATO M., 2005 Nuclear translocation of the heterotrimeric CCAAT binding factor of Aspergillus oryzae is dependent on two redundant localising signals in a single subunit. Arch. Microbiol. **184**: 93–100.

GOFFEAU A., BARRELL B. G., BUSSEY H., DAVIS R. W., DUJON B., FELDMANN H., GALIBERT F., HOHEISEL J. D., JACQ C., JOHNSTON M., LOUIS E. J., MEWES H. W., MURAKAMI Y., PHILIPPSEN P., TETTELIN H., OLIVER S. G., 1996 Life with 6000 genes. Science **274**: 546, 563–7.

GOLDFARB D. S., CORBETT A. H., MASON D. A., HARREMAN M. T., ADAM S. a, 2004 Importin alpha: a multipurpose nuclear-transport receptor. Trends Cell Biol. **14**: 505–14.

GÖRLICH D., HENKLEIN P., LASKEY R. A., HARTMANN E., 1996 A 41 amino acid motif in importin-alpha confers binding to importin-beta and hence transit into the nucleus. EMBO J. **15**: 1810–7.

GÖRLICH D., KOSTKA S., KRAFT R., DINGWALL C., LASKEY R. A., HARTMANN E., PREHN S., 1995 Two different subunits of importin cooperate to recognize nuclear localization signals and bind them to the nuclear envelope. Curr. Biol. **5**: 383–92.

HAAS H., ANGERMAYR K., STÖFFLER G., 1997 Molecular analysis of a Penicillium chrysogenum GATA factor encoding gene (sreP) exhibiting significant homology to the Ustilago maydis urbs1 gene. Gene **184**: 33–7.

HAAS H., EISENDLE M., TURGEON B. G., 2008 Siderophores in fungal physiology and virulence. Annu. Rev. Phytopathol. **46**: 149–87.

HAAS H., ZADRA I., STÖFFLER G., ANGERMAYR K., 1999 The Aspergillus nidulans GATA factor SREA is involved in regulation of siderophore biosynthesis and control of iron uptake. J. Biol. Chem. **274**: 4613–9.

HALLIWELL B., CHIRICO S., 1993 Lipid peroxidation: its mechanism, measurement, and significance. Am. J. Clin. Nutr. **57**: 715S–724S; discussion 724S–725S.

HALLIWELL B., GUTTERIDGE J. M. C., 1992 Biologically relevant metal ion-dependent hydroxyl radical generation An update. FEBS Lett. **307**: 108–112.

HARREMAN M. T., KLINE T. M., MILFORD H. G., HARBEN M. B., HODEL A. E., CORBETT A. H., 2004 Regulation of nuclear import by phosphorylation adjacent to nuclear localization signals. J. Biol. Chem. **279**: 20613–21.

HASSETT R. F., ROMEO A. M., KOSMAN D. J., 1998a Regulation of high affinity iron uptake in the yeast Saccharomyces cerevisiae. Role of dioxygen and Fe. J. Biol. Chem. **273**: 7628–36.

HASSETT R. F., YUAN D. S., KOSMAN D. J., 1998b Spectral and kinetic properties of the Fet3 protein from Saccharomyces cerevisiae, a multinuclear copper ferroxidase enzyme. J. Biol. Chem. **273**: 23274–82.

HELM D. VAN DER, WINKELMANN G., 1994 *Hydroxamates and polycarboxylates as iron transport agents (siderophores) in fungi.* (WD Winkelmann G, Ed.). Marcel Dekker, New York.

HEYMANN P., ERNST J. F., WINKELMANN G., 2000 Identification and substrate specificity of a ferrichrome-type siderophore transporter (Arn1p) in Saccharomyces cerevisiae. FEMS Microbiol. Lett. **186**: 221–7.

HO A. VAN, WARD D. M., KAPLAN J., 2002 Transition metal transport in yeast. Annu. Rev. Microbiol. **56**: 237–61.

HOELZ A., DEBLER E. W., BLOBEL G., 2011 The structure of the nuclear pore complex. Annu. Rev. Biochem. **80**: 613–43.

HORTSCHANSKY P., EISENDLE M., AL-ABDALLAH Q., SCHMIDT A. D., BERGMANN S., THÖN M., KNIEMEYER O., ABT B., SEEBER B., WERNER E. R., KATO M., BRAKHAGE A. A., HAAS H., 2007 Interaction of HapX with the CCAAT-binding complex--a novel mechanism of gene regulation by iron. EMBO J. **26**: 3157–68.

HSU P.-C., YANG C.-Y., LAN C.-Y., 2011 Candida albicans Hap43 is a repressor induced under low-iron conditions and is essential for iron-responsive transcriptional regulation and virulence. Eukaryot. Cell **10**: 207–25.

IWEMA T., PICCIOCCHI A., TRAORE D. A. K., FERRER J.-L., CHAUVAT F., JACQUAMET L., 2009 Structural basis for delivery of the intact [Fe2S2] cluster by monothiol glutaredoxin. Biochemistry **48**: 6041–3.

JACQUES J.-F., JANG S., PRÉVOST K., DESNOYERS G., DESMARAIS M., IMLAY J., MASSÉ E., 2006 RyhB small RNA modulates the free intracellular iron pool and is essential for normal growth during iron limitation in Escherichia coli. Mol. Microbiol. **62**: 1181–90.

JACQUES J.-F., MERCIER A., BRAULT A., MOURER T., LABBÉ S., 2014 Fra2 is a co-regulator of fep1 inhibition in response to iron starvation. (J Mata, Ed.). PLoS One **9**: e98959.

JBEL M., MERCIER A., LABBÉ S., 2011 Grx4 monothiol glutaredoxin is required for iron limitation-dependent inhibition of Fep1. Eukaryot. Cell **10**: 629–45.

JBEL M., MERCIER A., PELLETIER B., BEAUDOIN J., LABBÉ S., 2009 Iron activates in vivo DNA binding of Schizosaccharomyces pombe transcription factor Fep1 through its amino-terminal region. Eukaryot. Cell **8**: 649–64.

JENSEN L. T., CULOTTA V. C., 2002 Regulation of Saccharomyces cerevisiae FET4 by oxygen and iron. J. Mol. Biol. **318**: 251–60.

JOHNSON D. C., CANO K. E., KROGER E. C., MCNABB D. S., 2005 Novel regulatory function for the CCAAT-binding factor in Candida albicans. Eukaryot. Cell **4**: 1662–76.

JOHNSON P. F., MCKNIGHT S. L., 1989 Eukaryotic transcriptional regulatory proteins. Annu. Rev. Biochem. **58**: 799–839.

JONKERS W., KAN J. A. L. VAN, TIJM P., LEE Y.-W., TUDZYNSKI P., REP M., MICHIELSE C. B., 2011 The FRP1 F-box gene has different functions in sexuality, pathogenicity and metabolism in three fungal pathogens. Mol. Plant Pathol. **12**: 548–63.

JUNG W. H., SAIKIA S., HU G., WANG J., FUNG C. K.-Y., D'SOUZA C., WHITE R., KRONSTAD J. W., 2010 HapX positively and negatively regulates the transcriptional response to iron deprivation in Cryptococcus neoformans. PLoS Pathog. **6**: e1001209.

JUNG W. H., SHAM A., LIAN T., SINGH A., KOSMAN D. J., KRONSTAD J. W., 2008 Iron source preference and regulation of iron uptake in Cryptococcus neoformans. PLoS Pathog. **4**: e45.

KALDERON D., ROBERTS B. L., RICHARDSON W. D., SMITH A. E., 1984 A short amino acid sequence able to specify nuclear location. Cell **39**: 499–509.

KHAN M. G. M., JACQUES J.-F., BEAUDOIN J., LABBÉ S., 2014 Characterization of the Nuclear Import Mechanism of the CCAAT-Regulatory Subunit Php4 (JM Di Noia, Ed.). PLoS One **9**: 15.

KHOROSJUTINA O., WANROOIJ P. H., WALFRIDSSON J., SZILAGYI Z., ZHU X., BARAZNENOK V., EKWALL K., GUSTAFSSON C. M., 2010 A chromatin-remodeling protein is a component of fission yeast mediator. J. Biol. Chem. **285**: 29729–37.

KIM Y., LAMPERT S. M., PHILPOTT C. C., 2005 A receptor domain controls the intracellular sorting of the ferrichrome transporter, ARN1. EMBO J. **24**: 952–62.

KIM Y., YUN C.-W., PHILPOTT C. C., 2002 Ferrichrome induces endosome to plasma membrane cycling of the ferrichrome transporter, Arn1p, in Saccharomyces cerevisiae. EMBO J. **21**: 3632–42.

KNIGHT S. A. B., LESUISSE E., STEARMAN R., KLAUSNER R. D., DANCIS A., 2002 Reductive iron uptake by Candida albicans: role of copper, iron and the TUP1 regulator. Microbiology **148**: 29–40.

KOSMAN D. J., 2003 Molecular mechanisms of iron uptake in fungi. Mol. Microbiol. **47**: 1185–1197.

KOSUGI S., HASEBE M., MATSUMURA N., TAKASHIMA H., MIYAMOTO-SATO E., TOMITA M., YANAGAWA H., 2009 Six classes of nuclear localization signals specific to different binding grooves of importin α. J. Biol. … **284**: 478–485.

KUERSTEN S., OHNO M., MATTAJ I. W., 2001 Nucleocytoplasmic transport: Ran, beta and beyond. Trends Cell Biol. **11**: 497–503.

KUMÁNOVICS A., CHEN O. S., LI L., BAGLEY D., ADKINS E. M., LIN H., DINGRA N. N., OUTTEN C. E., KELLER G., WINGE D., WARD D. M., KAPLAN J., 2008 Identification of FRA1 and FRA2 as genes involved in regulating the yeast iron regulon in response to decreased mitochondrial iron-sulfur cluster synthesis. J. Biol. Chem. **283**: 10276–86.

KWOK E. Y., SEVERANCE S., KOSMAN D. J., 2006 Evidence for iron channeling in the Fet3p-Ftr1p high-affinity iron uptake complex in the yeast plasma membrane. Biochemistry **45**: 6317–27.

LABBÉ S., 2010 Simon Labbé's work on iron and copper homeostasis. World J. Biol. Chem. **1**: 196–200.

LABBÉ S., KHAN M. G. M., JACQUES J.-F., 2013 Iron uptake and regulation in Schizosaccharomyces pombe. Curr. Opin. Microbiol. **16**: 669–76.

LABBÉ S., PELLETIER B., MERCIER A., 2007 Iron homeostasis in the fission yeast Schizosaccharomyces pombe. Biometals **20**: 523–37.

LAN C.-Y., RODARTE G., MURILLO L. A., JONES T., DAVIS R. W., DUNGAN J., NEWPORT G., AGABIAN N., 2004 Regulatory networks affected by iron availability in Candida albicans. Mol. Microbiol. **53**: 1451–69.

LANGE A., MILLS R. E., CHRISTOPHER J., STEWART M., DEVINE S. E., CORBETT A. H., LANGE C. J., 2007 Classical Nuclear Localization Signals : Definition , Function ,. J. Biol. Chem. **282**: 5101–5105.

LANGE A., MILLS R. E., DEVINE S. E., CORBETT A. H., 2008 A PY-NLS nuclear targeting signal is required for nuclear localization and function of the Saccharomyces cerevisiae mRNA-binding protein Hrp1. J. Biol. Chem. **283**: 12926–34.

LAPINSKAS P. J., LIN S. J., CULOTTA V. C., 1996 The role of the Saccharomyces cerevisiae CCC1 gene in the homeostasis of manganese ions. Mol. Microbiol. **21**: 519–28.

LEE B. J., CANSIZOGLU A. E., SÜEL K. E., LOUIS T. H., ZHANG Z., CHOOK Y. M., 2006 Rules for nuclear localization sequence recognition by karyopherin beta 2. Cell **126**: 543–58.

LESUISSE E., BLAISEAU P. L., DANCIS A., CAMADRO J. M., 2001 Siderophore uptake and use by the yeast Saccharomyces cerevisiae. Microbiology **147**: 289–98.

LESUISSE E., KNIGHT S. A. B., COUREL M., SANTOS R., CAMADRO J.-M., DANCIS A., 2005 Genome-wide screen for genes with effects on distinct iron uptake activities in Saccharomyces cerevisiae. Genetics **169**: 107–22.

LESUISSE E., RAGUZZI F., CRICHTON R. R., 1987 Iron uptake by the yeast Saccharomyces cerevisiae: involvement of a reduction step. J. Gen. Microbiol. **133**: 3229–36.

LESUISSE E., SIMON-CASTERAS M., LABBE P., 1998 Siderophore-mediated iron uptake in Saccharomyces cerevisiae: the SIT1 gene encodes a ferrioxamine B permease that belongs to the major facilitator superfamily. Microbiology **144**: 3455–3462.

LI L., BAGLEY D., WARD D. M., KAPLAN J., 2008 Yap5 is an iron-responsive transcriptional activator that regulates vacuolar iron storage in yeast. Mol. Cell. Biol. **28**: 1326–37.

LI L., CHEN O. S., MCVEY WARD D., KAPLAN J., 2001 CCC1 is a transporter that mediates vacuolar iron storage in yeast. J. Biol. Chem. **276**: 29515–9.

LI L., KAPLAN J., 1998 Defects in the yeast high affinity iron transport system result in increased metal sensitivity because of the increased expression of transporters with a broad transition metal specificity. J. Biol. Chem. **273**: 22181–7.

LI H., MAPOLELO D. T., DINGRA N. N., KELLER G., RIGGS-GELASCO P. J., WINGE D. R., JOHNSON M. K., OUTTEN C. E., 2011 Histidine 103 in Fra2 is an iron-sulfur cluster ligand in the [2Fe-2S] Fra2-Grx3 complex and is required for in vivo iron signaling in yeast. J. Biol. Chem. **286**: 867–76.

LI H., MAPOLELO D. T., DINGRA N. N., NAIK S. G., LEES N. S., HOFFMAN B. M., RIGGS-GELASCO P. J., HUYNH B. H., JOHNSON M. K., OUTTEN C. E., 2009a The yeast iron regulatory proteins Grx3/4 and Fra2 form heterodimeric complexes containing a [2Fe-2S] cluster with cysteinyl and histidyl ligation. Biochemistry **48**: 9569–81.

LI H., OUTTEN C. E., 2012 Monothiol CGFS glutaredoxins and BolA-like proteins: [2Fe-2S] binding partners in iron homeostasis. Biochemistry **51**: 4377–89.

LI H., SWIERCZ R., ENGLANDER E. W., 2009b Elevated metals compromise repair of oxidative DNA damage via the base excision repair pathway: implications of pathologic iron overload in the brain on integrity of neuronal DNA. J. Neurochem. **110**: 1774–83.

LIM R. Y. H., HUANG N.-P., KÖSER J., DENG J., LAU K. H. A., SCHWARZ-HERION K., FAHRENKROG B., AEBI U., 2006 Flexible phenylalanine-glycine nucleoporins as entropic barriers to nucleocytoplasmic transport. Proc. Natl. Acad. Sci. U. S. A. **103**: 9512–7.

LIN S.-J., AUSTRIACO N., 2013 Aging and cell death in the other yeasts, Schizosaccharomyces pombe and Candida albicans. FEMS Yeast Res.

LIN S.-J. J., WARDLAW C. P., MORISHITA T., MIYABE I., CHAHWAN C., CASPARI T., SCHMIDT U., CARR A. M., GARCIA V., 2012 The Rad4(TopBP1) ATR-activation domain functions in G1/S phase in a chromatin-dependent manner. (S Jinks-Robertson, Ed.). PLoS Genet. **8**: e1002801.

LOPEZ-BERGES M. S., CAPILLA J., TURRA D., SCHAFFERER L., MATTHIJS S., JOCHL C., CORNELIS P., GUARRO J., HAAS H., PIETRO A. DI, LÓPEZ-BERGES M. S., TURRÀ D., JÖCHL C., 2012 HapX-mediated iron homeostasis is essential for rhizosphere competence and virulence of the soilborne pathogen Fusarium oxysporum. Plant Cell **24**: 3805–3822.

LOW C. P., YANG H., 2008 Programmed cell death in fission yeast Schizosaccharomyces pombe. Biochim. Biophys. Acta **1783**: 1335–49.

LYKKE-ANDERSEN J., WAGNER E., 2005 Recruitment and activation of mRNA decay enzymes by two ARE-mediated decay activation domains in the proteins TTP and BRF-1. Genes Dev. **19**: 351–61.

MACKINNON M. A., CURWIN A. J., GASPARD G. J., SURACI A. B., FERNÁNDEZ-MURRAY J. P., MCMASTER C. R., 2009 The Kap60-Kap95 karyopherin complex directly regulates phosphatidylcholine synthesis. J. Biol. Chem. **284**: 7376–84.

MAITY S. N., VUORIO T., CROMBRUGGHE B. DE, 1990 The B subunit of a rat heteromeric CCAAT-binding transcription factor shows a striking sequence identity with the yeast Hap2 transcription factor. Proc. Natl. Acad. Sci. U. S. A. **87**: 5378–82.

MALLET P.-L., BACHAND F., 2013 A proline-tyrosine nuclear localization signal (PY-NLS) is required for the nuclear import of fission yeast PAB2, but not of human PABPN1. Traffic **14**: 282–94.

MANTOVANI R., 1999 The molecular biology of the CCAAT-binding factor NF-Y. Gene **239**: 15–27.

MARFORI M., MYNOTT A., ELLIS J. J., MEHDI A. M., SAUNDERS N. F. W., CURMI P. M., FORWOOD J. K., BODÉN M., KOBE B., 2011 Biochimica et Biophysica Acta Molecular basis for speci fi city of nuclear import and prediction of nuclear localization ☆. BBA - Mol. Cell Res. **1813**: 1562–1577.

MARTÍNEZ-PASTOR M., VERGARA S. V, PUIG S., THIELE D. J., 2013 Negative feedback regulation of the yeast CTH1 and CTH2 mRNA binding proteins is required for adaptation to iron deficiency and iron supplementation. Mol. Cell. Biol. **33**: 2178–87.

MCNABB D. D. S., PINTO I., 2005 Assembly of the Hap2p/Hap3p/Hap4p/Hap5p-DNA complex in Saccharomyces cerevisiae. Eukaryot. Cell **4**: 1829–1839.

MCNABB D. S., TSENG K. A., GUARENTE L., 1997 The Saccharomyces cerevisiae Hap5p homolog from fission yeast reveals two conserved domains that are essential for assembly of heterotetrameric CCAAT-binding factor. Mol. Cell. Biol. **17**: 7008–18.

MCNABB D. S., XING Y., GUARENTE L., 1995 Cloning of yeast HAP5: a novel subunit of a heterotrimeric complex required for CCAAT binding. Genes Dev. **9**: 47–58.

MERCIER A., LABBÉ S., 2009 Both Php4 function and subcellular localization are regulated by iron via a multistep mechanism involving the glutaredoxin Grx4 and the exportin Crm1. J. Biol. Chem. **284**: 20249–62.

MERCIER A., LABBÉ S., 2010 Iron-dependent remodeling of fungal metabolic pathways associated with ferrichrome biosynthesis. Appl. Environ. Microbiol. **76**: 3806–17.

MERCIER A., PELLETIER B., LABBÉ S., 2006 A transcription factor cascade involving Fep1 and the CCAAT-binding factor Php4 regulates gene expression in response to iron deficiency in the fission yeast Schizosaccharomyces pombe. Eukaryot. Cell **5**: 1866–81.

MERCIER A., WATT S., BÄHLER J., LABBÉ S., 2008 Key function for the CCAAT-binding factor Php4 to regulate gene expression in response to iron deficiency in fission yeast. Eukaryot. Cell **7**: 493–508.

MOORE R. E., KIM Y., PHILPOTT C. C., 2003 The mechanism of ferrichrome transport through Arn1p and its metabolism in Saccharomyces cerevisiae. Proc. Natl. Acad. Sci. U. S. A. **100**: 5664–9.

MÜHLENHOFF U., MOLIK S., GODOY J. R., UZARSKA M. A., RICHTER N., SEUBERT A., ZHANG Y., STUBBE J., PIERREL F., HERRERO E., LILLIG C. H., LILL R., 2010 Cytosolic monothiol glutaredoxins function in intracellular iron sensing and trafficking via their bound iron-sulfur cluster. Cell Metab. **12**: 373–85.

NARDOZZI J. D., LOTT K., CINGOLANI G., 2010 Phosphorylation meets nuclear import: a review. Cell Commun. Signal. **8**: 32.

NEILANDS J. B., 1993 Siderophores. Arch. Biochem. Biophys. **302**: 1–3.

NEILANDS J. B., 1995 Siderophores: structure and function of microbial iron transport compounds. J. Biol. Chem. **270**: 26723–6.

OHTSUKA H., OGAWA S., KAWAMURA H., SAKAI E., ICHINOSE K., MURAKAMI H., AIBA H., 2013 Screening for long-lived genes identifies Oga1, a guanine-quadruplex associated protein that affects the chronological lifespan of the fission yeast Schizosaccharomyces pombe. Mol. Genet. Genomics **288**: 285–95.

PARK J., FREITAG S. I., YOUNG P. G., HOBMAN T. C., 2012 The karyopherin Sal3 is required for nuclear import of the core RNA interference pathway protein Rdp1. Traffic **13**: 520–31.

PATHOGEN F., CHAO L. Y., MARLETTA M. A., RINE J., 2008 Sre1 , an Iron-Modulated GATA DNA-Binding Protein of Iron-Uptake Genes in the. Biochemistry **47**: 7274–7283.

PEDRO-SEGURA E., VERGARA S. V, RODRÍGUEZ-NAVARRO S., PARKER R., THIELE D. J., PUIG S., 2008 The Cth2 ARE-binding protein recruits the Dhh1 helicase to promote the decay of succinate dehydrogenase SDH4 mRNA in response to iron deficiency. J. Biol. Chem. **283**: 28527–35.

PELÁEZ R., FERNÁNDEZ-GARCÍA P., HERRERO P., MORENO F., 2012 Nuclear import of the yeast hexokinase 2 protein requires α/β-importin-dependent pathway. J. Biol. Chem. **287**: 3518–29.

PELLETIER B., BEAUDOIN J., MUKAI Y., LABBÉ S., 2002 Fep1, an iron sensor regulating iron transporter gene expression in Schizosaccharomyces pombe. J. Biol. Chem. **277**: 22950–8.

PELLETIER B., BEAUDOIN J., PHILPOTT C. C., LABBÉ S., 2003 Fep1 represses expression of the fission yeast Schizosaccharomyces pombe siderophore-iron transport system. Nucleic Acids Res. **31**: 4332–4344.

PELLETIER B., TROTT A., MORANO K. a, LABBÉ S., 2005 Functional characterization of the iron-regulatory transcription factor Fep1 from Schizosaccharomyces pombe. J. Biol. Chem. **280**: 25146–61.

PHILPOTT C. C., 2006 Iron uptake in fungi: a system for every source. Biochim. Biophys. Acta **1763**: 636–45.

PHILPOTT C. C., LEIDGENS S., FREY A. G., 2012 Metabolic remodeling in iron-deficient fungi. Biochim. Biophys. Acta **1823**: 1509–20.

PHILPOTT C. C., PROTCHENKO O., 2008 Response to iron deprivation in Saccharomyces cerevisiae. Eukaryot. Cell **7**: 20–7.

PICCIOCCHI A., SAGUEZ C., BOUSSAC A., CASSIER-CHAUVAT C., CHAUVAT F., 2007 CGFS-type monothiol glutaredoxins from the cyanobacterium Synechocystis PCC6803 and other evolutionary distant model organisms possess a glutathione-ligated [2Fe-2S] cluster. Biochemistry **46**: 15018–26.

PINKHAM J. L., GUARENTE L., 1985 Cloning and molecular analysis of the HAP2 locus: a global regulator of respiratory genes in Saccharomyces cerevisiae. Mol. Cell. Biol. **5**: 3410–6.

PORTNOY M. E., LIU X. F., CULOTTA V. C., 2000 Saccharomyces cerevisiae expresses three functionally distinct homologues of the nramp family of metal transporters. Mol. Cell. Biol. **20**: 7893–902.

POULIOT B., JBEL M., MERCIER A., LABBÉ S., 2010 abc3+ encodes an iron-regulated vacuolar ABC-type transporter in Schizosaccharomyces pombe. Eukaryot. Cell **9**: 59–73.

PUIG S., ASKELAND E., THIELE D. J., 2005 Coordinated remodeling of cellular metabolism during iron deficiency through targeted mRNA degradation. Cell **120**: 99–110.

PUIG S., VERGARA S. V, THIELE D. J., 2008 Cooperation of two mRNA-binding proteins drives metabolic adaptation to iron deficiency. Cell Metab. **7**: 555–64.

QU M., RAPPAS M., WARDLAW C. P., GARCIA V., REN J.-Y., DAY M., CARR A. M., OLIVER A. W., DU L.-L., PEARL L. H., 2013 Phosphorylation-dependent assembly and coordination of the DNA damage checkpoint apparatus by Rad4(TopBP[1]). Mol. Cell **51**: 723–36.

QU M., YANG B., TAO L., YATES J. R., RUSSELL P., DONG M.-Q., DU L.-L., 2012 Phosphorylation-dependent interactions between Crb2 and Chk1 are essential for DNA damage checkpoint. PLoS Genet. **8**: e1002817.

RAMANAN N., WANG Y., 2000 A high-affinity iron permease essential for Candida albicans virulence. Science **288**: 1062–4.

RAMSAY L., 1997 Mutants of Saccharomyces cerevisiae defective in vacuolar function confirm a role for the vacuole in toxic metal ion detoxification. FEMS Microbiol. Lett. **152**: 293–298.

RAYMONDJEAN M., CEREGHINI S., YANIV M., 1988 Several distinct "CCAAT" box binding proteins coexist in eukaryotic cells. Proc. Natl. Acad. Sci. U. S. A. **85**: 757–61.

REES E. M., LEE J., THIELE D. J., 2004 Mobilization of intracellular copper stores by the ctr2 vacuolar copper transporter. J. Biol. Chem. **279**: 54221–9.

REES E. M., THIELE D. J., 2007 Identification of a vacuole-associated metalloreductase and its role in Ctr2-mediated intracellular copper mobilization. J. Biol. Chem. **282**: 21629–38.

REITER R. J., MELCHIORRI D., SEWERYNEK E., POEGGELER B., BARLOW-WALDEN L., CHUANG J., ORTIZ G. G., ACUÑA-CASTROVIEJO D., 1995 A review of the evidence supporting melatonin's role as an antioxidant. J. Pineal Res. **18**: 1–11.

REYES-TURCU F. E., GREWAL S. I., 2012 Different means, same end-heterochromatin formation by RNAi and RNAi-independent RNA processing factors in fission yeast. Curr. Opin. Genet. Dev. **22**: 156–63.

ROMAN D. G., DANCIS A., ANDERSON G. J., KLAUSNER R. D., 1993 The fission yeast ferric reductase gene frp1+ is required for ferric iron uptake and encodes a protein that is homologous to the gp91-phox subunit of the human NADPH phagocyte oxidoreductase. Mol. Cell. Biol. **13**: 4342–50.

RÓNA G., MARFORI M., BORSOS M., SCHEER I., TAKÁCS E., TÓTH J., BABOS F., MAGYAR A., ERDEI A., BOZÓKY Z., BUDAY L., KOBE B., VÉRTESSY B. G., 2013 Phosphorylation adjacent to the nuclear localization signal of human dUTPase abolishes nuclear import: structural and mechanistic insights. Acta Crystallogr. D. Biol. Crystallogr. **69**: 2495–505.

ROUHIER N., COUTURIER J., JOHNSON M. K., JACQUOT J.-P., 2010 Glutaredoxins: roles in iron homeostasis. Trends Biochem. Sci. **35**: 43–52.

RUTHERFORD J. C., JARON S., RAY E., BROWN P. O., WINGE D. R., 2001 A second iron-regulatory system in yeast independent of Aft1p. Proc. Natl. Acad. Sci. U. S. A. **98**: 14322–7.

RUTHERFORD J. C., JARON S., WINGE D. R., 2003 Aft1p and Aft2p mediate iron-responsive gene expression in yeast through related promoter elements. J. Biol. Chem. **278**: 27636–43.

SANTORO C., MERMOD N., ANDREWS P. C., TJIAN R., 1988 A family of human CCAAT-box-binding proteins active in transcription and DNA replication: cloning and expression of multiple cDNAs. Nature **334**: 218–24.

SARKAR B., 1995 Metal replacement in DNA-binding zinc finger proteins and its relevance to mutagenicity and carcinogenicity through free radical generation. Nutrition **11**: 646–9.

SCHRETTL M., BECKMANN N., VARGA J., HEINEKAMP T., JACOBSEN I. D., JÖCHL C., MOUSSA T. A., WANG S., GSALLER F., BLATZER M., WERNER E. R., NIERMANN W. C., BRAKHAGE A. A., HAAS H., 2010 HapX-Mediated adaption to iron starvation is crucial for virulence of Aspergillus fumigatus. PLoS Pathog. **6**: e1001124.

SCHRETTL M., WINKELMANN G., HAAS H., 2004 Ferrichrome in Schizosaccharomyces pombe ? an iron transport and iron storage compound. BioMetals **17**: 647–654.

SCHWECKE T., GÖTTLING K., DUREK P., DUEÑAS I., KÄUFER N. F., ZOCK-EMMENTHAL S., STAUB E., NEUHOF T., DIECKMANN R., DÖHREN H. VON, 2006 Nonribosomal peptide synthesis in Schizosaccharomyces pombe and the architectures of ferrichrome-type siderophore synthetases in fungi. Chembiochem **7**: 612–22.

SHAKOURY-ELIZEH M., TIEDEMAN J., RASHFORD J., FEREA T., DEMETER J., GARCIA E., ROLFES R., BROWN P. O., BOTSTEIN D., PHILPOTT C. C., 2004 Transcriptional remodeling in response to iron deprivation in Saccharomyces cerevisiae. Mol. Biol. Cell **15**: 1233–43.

SICKMANN A., REINDERS J., WAGNER Y., JOPPICH C., ZAHEDI R., MEYER H. E., SCHÖNFISCH B., PERSCHIL I., CHACINSKA A., GUIARD B., REHLING P., PFANNER N., MEISINGER C., 2003 The proteome of Saccharomyces cerevisiae mitochondria. Proc. Natl. Acad. Sci. U. S. A. **100**: 13207–12.

SILVA D. M. DE, ASKWITH C. C., KAPLAN J., 1996 Molecular mechanisms of iron uptake in eukaryotes. Physiol. Rev. **76**: 31–47.

SIMM C., LAHNER B., SALT D., LEFURGEY A., INGRAM P., YANDELL B., EIDE D. J., 2007 Saccharomyces cerevisiae vacuole in zinc storage and intracellular zinc distribution. Eukaryot. Cell **6**: 1166–77.

SINGH A., KAUR N., KOSMAN D. J., 2007 The metalloreductase Fre6p in Fe-efflux from the yeast vacuole. J. Biol. Chem. **282**: 28619–26.

SINGH A., SEVERANCE S., KAUR N., WILTSIE W., KOSMAN D. J., 2006 Assembly, activation, and trafficking of the Fet3p.Ftr1p high affinity iron permease complex in Saccharomyces cerevisiae. J. Biol. Chem. **281**: 13355–64.

SINHA S., MAITY S. N., LU J., CROMBRUGGHE B. DE, 1995 Recombinant rat CBF-C, the third subunit of CBF/NFY, allows formation of a protein-DNA complex with CBF-A and CBF-B and with yeast HAP2 and HAP3. Proc. Natl. Acad. Sci. U. S. A. **92**: 1624–8.

SMIALOWSKA A., DJUPEDAL I., WANG J., KYLSTEN P., SWOBODA P., EKWALL K., 2014 RNAi mediates post-transcriptional repression of gene expression in fission yeast Schizosaccharomyces pombe. Biochem. Biophys. Res. Commun. **444**: 254–9.

SOROKIN A. V, KIM E. R., OVCHINNIKOV L. P., 2007 Nucleocytoplasmic transport of proteins. Biochem. Biokhimiia **72**: 1439–57.

STEARMAN R., YUAN D. S., YAMAGUCHI-IWAI Y., KLAUSNER R. D., DANCIS A., 1996 A permease-oxidase complex involved in high-affinity iron uptake in yeast. Science **271**: 1552–7.

STEIDL S., PAPAGIANNOPOULOS P., LITZKA O., ANDRIANOPOULOS A., DAVIS M. A., BRAKHAGE A. A., HYNES M. J., 1999 AnCF, the CCAAT binding complex of Aspergillus nidulans, contains products of the hapB, hapC, and hapE genes and is required for activation by the pathway-specific regulatory gene amdR. Mol. Cell. Biol. **19**: 99–106.

STEIDL S., TÜNCHER A., GODA H., GUDER C., PAPADOPOULOU N., KOBAYASHI T., TSUKAGOSHI N., KATO M., BRAKHAGE A. a, 2004 A single subunit of a heterotrimeric CCAAT-binding complex carries a nuclear localization signal: piggy back transport of the pre-assembled complex to the nucleus. J. Mol. Biol. **342**: 515–24.

SYBIRNA K., GUIARD B., LI Y. F., BAO W. G., BOLOTIN-FUKUHARA M., DELAHODDE A., 2005 A new Hansenula polymorpha HAP4 homologue which contains only the N-terminal conserved domain of the protein is fully functional in Saccharomyces cerevisiae. Curr. Genet. **47**: 172–81.

SZCZYPKA M. S., ZHU Z., SILAR P., THIELE D. J., 1997 Saccharomyces cerevisiae mutants altered in vacuole function are defective in copper detoxification and iron-responsive gene transcription. Yeast **13**: 1423–35.

TABERNER F. J., IGUAL J. C., 2010 Yeast karyopherin Kap95 is required for cell cycle progression at Start. BMC Cell Biol. **11**: 47.

THIEKEN A., WINKELMANN G., 1992 Rhizoferrin: a complexone type siderophore of the Mucorales and entomophthorales (Zygomycetes). FEMS Microbiol. Lett. **73**: 37–41.

THOMPSON M. J., LAI W. S., TAYLOR G. A., BLACKSHEAR P. J., 1996 Cloning and characterization of two yeast genes encoding members of the CCCH class of zinc finger proteins: zinc finger-mediated impairment of cell growth. Gene **174**: 225–33.

TRAN E. J., BOLGER T. A., WENTE S. R., 2007 SnapShot: nuclear transport. Cell **131**: 420.

TWYFFELS L., WAUQUIER C., SOIN R., DECAESTECKER C., GUEYDAN C., KRUYS V., 2013 A masked PY-NLS in Drosophila TIS11 and its mammalian homolog tristetraprolin. PLoS One **8**: e71686.

UETA R., FUJIWARA N., IWAI K., YAMAGUCHI-IWAI Y., 2007 Mechanism underlying the iron-dependent nuclear export of the iron-responsive transcription factor Aft1p in Saccharomyces cerevisiae. Mol. Biol. Cell **18**: 2980–90.

UMEDA M., IZADDOOST S., CUSHMAN I., MOORE M. S., SAZER S., 2005 The Fission Yeast Schizosaccharomyces pombe Has Two Importin- a Proteins, Imp1p and Cut15p, Which Have Common and Unique Functions in Nucleocytoplasmic Transport and Cell Cycle Progression. **21**: 7–21.

URBANOWSKI J. L., PIPER R. C., 1999 The iron transporter Fth1p forms a complex with the Fet5 iron oxidase and resides on the vacuolar membrane. J. Biol. Chem. **274**: 38061–38070.

VACHON P., MERCIER A., JBEL M., LABBÉ S., 2012 The monothiol glutaredoxin Grx4 exerts an iron-dependent inhibitory effect on Php4 function. Eukaryot. Cell **11**: 806–19.

VERGARA S. V, PUIG S., THIELE D. J., 2011 Early recruitment of AU-rich element-containing mRNAs determines their cytosolic fate during iron deficiency. Mol. Cell. Biol. **31**: 417–29.

WOOD V., GWILLIAM R., RAJANDREAM M.-A., LYNE M., LYNE R., STEWART A., SGOUROS J., PEAT N., HAYLES J., BAKER S., BASHAM D., BOWMAN S., BROOKS K., BROWN D., BROWN S., CHILLINGWORTH T., CHURCHER C., COLLINS M., CONNOR R., CRONIN A., DAVIS P., FELTWELL T., FRASER A., GENTLES S., GOBLE A., HAMLIN N., HARRIS D., HIDALGO J., HODGSON G., HOLROYD S., HORNSBY T., HOWARTH S., HUCKLE E. J., HUNT S., JAGELS K., JAMES K., JONES L., JONES M., LEATHER S., MCDONALD S., MCLEAN J., MOONEY P., MOULE S., MUNGALL K., MURPHY L., NIBLETT D., ODELL C., OLIVER K., O'NEIL S., PEARSON D., QUAIL M. A., RABBINOWITSCH E., RUTHERFORD K., RUTTER S., SAUNDERS D., SEEGER K., SHARP S., SKELTON J., SIMMONDS M., SQUARES R., SQUARES S., STEVENS K., TAYLOR K., TAYLOR R. G., TIVEY A., WALSH S., WARREN T., WHITEHEAD S., WOODWARD J., VOLCKAERT G., AERT R., ROBBEN J., GRYMONPREZ B., WELTJENS I., VANSTREELS E., RIEGER M., SCHÄFER M., MÜLLER-AUER S., GABEL C., FUCHS M., DÜSTERHÖFT A., FRITZC C., HOLZER E., MOESTL D., HILBERT H., BORZYM K., LANGER I., BECK A., LEHRACH H., REINHARDT R., POHL T. M., EGER P., ZIMMERMANN W., WEDLER H., WAMBUTT R., PURNELLE B., GOFFEAU A., CADIEU E., DRÉANO S., GLOUX S., LELAURE V., MOTTIER S., GALIBERT F., AVES S. J., XIANG Z., HUNT C., MOORE K., HURST S. M., LUCAS M., ROCHET M., GAILLARDIN C., TALLADA V. A., GARZON A., THODE G., DAGA R. R., CRUZADO L., JIMENEZ J., SÁNCHEZ M., REY F. DEL, BENITO J., DOMÍNGUEZ A., REVUELTA J. L., MORENO S., ARMSTRONG J., FORSBURG S. L., CERUTTI L., LOWE T., MCCOMBIE W. R., PAULSEN I., POTASHKIN J., SHPAKOVSKI G. V, USSERY D., BARRELL B. G., NURSE P., CERRUTTI L., 2002 The genome sequence of Schizosaccharomyces pombe. Nature **415**: 871–80.

XU N., DONG Y., CHENG X., YU Q., QIAN K., MAO J., JIA C., DING X., ZHANG B., CHEN Y., ZHANG B., XING L., LI M., 2013 Cellular iron homeostasis mediated by the Mrs4-Ccc1-Smf3 pathway is essential for mitochondrial function, morphogenesis and virulence in Candida albicans. Biochim. Biophys. Acta **1843**: 629–639.

YAMAGUCHI-IWAI Y., DANCIS A., KLAUSNER R. D., 1995 AFT1: a mediator of iron regulated transcriptional control in Saccharomyces cerevisiae. EMBO J. **14**: 1231–9.

YOSHIDA K., BLOBEL G., 2001 The karyopherin Kap142p/Msn5p mediates nuclear import and nuclear export of different cargo proteins. J. Cell Biol. **152**: 729–40.

YUAN D. S., DANCIS A., KLAUSNER R. D., 1997 Restriction of copper export in Saccharomyces cerevisiae to a late Golgi or post-Golgi compartment in the secretory pathway. J. Biol. Chem. **272**: 25787–93.

YUAN D. S., STEARMAN R., DANCIS A., DUNN T., BEELER T., KLAUSNER R. D., 1995 The Menkes/Wilson disease gene homologue in yeast provides copper to a ceruloplasmin-like oxidase required for iron uptake. Proc. Natl. Acad. Sci. U. S. A. **92**: 2632–6.

YUN C. W., BAULER M., MOORE R. E., KLEBBA P. E., PHILPOTT C. C., 2001 The role of the FRE family of plasma membrane reductases in the uptake of siderophore-iron in Saccharomyces cerevisiae. J. Biol. Chem. **276**: 10218–23.

YUN C. W., TIEDEMAN J. S., MOORE R. E., PHILPOTT C. C., 2000 Siderophore-iron uptake in saccharomyces cerevisiae. Identification of ferrichrome and fusarinine transporters. J. Biol. Chem. **275**: 16354–9.

ZHOU L., MARZLUF G. A., 1999 Functional analysis of the two zinc fingers of SRE, a GATA-type factor that negatively regulates siderophore synthesis in Neurospora crassa. Biochemistry **38**: 4335–41.

ZNAIDI S., PELLETIER B., MUKAI Y., LABBÉ S., 2004 The Schizosaccharomyces pombe corepressor Tup11 interacts with the iron-responsive transcription factor Fep1. J. Biol. Chem. **279**: 9462–74.